

ELECTROCHEMICAL BEHAVIOUR OF
POLYANILINE ELECTRODEPOSITED ON A
REDOX ION-EXCHANGER MODIFIED
ELECTRODE.

THIS THESIS HAS BEEN ACCEPTED FOR
THE DEGREE OF M.Sc. 1996
AND MAY BE CONSULTED IN THE
LIBRARY

UNIVERSITY OF NAIROBI
P. O. BOX 30197
NAIROBI

By

KARIUKI BENSON
Bed. Sci. (Hons)
KENYATTA UNIVERSITY

A thesis submitted in partial fulfilment for the degree of Master of Science of the
[University of Nairobi.]

1996

UNIVERSITY OF NAIROBI LIBRARY




0133986 0


DECLARATION

This thesis is my original work and has not been presented for a degree in any other university.

Sign. 
Kariuki Benson

This thesis has been submitted for examination with our approval as university supervisors.

Sign.  8/11/96.
DR. D.O. ORATA,
DEPT. OF CHEMISTRY,
UNIVERSITY OF NAIROBI.

Sign. 
PROF. G.N. KAMAU,
DEPT. OF CHEMISTRY,
UNIVERSITY OF NAIROBI.

DEDICATION

Dedicated to my mother, Jedidah Watetu, and my sisters, Pauline and Ciru.

ACKNOWLEDGEMENT

I wish to express my sincere gratitude to my supervisors, Dr. D.O. Orata and Prof. G.N. Kamau for their supervision, advice and encouragement during the course of this work. I am particularly thankful to Dr. D.O. Orata, my first supervisor, for his inspiration throughout the course of investigation and compilation of this work.

I am also indebted to the Gandhi Smarak Nidhi Fund for the provision of a scholarship which enabled me to carry out my M.Sc work. I also wish to thank all the technical staff of the Dept. of Chemistry, University of Nairobi, in particular Moses Njau for all the help they so willingly rendered to me during the course.

My parents, relatives and friends have continuously given me constant support and encouragement for all the years I have been involved in academic pursuits. I am indeed thankful for their patience and they always remain sincerely and earnestly loved. Special thanks go to Miss Irene Wangari for her understanding and encouragement throughout this course.

LIST OF ABBREVIATIONS

B-NAC	Bentonite No Acid
B-WAC	Bentonite With Acid
B-WPN	Bentonite With Potassium Nitrate
B-NPN	Bentonite No Potassium Nitrate
A-NAC	Amberlite No Acid
A-WAC	Amberlite With Acid
A-WPN	Amberlite With Potassium Nitrate
A-NPN	Amberlite No Potassium Nitrate

These materials used for electrode modification were made according to procedure outlined in page 70.

TABLE OF CONTENT

Title	i
Declaration	ii
Dedication	iii
Acknowledgement	iv
List of Abbreviations	v
Table of Content	vi
Abstract	ix
List of tables	xi
List of schemes	xii
List of figures	xii

CHAPTER ONE

1.0 Introduction	1
1.1 Literature review	2
1.1.1 Electrode modification	2
a) Derivatization of metal oxide electrodes.	3
b) Derivatization of carbon electrodes.	4
1.1.2 Derivatization of electrode surfaces by film formation	9
a) Ion exchangers	11
b) Redox polymers.	28
c) Conducting polymers.	30

CHAPTER TWO

2.0 Proposed research.	43
Experimental section	44
2.1 Methods of analysis	44
2.1.1. An overview of the electrochemical technique.	44
a) Mode of Operation of a Potentiostat.	51

2.1.2 X-ray fluorescence analysis (X-RF)	59
a) X-RF instrumentation	65
b) Sample preparation	67
2.2 Chemical reagents	69
2.3 Electrodes	69
2.3.1 Modification of the working electrode.	70
2.3.2 Reference electrodes	71

CHAPTER THREE

Results and discussion	75
3.1 Enhancement of lead redox characteristics and detection by clay modification of the working electrode.	75
3.1.1 Electrochemistry of Lead on a Carbon Graphite Electrode.	75
3.1.2. Redox Chemistry of Lead on a Bentonite Modified Electrode.	77
3.1.3 Electrode Modification with Pre-treated Bentonite	79
3.1.4 Electrochemical Analysis of Polyaniline Redox Properties on Pre-Treated Bentonite Host-matrix	84
3.2 Lead (II) and polyaniline electrochemistry on an ion-exchange resin modified electrode.	87
3.2.1 Electrochemistry of Lead on an Amberlite Modified Electrode	87
3.2.2 Electrode modification with pre-treated amberlite	94

3.2.3 Polyaniline Redox Features on a pre-treated Amberlite Modified Electrode	97
3.3 Polyaniline-copper redox chemistry on clay mineral(bentonite) host matrix.	100
3.3.1 Electrochemistry of Copper on a Bare Carbon Graphite Electrode	100
3.3.2 Electrochemistry of Copper on a bentonite Modified Electrode.	102
3.3.3 Electrode Modification with Pre-Treated Bentonite	105
3.3.4 Electrodeposition of Polyaniline on a Copper Loaded Bentonite Modified electrode.	109
3.4 Charge state trapping at a conducting polymer-redox ion exchanger interface - a bilayer electrode.	113
3.4.1 Electrochemical Behaviour of Copper on an Amberlite Modified Electrode	113
3.4.2 Electrode Modification using Pre-Treated Amberlite	115
3.4.3 Electrochemical Behaviour of Polyaniline on a Pre-Treated Amberlite Modified Electrode.	118
Conclusion	125
References	126

ABSTRACT

Polyaniline is one of the most widely studied conducting polymer. It's domain of application is however limited by the fact that it crystallises if large amounts of it are electrodeposited on a bare electrode surface. One method that has already been tried to overcome the problem is the use of an insulating host matrix for example Nafion. This method has however adversely reduced the rate of polymerization of the aniline monomers.

Also, bilayer electrodes so far known have been made from a combination of redox polymers. No bilayer electrodes have however been made from a combination of a redox and a conducting polymer. It is these areas that this research project seeked to address.

All electrochemical analysis were carried out using the cyclic voltammetric technique. A PAR model 173 Potentiostat/Galvanostat was used in conjunction with a model 175 Universal programmer. The output was fed into a PAR model RE-0089 X-Y recorder. A three electrode assembly was used in an undivided cell.

The results obtained showed that lead redox chemistry can be studied in sulphuric acid for cases where the lead has been exchanged in a clay mineral (bentonite) or a cation exchange resin (amberlite).

The redox peaks of polyaniline and lead been shown to be about 500 mV apart and thus independent of each other. The presence of lead in the host matrix was however observed to cause electrocatalyses in the deposition of polyaniline.

Experiments also revealed the versatility of bentonite and amberlite modified electrodes in the detection of very low concentrations of lead i.e., upto 10^{-5} M.

When copper was exchanged for the protons in amberlite, and the copper loaded amberlite used as a host matrix for electrodeposition of polyaniline, an interface whose electrochemical features are characteristic of bilayer electrodes was formed.

On the contrary, when a copper loaded bentonite was used as a host matrix, distinct copper and polyaniline redox peaks are observed (no features of bilayer electrodes). Nevertheless a remarkable improvement in the copper peak currents was observed.

LIST OF TABLES

Table 1.1 : Composition of Amboseli and Wyoming bentonite obtained from mineralogical and X-ray diffraction tests	18
Table 1.2: Oxides in Kriegers, parminters and Athi river bentonite	19
Table 2.1: Elemental composition of bentonite as determined by X-ray fluorescence	70
Table 2.2: Standard potentials for the various types of calomel electrodes	73
Table 3.1: Rate of change of i_{pa} and redox efficiency of polyaniline on various types of bentonite modified electrodes	86
Table 3.2: Peak current ratios at different scan rates for a bentonite modified electrode	104
Table 3.3: Maximum anodic peak current versus mass of B-NAC used in electrode modification	107
Table 3.4: Maximum anodic peak current versus mass of B-WAC used in electrode modification	108
Table 3.5: X-ray fluorescence measurements on various samples of bentonite	109
Table 3.6: Copper concentration in A-WAC and A-NAC as determined by X-RF analysis	118

LIST OF SCHEMES

Scheme I: A scheme illustrating the attachment of Tetra-(Amino phenyl) porphyrin (TAPP) on a thionyl chloride activated carbon electrode	8
Scheme II: Preparation of a strongly acidic cation exchange resin	23
Scheme III: Preparation of a weakly acidic cation exchange resin	24
Scheme IV: Polaron and bipolaron formation on reduction of parapolyphenylene	33
Scheme V: Formation of solitons in polyacetylene	34
Scheme VI: Oxidation products of polyaniline	37

LIST OF FIGURES

Fig. 1.2.1: Schematic illustration of the chemical functionalities on a carbon electrode	6
Fig. 1.2.2: A unit cell of the crystal of sodalite	16
Fig. 1.2.3: The general structure of montmorillonite clays	16

Fig. 1.2.4.: Conducting polymer rechargeable battery (Button cell, Bridgestone design)	40
Fig. 2.1: The general shape of a cyclic voltammogram	47
Fig. 2.2.: Block diagram of a differential amplifier (current follower)	51
Fig. 2.3: Block diagram of a voltage follower	53
Fig. 2.4: Block diagram of a control amplifier	54
Fig. 2.5: An adder potentiostat with a positive feedback compensation	56
Fig. 2.6.: A schematic representation of X-RF geometry	62
Fig. 2.7.: Block diagram of the electronic set-up of a X-RF unit	66
Fig. 2.8.: A commercial calomel electrode	74
Fig. 3.1.1: CV for bare carbon graphite electrode in a solution containing 0.001 M $\text{Pb}(\text{NO}_3)_2$ and 0.1 M KNO_3 . Potential range -0.8 V to 0.4 V. Scan rate 20 mV/sec.	76
Fig. 3.1.2: A plot of anodic peak current versus square root of scan rate for a bare carbon electrode in a solution containing 0.001 M $\text{Pb}(\text{NO}_3)_2$ and 0.1 M KNO_3 . Potential range -0.8 V to 0.4 V.	77

Fig. 3.1.3: CVs for a bentonite modified electrode
in a solution containing 0.1 M $\text{Pb}(\text{NO}_3)_2$
and 0.1 M KNO_3 . Potential range -0.8 V to
0.4 V. Scan rate 50 mV/sec. 76

Fig. 3.1.4: CVs for a bentonite modified electrode
in a solution containing 1 M HCl
(full lines) after transfer from a
solution containing 1 mM $\text{Pb}(\text{NO}_3)_2$ and
0.1 M KNO_3 (dashed line). Potential
range -0.8 V to 0.4 V. Scan rate
20 mV/sec. 80

Fig. 3.1.5: CVs for a B-NPN modified electrode
in a solution containing 0.1 M KNO_3 .
Potential range -0.8 V to 0.8 V. Scan
rate 20 mV/sec. 81

Fig. 3.1.6: CVs for a B-NPN modified electrode in a
solution containing 1.0 M H_2SO_4 . Potential
range -0.8 V to 0.8 V. Scan rate 20 mV/sec. 81

Fig. 3.1.7: CVs a B-WPN modified electrode in a
solution containing 0.1 M KNO_3 .
Potential range -0.8 V to 0.8 V.
Scan rate 20 mV/sec. 83

Fig. 3.1.8: CVs for a B-WPN modified electrode in a solution containing 1.0 M H ₂ SO ₄ . Potential range -0.8 V to 0.80 V. Scan rate 20 mV/sec.	83
Fig. 3.1.9: CVs for a B-NPN modified electrode in a solution containing 1.0 M H ₂ SO ₄ and 0.1 M aniline. Potential range -0.8 V to 0.8 V. Scan rate 20 mV/sec.	85
Fig. 3.1.10 CVs for a B-WPN modified electrode in a solution containing 1 M H ₂ SO ₄ and 0.1 M aniline. Potential range -0.8 V to 0.8 V. Scan rate 20 mV/sec.	85
Fig. 3.2.1: CVs for an amberlite modified electrode in a solution containing 0.1 M Pb(NO ₃) ₂ and 0.1 M KNO ₃ . Potential range -0.8 V to 0.4 V. Scan rate 20 mV/sec.	88
Fig. 3.2.2: A plot of anodic peak current versus time for an amberlite modified electrode in a solution containing 0.1 M Pb(NO ₃) ₂ and 0.1 M KNO ₃ . Potential range -0.8 V to 0.4 V. Scan rate 20 mV/sec.	89

Fig. 3.2.3: CVs for an amberlite modified electrode
on transfer into a solution containing
1.0 M H₂SO₄ (full lines) from a solution
containing 0.1 M PbNO₃ and 0.1 M KNO₃
(dashed line). Potential range -0.8 V to
0.4 V. Scan rate 20 mV/sec 91

Fig. 3.2.4: A plot of anodic peak current versus
time for an amberlite modified electrode
(after incorporation of lead (II) from
solution) after being transferred in a
solution containing 1.0 M H₂SO₄. 92

Fig. 3.2.5: CVs on transfer of an amberlite
modified electrode (after incorporation
of Lead (II) from solution) into a solution
containing 0.1 M KNO₃. Potential range
-0.8 V to 0.4 V. Scan rate 20 mV/sec. 93

Fig. 3.2.6: CVs for an amberlite modified electrode
on transfer into a solution containing
1.0 M HCl (full lines) from a solution
containing of 10⁻⁵ Pb(NO₃)₂ and 0.1 M KNO₃
(dashed line). Potential range -0.8 V to
0.4 V. Scan rate 20 mV/sec. 93

Fig. 3.2.7: CVs for a A-WPN modified electrode
in a solution containing 1.0 M H₂SO₄.
Potential range -0.8 V to 0.8 V. Scan
rate 20 mV/sec. 95

Fig. 3.2.8: CV for a A-NPN modified electrode in a solution containing 1.0 M H ₂ SO ₄ . Potential range -0.8 V to 0.8 V. Scan rate 20 mV/sec.	95
Fig. 3.2.9: A plot of anodic peak current versus square root of scan rate for a A-NPN modified electrode in a solution containing 1.0 M H ₂ SO ₄ . Potential range -0.8 V to 0.8 V.	96
Fig. 3.2.10 CVs a A-NPN modified electrode in a solution containing 1.0 M H ₂ SO ₄ and 0.1 M aniline. Potential range -0.8 V to 0.8 V. Scan rate 20 mV/sec.	98
Fig. 3.2.11 CVs for an amberlite modified electrode (after incorporation of lead (II) from solution) in a solution containing 1.0 M H ₂ SO ₄ and 0.1 M aniline. Potential range -0.8 V to 0.8 V. Scan rate 20 mV/sec.	98
Fig. 3.3.1: CVs on a bare carbon electrode in a solution containing 0.1 M H ₂ SO ₄ and 0.01 M CuSO ₄ . Potential range -0.3 V to 0.6 V. Scan rate of 20 mV/sec.	101

Fig. 3.3.2: The CVs for a bentonite modified electrode in a solution containing 0.1 M H ₂ SO ₄ and 0.01 M CuSO ₄ . Potential range -0.3 V to 0.6 V. Scan rate 20 mV/sec.	101
Fig. 3.3.3: A plot of the cathodic versus anodic peak current used in calculating the redox efficiency for copper redox process on a bentonite modified electrode.	102
Fig. 3.3.4: A plot of anodic peak current versus square root of scan rate for a bentonite modified electrode in a solution containing 0.1 M H ₂ SO ₄ and 0.01 M CuSO ₄ . Potential range -0.3 V to 0.6 V.	103
Fig. 3.3.5: CVs for a B-WAC modified electrode in a solution containing 1.0 M H ₂ SO ₄ . Potential range -0.3 V to 0.8 V. Scan rate 20 mV/sec.	106
Fig. 3.3.6: CVs for a B-NAC modified electrode in a solution containing 1 M H ₂ SO ₄ . Potential range -0.3 V to 0.8 V. Scan rate 20 mV/sec.	106
Fig. 3.3.7: CVs for a B-WAC modified electrode in a solution containing 0.1 M aniline and 1.0 M H ₂ SO ₄ . Potential range -0.3 V to 0.85 V. Scan rate 20 mV/sec.	111

Fig. 3.3.8: CVs for a B-NAC modified electrode in a solution containing 0.1 M aniline and 1.0 M H ₂ SO ₄ . Potential range -0.3 V to 0.85 V. Scan rate 20 mV/sec.	111
Fig. 3.3.9: CV depicting only the polyaniline redox peaks. The solution contains 0.1 M aniline and 1.0 M H ₂ SO ₄ . Potential range -0.3 V to 0.85 V. Scan rate 20 mV/sec.	112
Fig. 3.3.10 Scan rate studies on B-NAC modified electrode after the merging of copper and polyaniline oxidation peaks in a solution containing 1 M H ₂ SO ₄ . Potential range -0.3 V to 0.6 V.. . . .	112
Fig. 3.4.1: CVs for an amberlite modified electrode in a solution containing 0.1 M H ₂ SO ₄ and 0.01 M CuSO ₄ . Potential range -0.3 V to 0.6 V. Scan rate 20 mV/sec	114
Fig. 3.4.2: A plot of oxidation peak current versus time for an amberlite modified electrode in a solution containing 0.1 M H ₂ SO ₄ and 0.01 M CuSO ₄ . Potential range -0.3 V to 0.6 V. Scan rate 20 mV/sec.	115

Fig. 3.4.3: A plot of maximum anodic peak current versus amount of A-WAC used in the electrode modification on dipping the electrode in 1 M H ₂ SO ₄ . Potential range -0.3 V to 0.8 V. Scan rate 20 mV/sec.	116
Fig. 3.4.4: CVs on transferring a copper loaded amberlite (by simultaneous exchange) into a solution containing 1 M H ₂ SO ₄ and 0.1 M aniline. Potential range -0.3 V to 0.8 V. Scan rate 20 mV/sec.	120
Fig. 3.4.5: CVs for A-WAC modified electrode in a solution containing 1 M H ₂ SO ₄ and 0.1 M aniline. Potential range -0.3 V to 0.8 V. Scan rate 20 mV/sec.	121
Fig. 3.4.6: CVs obtained after the merging of the copper and polyaniline oxidation peaks for A-WAC modified electrode.	121

CHAPTER ONE

1.0 INTRODUCTION

The alteration of an electrode's chemical, physical, optical and electrochemical characteristics is called electrode modification. Various methods to achieve this have been developed and they depend on the physical and chemical properties of both the material to be used for the purpose of modification and the electrode surface.

The most commonly modified electrodes are those of metal oxides and carbon. These are favoured because of the functional groups on their surfaces. The materials used for modification include ion exchangers, redox polymers, conducting polymers and compounds that can be attached to the electrode surface by silanization.

Modified electrodes have found use as reference electrodes, sensory devices, pre-concentrators of ions and molecules from dilute solutions, ion selective electrodes and as electrodes in rechargeable batteries. These electrodes have a lot of potential in the industrial world, and its for this reason that many researchers especially from the fields of electrochemistry, material science, electrical engineering and physics have shifted their attention towards them.

Currently, modification of electrodes with a combination of two or more materials has proved to be more interesting and opens up new domains/areas which these electrodes may be used. Such modifications usually involve co-polymers, composites or bilayers, an example being the combination of redox polymers and conducting polymers.

1.1 LITERATURE REVIEW

1.1.1 ELECTRODE MODIFICATION

Surface derivatization, also known as electrostatic trapping or polymer coating, involves the deliberate immobilization of materials on the electrode surface. The electrode thereafter displays the chemical, electrochemical and optical properties of that material. These materials are selected on the basis of their known and desired properties. For example, chiral centres, electron transfer mediation catalysis, ability to inhibit corrosion e.t.c. [1].

The main methods used for the purpose of attachment or immobilization of these materials on the electrode surface depend on:-

1) Chemisorptive abilities of some chemical functionalities to which a redox functionality may be linked [2]. This leads to irreversible or strong adsorption of electroactive materials on the electrode surface. Hubbard and Lane [3,4] for example took advantage of these forces to chemisorb quinone bearing olefins on platinum electrodes.

2) Formation of covalent bonds between the material and the electrode surface or on an already chemisorbed material. In the 1970s when the study of electrode modification became important, this method became very popular as it could be used to attach optically active molecules on electrodes [5], electroactive species on metal oxide surfaces [1,2] and also the attachment of catalytically active groups on carbon electrodes [6].

3) Electrodeposition of a conducting polymer on the electrode surface. In this method, the resulting film is held on the electrode surface by a combination of chemisorption forces and low solubility in the electrolytic media. This method of film formation has proved to be more superior and it's currently the most widely used method for the purpose of electrode modification using conducting polymers [7-10].

The choice of a particular method to be used in the modification process depends not only on the properties of the material, but also on those of the electrode. The metal oxide surfaces are most preferred due to their ability to form covalent bonds with most compounds [2,11,12]. The carbon electrodes on the other hand rely heavily on their chemisorptive abilities present in the basal plane and covalent bonds formation abilities present in the edge plane [13-15].

a) DERIVATIZATION OF METAL OXIDE ELECTRODES.

A number of metal oxides have been identified as useful electrodes. For example, tin oxide (SnO_2) films on glass or titanium have been shown to contain many $-\text{SnOH}$ sites [16-17], which are quite reactive towards chlorosilanes and alkoxy silanes. If the SnO_2 electrode comes into contact with a solution containing dichlorodimethyl silane, $\text{Cl}_2\text{Si}(\text{CH}_3)_2$ under anhydrous conditions for example, the organosilane becomes immobilized by the formation of $-\text{SnOSi}-$ bonds [1,2,21].

This procedure is called silanization and is the most commonly used procedure for attachment of materials to metal oxide surfaces. Other metal oxides that can be

derivatized using this procedure include RuO₂, Pt/PtO, Au/AuO, TiO₂ Ge/GeO and Si/SiO [1,2,11,19-21]. The M/MO (for M = Pt, Au, Ge and Si) refer to bulk metals or semiconductors treated in a manner calculated to introduce a few monolayers of surface oxides - with the associated hydroxyl groups to enable reaction with the organosilanes.

Organosilanes like (CH₃O)₃Si(CH₂)₃NH(CH₂)₂NH₂Si (ensilane), (CH₃CH₂O)₃Si(CH₂)₃NH₂ (prNH₂ silane) e.t.c have been successfully immobilized on these electrodes [1].

The most important organosilanes however, are those that contain secondary reactive coupling functionalities. The secondary groups may then be used for further electrode modification. For example, the -N- group on ensilane modified electrode may be treated with an acid chloride to form amides on the electrode surface [21].

Other methods used for derivatization of these electrodes are based on ester bond linkages [18], cyanuric chloride [16] and the use of basic chromium complexes. Surface ester formation for example has been proposed to explain the fairly stable attachment of Rhodamine B on SnO₂ surfaces, which occurs without the assistance of organosilanes [1]. Surface esterification has also been used to attach anthracene derivatives onto tin oxide electrodes [16].

b) DERIVATIZATION OF CARBON ELECTRODES.

The derivatization of carbon graphite or glassy carbon electrodes is best understood when we critically examine the properties of their surface. Carbon graphite

has been shown to consist of giant sheets of fused aromatic rings which are stacked coplanarly as shown in Fig. 1.2.1.

The basal plane surface is non ionic, has low polarity, is hydrophobic and rich in π -electrons. It is thus barren to synthetic coupling reactions. The high π -electron density however is conducive to strong chemisorptive interactions especially with unsaturated compounds, including those of aromatic origin [13,22].

The edge plane on the other hand consists of groups such as phenolic, quinone, carboxylic, lactone and ketones. These have a high affinity for oxygen and water and as such, the edge plane is important in chemical coupling and modification of the electrode [13,14,23]. The absolute populations and relative reactivities of these groups are still not yet known. Their concentrations are however known to be very low especially on glassy carbon electrodes [1,13].

The pyrolytic graphite is a highly imperfect approximation to single crystal graphite with a basal plane while the glassy carbon is described as a random tangle of graphite strips, so that any given exposed surface exhibits a mixture of basal and edge plane characteristics [1]. The extent to which each of these planes are exposed depends on the pretreatment procedures which may be thermal or physical. For example, polishing of the basal plane in pyrolytic graphite exposes the edge plane sites. Conversely, polished edge plane surfaces displays some basal plane characteristics. This then leads to varying densities of modification materials on the electrode surface [13].

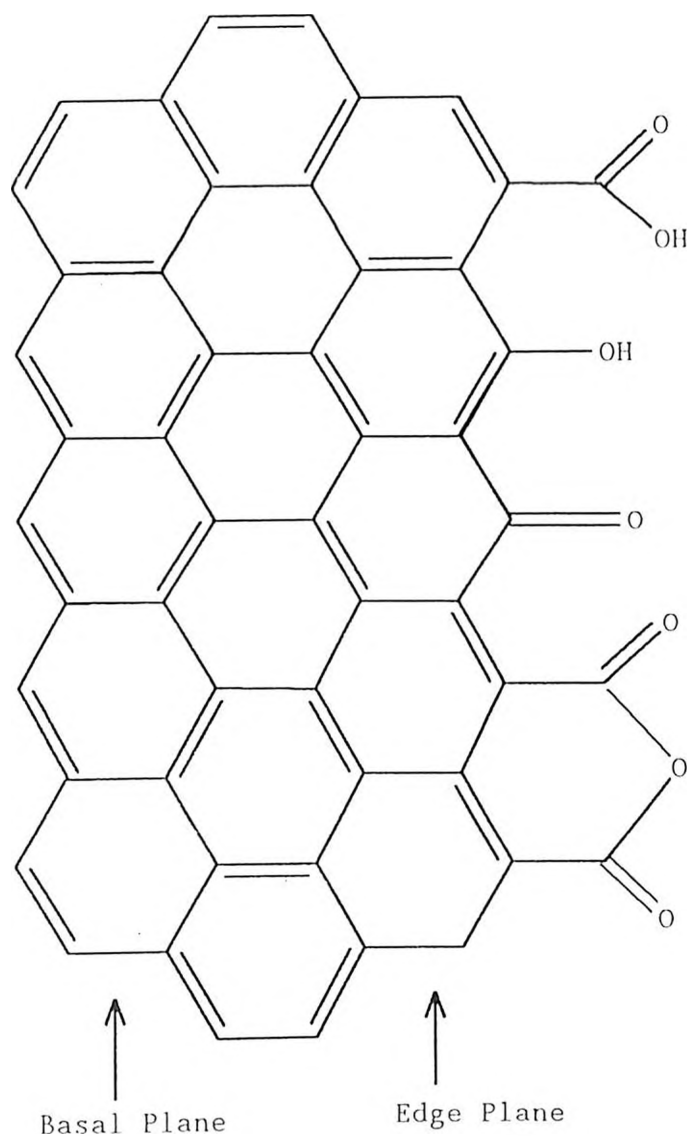
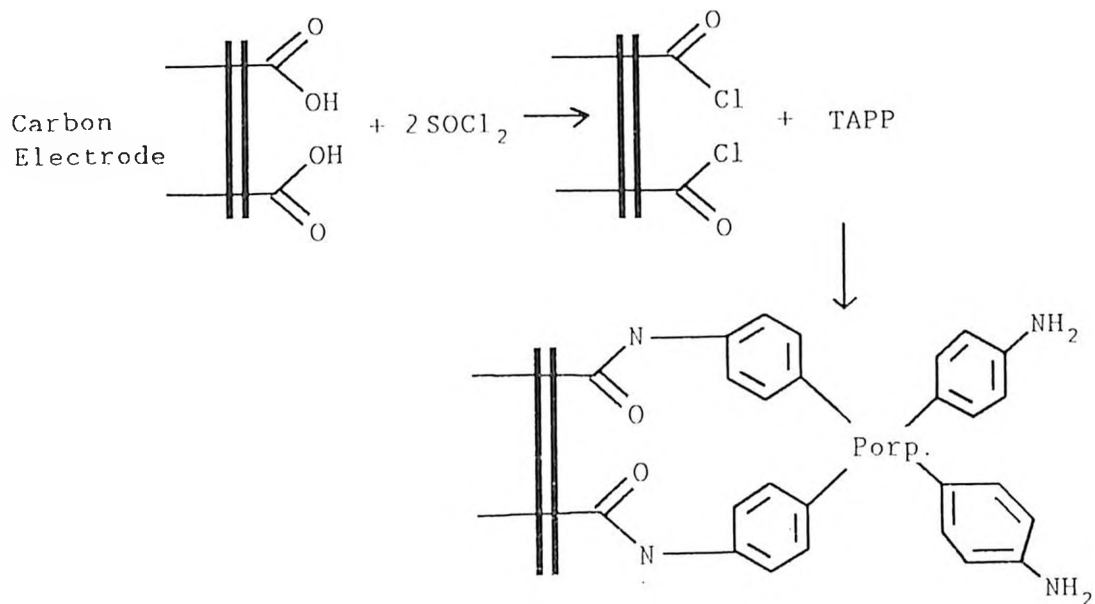


Fig. 1.2.1: Schematic illustration of the chemical functionalities on a carbon electrode [1].

To enhance the synthetic usefulness of the groups on the edge plane, the activation of the carbon surface is at times necessary. The -COOH group for example is activated by heating the electrode in air to 400°C - 500°C [14,23], while the -OH group has been shown to be activated by initial oxidation of all the groups on the surface using O₂ RF plasma followed by reduction with LiAlH₄ [1].

The introduction of various chemical groups on a carbon electrode via -COOH may be achieved by reacting a suitable reagent with a thionyl chloride activated and thermally oxidized carbon electrode. For example, the addition of the amine S(-)phenylalanine methylester has been reported to enable the immobilization of not only an amide, but also a chiral centre on the electrode surface [5,24]. Tetra-(aminophenyl)porphyrin, an electroactive redox substance, has also been successfully attached on a thionyl chloride activated carbon electrode after thermal treatment (see Scheme 1) [25]. A transition metal impregnated in the porphyrin before [23,68] or after [25] the immobilization has also been shown to yield a series of porphyrin donor sites for electron transfer mediation on reduction. For example, cobalt metallated porphyrin has been reported to be effective as an electrocatalyst in the reduction of 1,2-dibromo-1-phenylethane [1].

As with metal oxide electrodes, carbon electrodes may also be derivatized via the -OH groups using organosilanes [24] and cyanuric chloride. These in turn provides an avenue for further electrode modification. For example, hydroxy-methylferrocene, O-tolidine and methylaminopropyl- viologen have been successfully attached on carbon electrode surfaces via the -OH groups by use of cyanuric chloride [1,26].



Scheme I: A scheme illustrating the attachment of tetra-(Amino phenyl) porphyrin(TAPP) on a thionyl chloride activated carbon electrode.

1.1.2 DERIVATIZATION OF ELECTRODE SURFACES BY FILM FORMATION

Unlike the materials used for electrode modification discussed so far, where the main forces between the electrode and the material were covalent bonds and chemisorption, modification of electrode surface with organic polymers and some inorganic equivalents is done by attachment of films formed from these materials.

The main advantage of this method over the others is that we are able to obtain films with a thickness ranging from 1 to 20,000 monolayers [1,27]. The modification processes relying on covalent bond formation or chemisorption properties only, hardly exceed a monolayer (where a monolayer refers to 1.5×10^{-10} mol/cm² of surface coverage depending on the size of molecules used for modification). The low solubilities combined with chemisorption, covalent bonding and adsorption of films allows the formation of very thick polymer films.

The most popular procedures used for electrode derivatization with films include:

1) Dip coating:- a process that involves dipping of the electrode in a dilute solution of the polymer for sometime and then allowing the electrode time to dry. This method relies on adsorptive properties of these polymers on the electrode surface. If the polymer does not contain redox sites, these may then be introduced by amide [7] or metal couple formation [26].

2) Droplet evaporation:- this method involves the application of micro-syringe quantities onto the electrode surface [27]. Like dip coating, this method leads to formation of non-homogenous films. It may however be improved by spinning the

applied polymer solution by placing the electrode at the centre of a rapidly rotating disk [1,27].

3) Oxidative or reductive polymerization:- the solubility of most polymers depends on their ionic forms. As such, by oxidizing or reducing a polymer to its most insoluble form (most adsorbable), the polymer may be deposited (precipitated) on the electrode surface. For example, polyvinylferrocene films may be deposited from dichloromethane solutions by electrochemical or photochemical oxidation of the polymer to its most insoluble form [27].

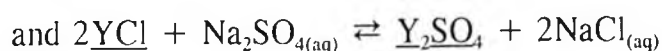
4) Electrochemical polymerization:- monomers in solution may be oxidized or reduced to intermediates which polymerize sufficiently rapidly on the electrode surface, forming a polymer film on the electrode [9,10,28,29]. To electrodeposit films of significant thickness, it's necessary that the polymer be redox active (so as to electrocatalytically oxidize or reduce fresh monomers) or be permeable to fresh monomers, otherwise, electrode passivation occurs and further polymerization is halted [1]. This is the most widely used procedure for modification of electrodes with conducting polymers such as polyaniline [29-31].

The most widely used materials for electrode modification, as films, are ion exchangers, redox polymers and conducting polymers. These materials are however of very different origins and display very different chemical and physical properties.

a) ION EXCHANGERS

Ion exchangers by definition, are insoluble solid materials which carry exchangeable ions. These ions can be exchanged for a stoichiometrically equivalent amounts of other ions of the same charge sign when the exchanger is in contact with an electrolyte solution. Carriers of exchangeable cations are called cationic exchangers while those that carry exchangeable anions are called anionic exchangers. Certain materials are capable of both cation and anion exchange and are referred to as amphoteric exchangers [32].

For the cationic or anionic exchangers $\underline{\text{NaX}}$ and $\underline{\text{YCl}}$ when in contact with the electrolyte solutions CaCl_2 and Na_2SO_4 respectively, the following reactions take place;



where X and Y represent a structural unit of the exchanger; solid phases are underlined and (aq) indicates that the electrolyte is in aqueous media.

In the above examples, the Na^+ and Cl^- ions act as the exchangeable cation and anion and are exchanged for Ca^{2+} and SO_4^{2-} respectively.

For more than a century now, ion exchangers have been used to an increasingly great extent both in the laboratory and in plant operations. Nature makes extensive use of them and has done so long before man attempted to elucidate, apply it's principles, copy and surpass its performance. Ion exchange occurs in inanimate soils, sands, rocks and in living organisms.

The materials responsible for ion exchange in soils have been identified as clays, glauconites, zeolites and humic acids [32]. Efforts to synthesize products with ion exchange abilities were met with success when in 1903, Harm and RÜmpler [33] prepared the first synthetic industrial ion exchanger. A spectacular evolution however began in 1935 when it was discovered that crushed phonograph records exhibit ion exchange properties. This directly led to the syntheses of organic ion exchange resins in the 1950s. These were found to have better properties than any of the previous products.

Currently, nearly all industrial and laboratory applications of ion exchange are based on such resins. These are used in such areas as recovery of metals from industrial wastes, separation of rare metals, catalysis of organic reactions and as ion exchange membranes [32,34].

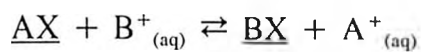
(i) Operation of ion exchangers.

Ion exchangers consist of a framework which is held together by chemical bonds or lattice energy. These frameworks carry excess positive or negative charges which are compensated for by ions of opposite charge, the so called counter ions. The counter ions are free to move within the framework and may be replaced by ions of the same charge sign. The framework of a cation exchange may be considered as a macromolecular or crystalline polyanion, while that of an anion exchanger as a polycation [32].

Ion exchange is, with very few exceptions, a reversible process [35]. The extent to which the exchange process proceeds to is determined by the equilibrium constant whose definition is given in equation 1.1;

$$K_B^A = \frac{[A^+]}{[B^+]} \dots \dots \dots Equ. 1.1$$

for the exchange process



This value is not constant but varies with experimental conditions. For example, the use of an exchange column yields higher values than those obtained from just soaking the exchanger in an electrolyte solution. The other factor that also determines its value is the selectivity of the exchanger for that particular ion. The most important factors that determine selectivity of an exchanger include:-

1) Electrostatic interactions between the charged framework of the exchanger and the counter ion. Ions with a high charge density are preferred due to the resulting strong electrostatic interaction.

2) Permeability of counter ions into the framework. In cases where the pore size or interlayer distance (channels) of the framework are small, large ions may be excluded other factors not withstanding. As such, small counter ions with less hinderance are preferred.

3) Special interactions between the framework or fixed ionic sites with the counter ion, such as chelation effects, may significantly affect the value of the equilibrium constant.

Besides the exchange of ions, an ion exchanger will always take up solvents and solution molecules which can fit within the channels of the framework ones it comes into contact with an electrolyte solution. This process is referred to as sorption and has a very significant role in the exchange process [36,37]. For example, sorption of solvent results to swelling of the framework (increasing the size of the channels) and as such large cations become more exchangeable. The sorption of electrolyte solution on the other hand leads to a higher concentration of the counter ions within the framework, thus affecting the value of the equilibrium constant.

The exchange properties of an exchanger are basically determined by the pore size, location of mobile ions and the general structure of the framework.

(ii) Structure of ion exchangers

a) Mineral ion exchangers

Most naturally occurring aluminosilicates such as zeolites, clays and glauconites have cationic exchange properties. All these materials have a crystalline structure with channels and interconnecting cavities within the lattice. Counter ions reside within these cavities and may be replaced by any other cations which for one reason or the other are more preferred by the framework and are able to permeate through the cavities [34-40].

Zeolites are formed from silica by substitution of some silicon atoms with aluminium atoms. This replacement leads to excess negative charge (as aluminium is trivalent while silicon is tetravalent) which is usually neutralized by alkali or alkali earth metals counter ions. They have the general composition represented by $M_{x/n}\{(AlO_x)(SiO_y)\}_n \cdot ZH_2O$ where n is the charge on cation M usually Na^+ , K^+ or Ca^+ and Z is the number of moles of water of hydration, which is highly variable [38]. Typical examples include, $Ca_6Al_{12}Si_{24}O_{72} \cdot 40H_2O$ (chabazite), $(Na_2Ca)_4Al_8Si_{16}O_{48} \cdot 24H_2O$, $Na_2Si_3Al_2O_{10} \cdot 2H_2O$ (natrolite) and $(K_2, Ba)Si_5Al_2O_{14} \cdot 5H_2O$ (harmotome) [32,38]. The lattice structure of a typical zeolite, sodalite, is shown in Fig. 1.2.2.

The structure consists of SiO_4 and AlO_4 tetrahedrals which share their oxygen atoms. The presence of counter ions within the cavities make zeolites useful as ion exchangers. It's however worth noting that the size of the cavities, usually ranging from 4 - 10 Å, changes insignificantly on sorption of solvents. This then implies that zeolites will not absorb all those molecules or ions which are too big to enter the cavities. Also, the fact that these pores are very uniform makes the zeolites absorb only weakly those small molecules or ions which can enter but also leave easily. This "sieving action" at a molecular level makes them very useful in laboratories and industries as molecular sieves [32,38,42,43].

Unlike the zeolites, montmorillonites and beidellite clays have a loose structure. They carry their counter ions within the layers and can swell in one dimension by increasing the interlayer distance. This leads to the fact that they have

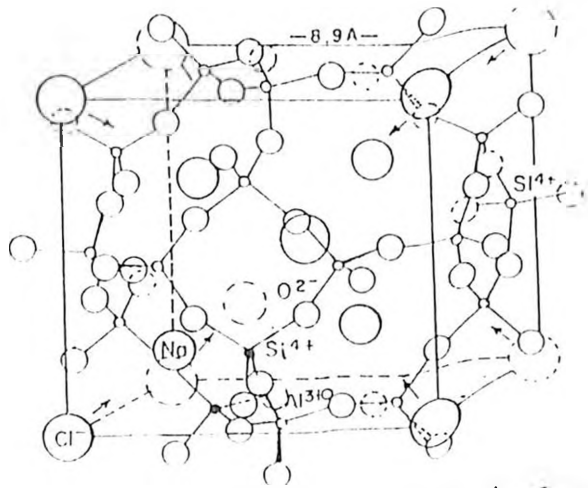


Fig 1.2.2: A unit cell of the crystal of sodalite $\text{Na}_4(\text{Si}_3\text{Al}_3\text{ClO}_{12})$. The arrows indicate channels which connect the cavities in the aluminosilicate framework (32).

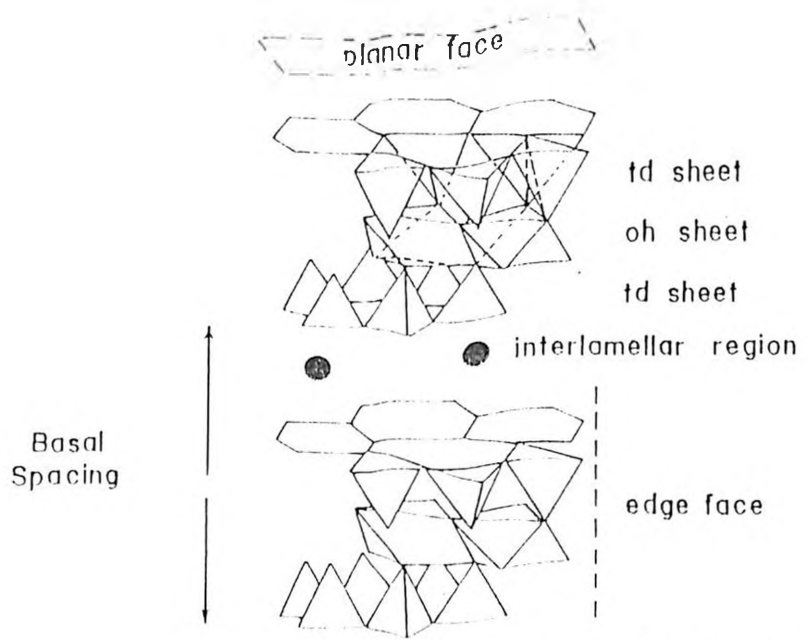


Fig 1.2.3: The general structure of montmorillonite clays

a high exchange capacity especially for large cations. The montmorillonites and beidellite clays have an approximate composition represented by $Al_2\{Si_4O_{10}(OH)_2\}.nH_2O$ and $Al_2\{(OH)_2AlSi_3O_9OH\}.4H_2O$ respectively [36-41]. The general structure of montmorillonites is shown in Fig. 1.2.3.

The structure is characterized by a layered structure where a layer of hydrated cations separate two dimensional oxyanions. The oxyanion layers are made up of two inverted silicate tetrahedral and octahedral sheets which share their apical oxygen. There is a 2:1 relationship between the tetrahedral and the octahedral sheets and as such, smectite clays are normally christened 2:1 phyllosilicates [41].

In most naturally occurring clays, we find alkali earth metals like Ca^{2+} intercalated within the layers. However, alkali metals like K^+ are also at times found to have been intercalated within the layers [40,41].

In kenya, we find bentonite (Ca-montmorillonite) at Amboseli, Athi river and in Nanyuki. Mineralogical and X-ray diffraction tests done on samples of Amboseli clays (see Table 1.1) showed [44] that these clays mainly contain seplotite. The swelling index was found to be 32, a very low value compared to that of Wyoming bentonites (U.S.A) of about 150.

At Athi river, Ca-montmorillonite is found as a grey-green clay at shallow beds as a matrix to gypsum modules in areas held by East Africa Portland Cement Company Ltd. This clay is usually converted into Na-montmorillonite by addition of soda ash before use [41,44].

Table 1.1: Composition of Amboseli and Wyoming bentonite obtained from mineralogical and X-ray diffraction tests.

OXIDE	% composition			
	1	2	3	4
SiO ₂	45.70	42.02	41.32	57.98
CaO	9.70	5.62	6.25	1.92
MgO	5.52	10.12	10.57	3.24
Na ₂ O + K ₂ O	3.96	6.84	6.42	1.35

Samples 1-3, Amboseli clays, Sample 4 Wyoming bentonite.

Kriegers and parminters deposits are found in Nanyuki. The former is underlain by a layer of brown-grey earth with yellowish mottling which does not swell appreciably in water. The latter is an unstratified greenish-grey and chocolate coloured clay which feels soapy in the hands.

The oxides in Kriegers, parminters and Athi river bentonites as obtained from mineralogical and X-ray diffraction are shown in Table 1.2 [44].

Glauconites are ferrous aluminosilicates containing exchangeable potassium. Their crystal lattice is rather dense and rigid, so that cation exchange can only occur at the crystal surfaces. They have nevertheless been shown to have a considerable capacity in the colloidal form [39,40].

Only a few aluminosilicates have been shown to act as anion exchangers. For example, the exchange of OH⁻ for Cl⁻, SO₄²⁻ and PO₄³⁻ has been observed in montmorillonites, kaolinite and feldspars belonging to the sodalite and cancrinite groups. However, only apatite {Ca₅(PO₄)₃}F and hydroxylapatite {Ca₅(PO₄)₃}OH [45] have been used as anion exchangers for any practical purposes.

Table 1.2: Oxides in Kriegers, Parminters and Athi river bentonite

Oxides	% composition			
	1	2	3	4
SiO ₂	51.66	46.24	43.93	52.97
Al ₂ O ₃	14.97	17.00	14.77	14.27
Fe ₂ O ₃		12.08	13.80	9.81
FeO	7.49	0.28	0.25	0.43
MgO	2.01	2.11	2.65	3.69
MnO	0.04	0.04	0.03	0.04
CaO	1.58	1.58	2.48	0.95
Na ₂ O	1.81	0.99	0.78	0.52
K ₂ O	1.98	1.31	1.77	4.28
TiO ₂	0.64	2.19	2.31	0.45
CO ₂	0.40		0.51	
H ₂ O ⁺	5.71	0.05	7.72	6.51
H ₂ O ⁻	11.88	7.75	8.47	5.50
P ₂ O ₅	0.06	0.27	0.57	0.03
Total %	97.23	99.94	100.02	99.95

Samples 1&2 Kriegers, Sample 3 Parminters and Sample 4 Athi river bentonite.

b) synthetic inorganic ion exchangers.

The first commercially available synthetic inorganic ion exchangers were called "fusion permutits". These compounds were made by fusion of a mixture of soda, potash, feldspar, kaolin and other similar compounds [32]. These were very much like the natural zeolites and the only difference was that their structure was irregular.

These were latter replaced by the "gel permutits" which were prepared by precipitation of aluminium sulphate and silicon silicate by use of caustic. The precipitates were then dried to a gelatinous form [32,34]. The chemical composition

of these compounds was similar to those of zeolites but they had an irregular structure. The above two types of "permutits" have however ceased to be in use since the discovery of better synthesis methods.

The crystallization of solutions containing silica, alumina and alkali at an elevated temperature has been shown to yield products that are exact counterparts of the natural zeolites [35,42,43,46]. This method is called hydrothermal preparation. These products have been shown to be very useful as highly specific sorbents and "molecular sieves" due to their narrow, rigid and uniform pore structure [43]. They are however of very little importance as ion exchangers.

Attempts to synthesize inorganic cation exchangers with other frameworks other than aluminosilicates have been made. This was done by replacing partly or completely the silicon with other tetravalent elements like titanium, tin and the aluminium with other trivalent elements like iron, manganese, vanadium e.t.c. These products were however found to be of poor qualities [45].

From the fact that most hydrous oxide gels like Fe_2O_3 , Al_2O_3 , Cr_2O_3 e.t.c. are amphoteric and can act as ion exchangers at pH values above their isoelectric points, synthetic cation exchangers with more satisfactory properties can now be made. These products are extremely insoluble and their chemical composition depends on the conditions under which they are prepared. They however tend to lose their fixed ionic groups on hydrolysis in solutions of high pH [1].

A few synthetic inorganic anion exchangers have been made. For example, gelatinous precipitates of aluminium and iron oxides have been shown to have anionic exchange properties.

c) Organic ion exchange resin.

This group of exchangers consist of the most widely used materials for the purpose of ion exchange. Their frameworks, the so called matrix, consists of an irregular macromolecular 3-dimensional network of hydrocarbon chains. The members of this class are all synthetic and contain fixed ionic groups like; $-\text{SO}_3^-$, $-\text{COO}^-$, $-\text{PO}_3^{2-}$ and $-\text{AsO}_3^{2-}$ for cation exchangers and $-\text{NH}_3^+$, $-\text{NH}_2^+$, $-\text{N}^+$ and $-\text{S}^+$ for anion exchangers.

The thermal, mechanical and ion exchange properties mostly depend on the structure, degree of crosslinking, nature and number of fixed ionic groups. Highly crosslinked materials are very compact, have small mesh width and low swelling abilities. This restricts the movement of counter ions within the framework leading to low electrical conductivity of the resin [32,48,49]. They are however very resistant to mechanical breakdown.

The number of fixed ionic groups in the matrix determines the maximum exchange capacity while the chemical nature of these groups determine such characteristics as selectivity and apparent capacity (exchangeable ions under a given experimental conditions). These groups are categorized as strongly acidic or basic and weakly acidic or basic.

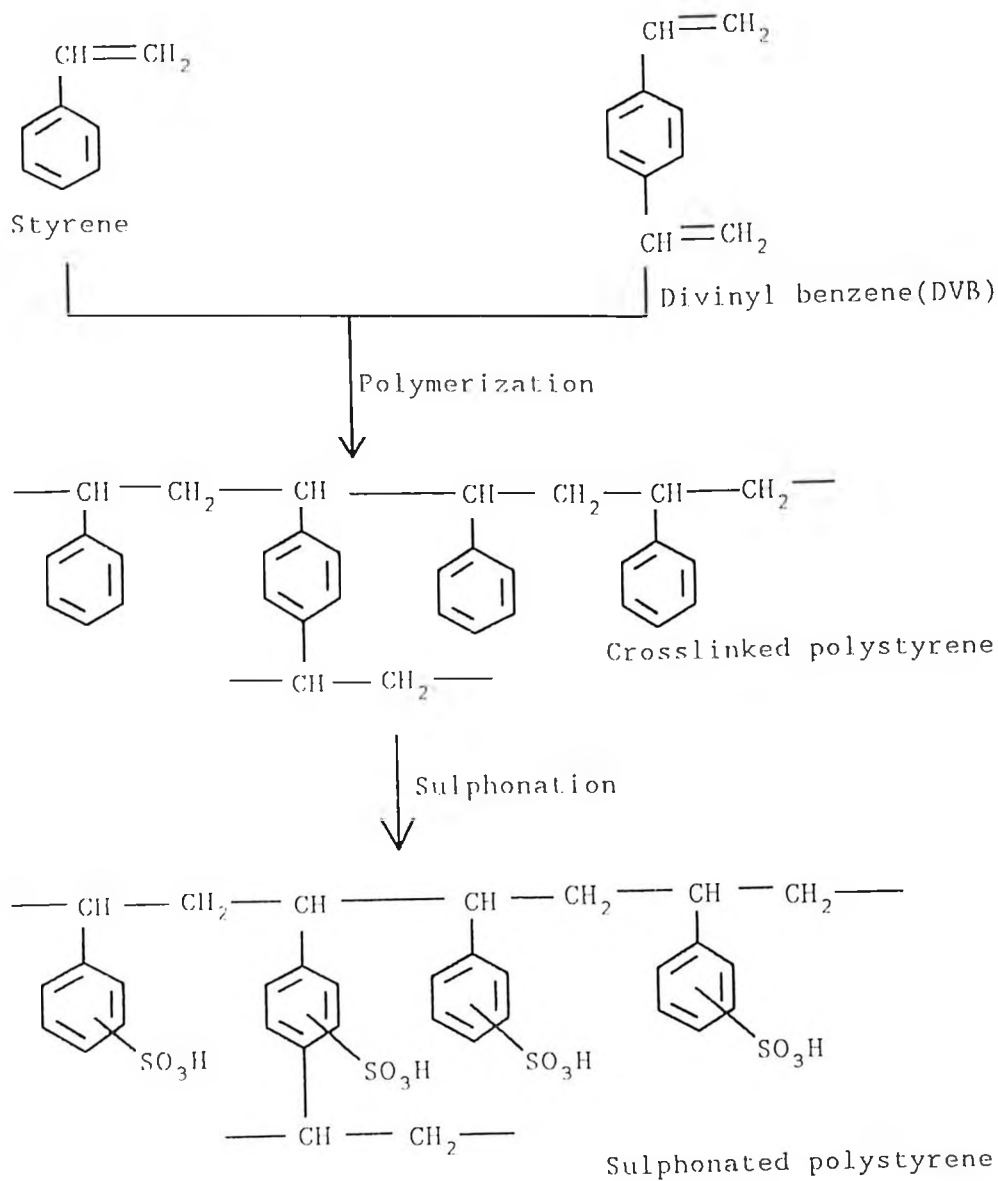
Strongly acidic/basic groups are able to dissociate fully in almost all solutions irrespective of the solution's pH. The weakly acidic groups e.g. $-\text{COO}^-$ are only ionizable in solutions of high pH. They exist in the undissociated form, as $-\text{COOH}$, in solutions of low pH. Similarly, weakly basic resins with groups like $-\text{NH}_3^+$ lose a proton to form uncharged $-\text{NH}_2$ in solutions of high pH. The salt form of these resins tend to hydrolyse in the same manner as the basic/acidic forms of these resins.

During the synthesis of these materials, organic molecules are polymerized in such a way that a crosslinked

3-dimensional network matrix is formed. The ionic groups if not incorporated before the polymerization process may be introduced after this process. Crosslinking here is very important as it ensures that the matrix is insoluble in most solvents besides those that react with the exchanger.

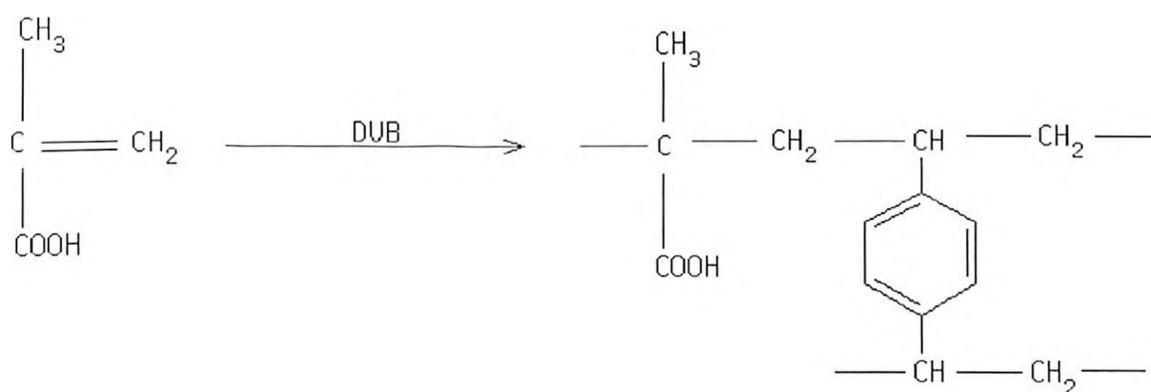
Initially, the method of synthesis of these type of resins involved condensation polymerization especially between phenol and formaldehyde [32]. This method has however been replaced by the more efficient addition polymerization using vinyl monomers and divinyl benzene as a crosslinking agent. This method offers the advantages that the degree of crosslinking may be adjusted conveniently during synthesis and it produces thermally stable polymers. The matrix may then be sulphonated using concentrated sulphuric acid or chlorosulphonic acid [50]. Such a synthesis is illustrated in Scheme II.

Similar exchangers with derivatives of styrene e.g. methylstyrene, vinylanisole and phenylacetylene have been prepared. Other crosslinking agents containing at least



Scheme II: Preparation of a strongly acidic cation exchange resin.

two unsaturated groups such as divinylacetylene and butadiene have also been shown to produce products with satisfactory properties. Weak acid exchangers are also synthesized in a similar manner e.g. copolymerization of an organic acid and an acid anhydride with a crosslinking agent [32]. An example is given in Scheme III.



Scheme III: Preparation of a weakly acidic cation exchange resin.

Bifunctional resins containing both sulphonic and carboxylic acid groups can also be prepared by sulphonation of acrylic and methylacrylic acid polymers. The ion exchanging properties of these resins are highly dependent on the solutions pH due to the -COOH group as already noted earlier [49].

Anion exchange resins are also prepared in similar manner, the only difference here being the nature of the fixed ionic groups. The introduction of these groups may be achieved by the reaction of the chloromethylated matrix with tris-(dialkylamino)phosphine to yield quaternary phosphonium groups as the fixed ionic

groups. Most of these resins are bifunctional and portray exchange properties that vary with the solution pH [32].

(iii) Other materials with ion exchange properties.

Materials such as coals, alumina, collodion e.t.c. also do have ion exchange abilities. These are however of very little practical importance due to their instability and low capacities. A large number of other materials which are soluble in common solvents but contain fixed ionic groups may also be converted to exchangers by making them ion exchange gels. For example, epichlorohydrin pectins and carrageen [49] may be crosslinked using formaldehyde. Conversely, many insoluble materials e.g. olive pits, nut shells, spent ground coffee, wood, paper, cotton e.t.c. can be converted into exchangers by the incorporation of ionic groups. Sulphonation and phosphorylation to cationic exchangers is the most widely used method [32].

(iv) Liquid ion exchangers

Even though most ion exchangers are solids, we also do have ion exchange especially between two immiscible liquid phases. These may be prepared by dissolving compounds with ionogenic groups in an organic solvent such as kerosene, trichloroethylene, chloroform, and xylene, which are immiscible with water. The compound containing these groups must be hydrophobic in order to remain in the organic phase even in presence of the aqueous solution. Compounds such as long

chain aliphatic amines, fatty acids and dialkylphosphates have been used this way as cation exchangers [51].

Liquid ion exchangers have the advantage of being easily synthesized, have high ion exchange rates and the concentration of the functional groups can be readily adjusted. The main difficulty in their use however is that losses of ion exchange can hardly be avoided during the phase separation more so if the compound containing the ionic groups is not completely insoluble in water [32].

(v) Use of ion exchangers as electrode modification materials.

Ion exchangers have found extensive usage as electrode modification materials and are applied from colloidal solutions by simple dip or spin coating [27]. In their electroinactive state, they have been shown not to affect the electrochemistry of a reasonable electron transfer rate even when their films are quite thick.

The clay mineral bentonites (Na-montmorillonite) has proved to be the most important and widely used for the purpose of electrode modification due to its excellent ion exchange and adsorption capacity. Its selectivity has been shown to segregate $\text{Ru}(\text{bpy})_3^{2+}$ from Na^+ [52]. Thicker films of approximately $3 \mu\text{M}$ can be made more stable by addition of polyvinyl alcohol, which also enhances the swelling of the clay. The fact that clays are inexpensive and are very stable under ambient conditions puts them as important candidates in organic electrochemistry [1,27].

Films of zeolite Y microplates, obtained from powdered molecular sieves, on the electrode surface have also been shown to allow selective electron exchange [53]

between the electrode and the substrate in solution. This is mainly achieved by the exclusion of some molecules from reaching the electrode surface due to their large sizes.

Ion exchangers have also been shown to exchange their counter ions with others that are redox active, thus, making the film electroactive. This exchange may be done electrochemically or by initial soaking of the exchanger in a solution containing the ions of interest [27,32] to form the so called redox ion exchanger modified electrodes.

(vi) Application of ion exchanger modified electrodes.

These electrodes have proved to be very important as pre-concentrators. Their ability to accumulate redox species from a dilute solution enables the voltammetric detection of trace elements and organic molecules [27]. The incorporation of minute amounts of certain ions into the exchanging film has been observed to enhance the electrochemical sensitivity of an electrode. For example, a nickel electrode modified with $[\text{FeNi}(\text{CN})_6]^{3+}$ has been shown to detect Na^+ and Cs^+ at a 10^{-8} M level [54].

These electrodes also have the potential of being used as ion selective electrodes in that they act as a substrate selective diffusion layer [27] which will only allow ions of a given charge and a size smaller than their pore size to diffuse through to the electrode surface. This ability may then allow their use in analyzing specific ions or molecules among other interfering ones.

Their ability to adsorb organic compounds and restrict them at the electrode surface has proved them to be valuable in electrocatalysis. The oxidation or reduction of a substrate suffering from sluggish electron transfer kinetics at the electrode surface can be mediated by a redox system that can exchange electrons rapidly with both the electrode and the substrate [1,27].

The possible areas in which these electrodes may find use are numerous and we have thus mentioned just but a few, which are most important.

b) REDOX POLYMERS.

Even though electroinactive films on the electrode surface have been shown to offer interesting applications, e.g. chiral centres imposing stereoselectivity [1,5], the use of redox active films has proved to be more attractive. Redox polymers contain redox species in their backbone and find use in areas such as macromolecular electronics, electrocatalysis, sensor electrodes, biological and medical chemistry [1,4,5,12,14,18,28,68].

These have the advantage that their behaviour in electrolyte solutions may be monitored and characterized by electroanalytical methods in situ. Due to the changing properties of molecules with change in potential (redox states), an electrode surface coated with a redox film may have its properties adjusted to suit specific needs [27].

Three classes of redox polymers are usually used. These include metal complexes e.g. ruthenium bipyridyl, polymers of the ferrocene origin and those of organic origin for example quinones, dopamine, nitrophenyl, azobenzene, viologens,

thionine and porphyrins [1,2,9,20,27,56]. Most of these are applied to the electrode surface as preformed polymeric materials by such methods as dip, spin or droplet coating or by insitu polymerization.

One of the earliest redox polymer modified electrode was coated with poly(p-nitro-styrene) on a platinum electrode [57] by dip coating. This electrode exhibited reduction peaks in acetonitrile at reduction potentials appropriate for the production of nitro aromatic radical anion sites in the polymer films, thus, making the polymer electroactive.

Quinodal and dopamine coated glassy electrodes prepared by Kuwana and co-workers [58] were interesting in that their electroactivity depended not only on the electron but also on the proton transfer for the redox system quinone/hydroquinone. These electrodes were found to electrocatalyse the oxidation of dihydronicotinamide adenine dinucleotide (NADH).

The reduction of O_2 to H_2O_2 has also been reported to be catalyzed by metalporphyrins modified electrodes e.g. Fe(III)tetra(O-aminophenyl) porphyrin [25] in sulphuric acid. The attachment of these porphyrins had been achieved by addition of poly(methacryl chloride) and then dip or spin coated on a glassy carbon electrode [68].

Most examples of redox polymers films and their areas of applications have been given in details in references 1 and 27. The most important ones include electrocatalysis, whereby the redox polymer used to modify the electrode is chosen in such a way that it's E°_{surf} is approximately equal to the formal potential E° , of the

substrate (where formal potential E° , is the average of the anodic and cathodic peak potentials). For example, polymeric ferrocene on platinum electrode surfaces has been shown to mediate the oxidation of cytochrome C [1].

One group of compounds in this class that has really attracted a lot of interest, of late, because of their conductivity mechanism, which is by delocalized band structure, rather than site to site hopping as is the case with other redox polymers, are the so called conducting polymers [27]. These polymers have attracted many researchers due to the wide range of possible areas in which they can be applied.

c) CONDUCTING POLYMERS.

The discovery that an explosive inorganic polymer, polysulphurnitride $-(SN)_x-$, was conductive [70] led researchers directly to the study of organic polymers which they thought would be formed as films on electrodes. They found out that some organic polymers could conduct electricity. These polymers were all found to have an extended conjugated system and their study has intensified since the late 1970s.

The very first conductive organic polymer to be identified was the simple conjugated polymer, polyacetylene [71,72]. This polymer was found to be of low conductivity but McDiarmid et. al. succeeded in increasing its conductivity by ten-fold on doping it (the chemical equivalent of oxidation or reduction) with iodine. They then suggested the use of this polymer as a polymer battery electrode which was hopefully to be commercialized by the 1980s. This was however not to be because polyacetylene was found to be unstable in air especially after doping.

The above notwithstanding, research intensified and it was soon discovered that other organic polymers such as polypyrrole, poly-anthracene, polythiophene, polyparaphenylene, polyaniline e.t.c. were also conductive [1,27]. With this increase in number of conducting polymers, many applications have been proposed which include electrochromic displays, information memories, antistatic materials, anticorrosives, electrocatalysts e.t.c. [1,27,59,60,69].

These polymers were however found to be of low conductivities, infusible, brittle and insoluble and they could as such not be conveniently used. To address these problems, it was necessary that these polymers be understood from a molecular level. This became a multidimensional problem involving researchers from fields such as theoretical physics, chemistry, electrical engineering and material science.

i) Mechanism of conduction in conducting polymers.

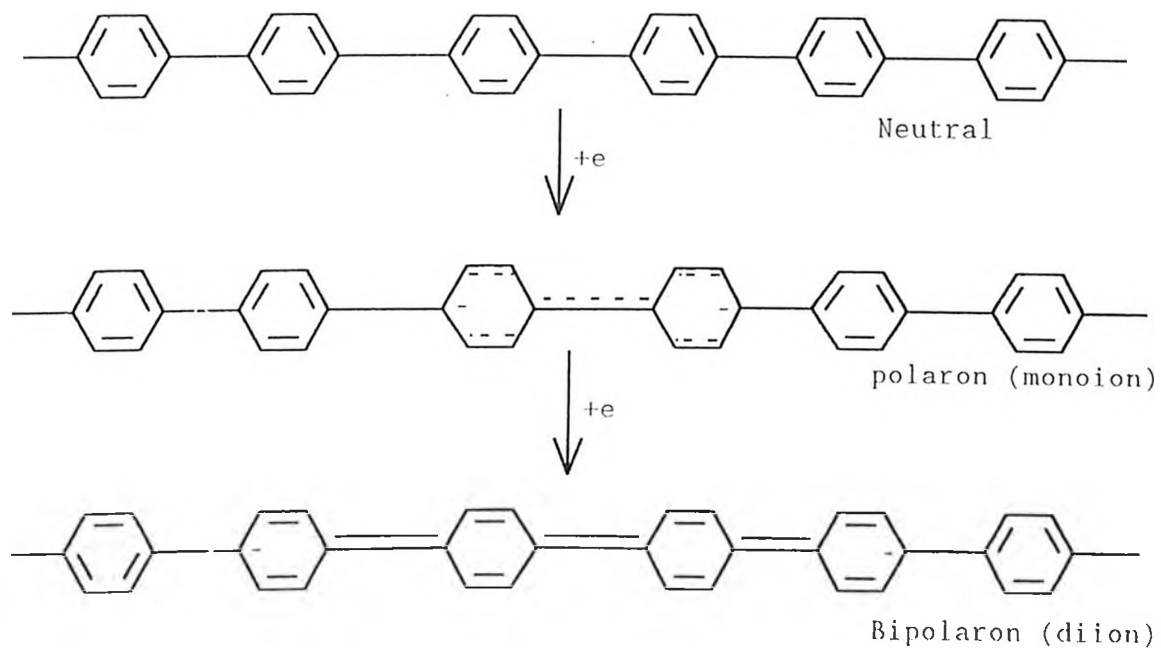
Unlike in metals and semiconductors where conduction can be adequately explained by the Band theory [61], this theory fails in the case of conducting polymers because all the electronic bands in these polymers are either completely filled or empty, a situation classically associated with the insulating state.

In semiconductors, doping leads to generation of excess positively charged holes or electrons which are free to move under an applied potential leading to conductivity. The resulting unpaired electron spins can thus be detected by techniques such as electron spin resonance (ESR). The conductivity of these polymers has

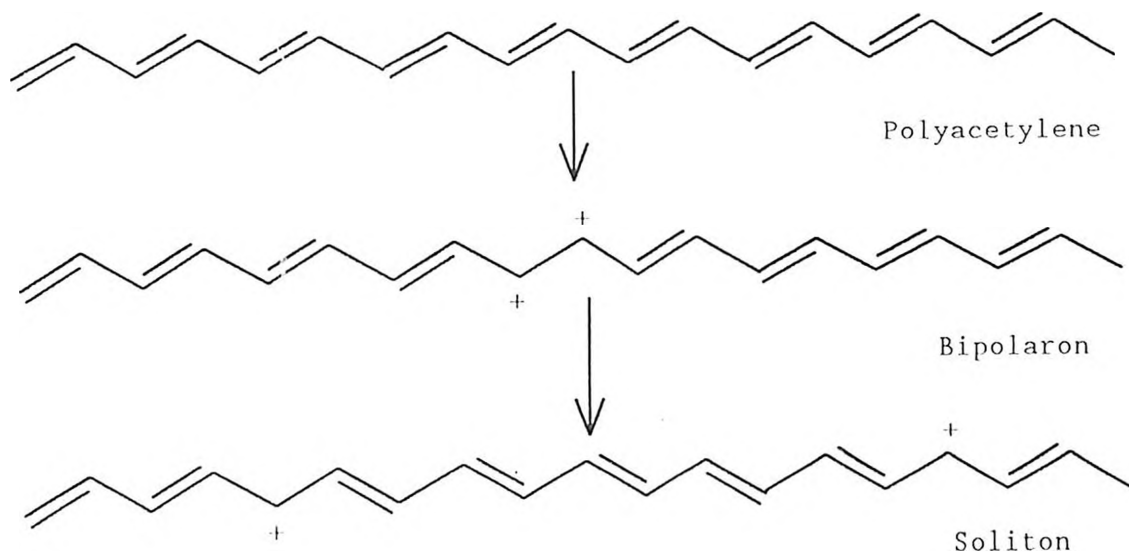
however been shown not to be associated with unpaired electron spin [62], even after doping, unlike in the case of semiconductors.

This then led researchers to accept the physicists model of conductivity based on the concept of polarons and bipolarons [27]. The physicists are of the view that when an electron is removed from a conducting polymer, the charge developed polarizes a segment of the molecule, inducing geometric modification, to form the so called polaron (a radical cation). This modification involves the rearrangement of the positions of the carbon - carbon single and double bonds [62] (its for this reason that only polymers with a conjugate system are able to conduct). On removing a second electron by further doping, we create a bipolaron (dication), rather than a second polaron. Calculations show this is energetically more favourable [63]. The polarons and bipolarons extend over several monomeric unit and are mobile along the polymer chain, carrying charge. For example, bipolarons in polypyrrole and polyparaphynelene have been shown to extend over four rings. The formation of polarons and bipolarons in poly-paraphenylene upon reduction to form radical anion and dianions is shown in scheme IV [27]. It is these bipolarons that carry charge by hopping, resulting to high conductivity in these films in the doped state. Bipolarons in conductive polymers with a degenerate ground state may split to form solitons as shown for polyacetylene in scheme V [65].

At low and intermediate doping levels, polarons even though more unstable than bipolarons, can still be seen due to the slow inter-conversion kinetics from a polaron to a bipolaron [64]. This model has now come to be accepted and it



Scheme IV: Polaron and bipolaron formation on reduction of polyparaphenylene.



Scheme V: Formation of solitons in polyacetylene.

adequately represents conductivity in these polymers. This mechanism, as already noted, is very different from that by other redox polymers and it is actually this difference that makes conducting polymers unique.

(ii) Use of conducting polymers in electrode modification.

Films of conducting polymers are conveniently applied on electrode surfaces by electropolymerization of the respective monomers from an aqueous or non-aqueous media. On oxidation or reduction of the monomer [1,27], precursors, typically cation radicals, are formed and these polymerize rather rapidly on the electrode surface. The conducting polymer films being redox active electrocatalyze the oxidation/reduction of fresh monomers enabling the formation of films with a significant thickness [1,9,10,27].

Even though polypyrrole, polyacetylene and polythiophene have attracted substantial research attention in the past, polyaniline is currently the most pursued of these polymers. This is because it has a well behaved electrochemistry, it's easily synthesized, is stable under ambient conditions and has a high conductivity unlike polypyrrole and polythiophene which have poor mechanical and electrical properties in aqueous media [8-10,30,31].

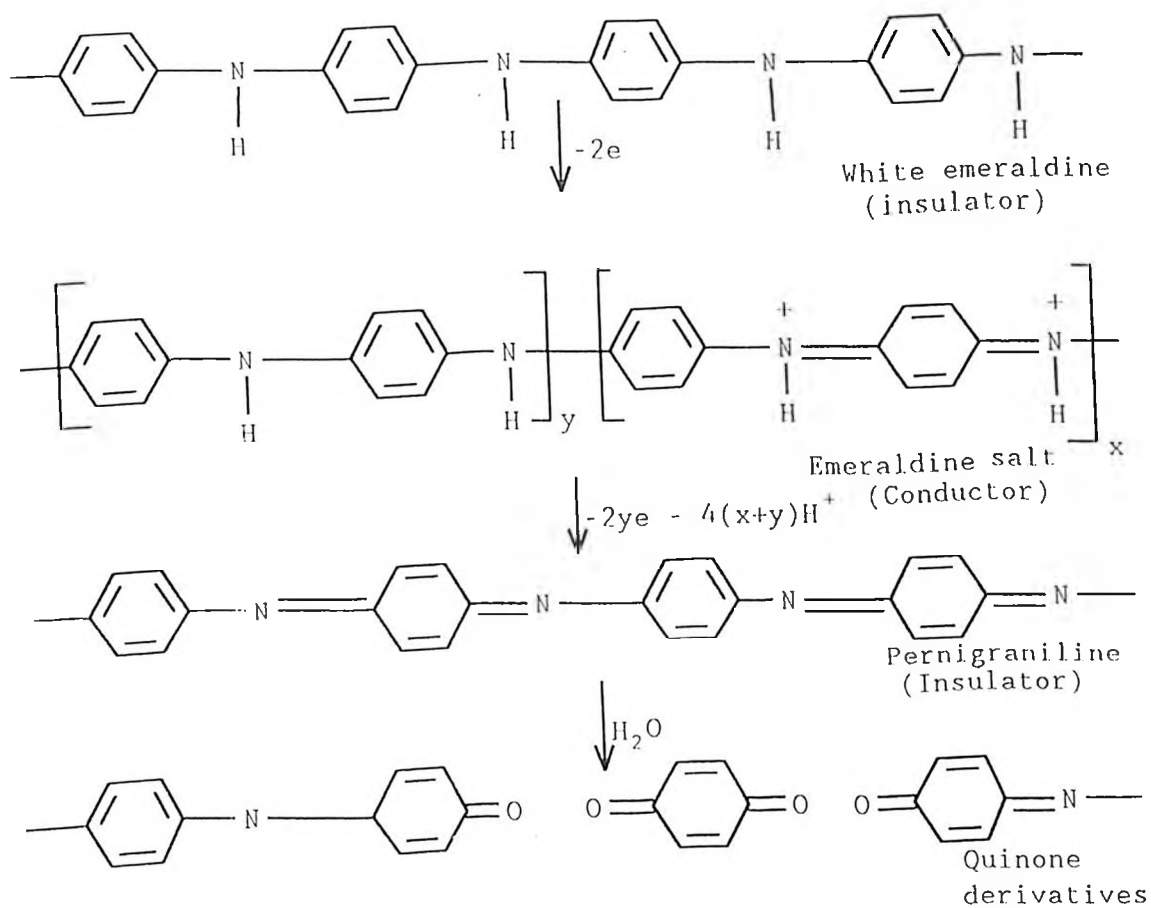
Polyaniline displays a sharp oxidation peak at around 0.2 V vs SCE in a process that has been proposed to involve the lose of two electrons to form its conductive form, the so called emeraldine salt. On reduction, the film is switched back to the insulating state, the white emeraldine. The reduction peak occurs at

approximately 0.04 V vs SCE in aqueous media. A large charging current and a small charging current are observed at the positive and the negative end of the redox process respectively. This behaviour is consistent with the transition from a conductor to an insulator.

The main handicap in the use of polyaniline however is that at potentials greater than 0.75 V vs SCE, it degrades irreversibly to the pernigraniline form, which due to its instability towards hydrolysis is oxidized to quinone-imine derivatives [8-10,31] see Scheme VI. These products are soluble leading to deterioration of polyaniline electrochemical features. Attempts made so far to extend the useful range of polyaniline include co-polymerization with p-aminophenol [9], incorporation of lead into the polymer film [10] and formation of composites between various non-conducting materials with polyaniline [66,67].

These attempts have allowed the extension of the potential window in polyaniline to as far as 0.85 V without significant degradation of the polymer. The other problem experienced with these polymers is that when electrodeposited beyond a certain thickness on a bare electrode, they tend to crystallize. This limits the applicability of these polymers as they find much use only when in the film form. It has however been shown that electrodeposition of polyaniline on an insulating host matrix, like nafion [66], or on clays, to form composites, allows the polymer thickness to be increased substantially without crystallization.

One area that has not been investigated, so far, is the formation of bilayers with these polymers. This is in spite of the fact that such a behaviour has been



Scheme VI: Oxidation products of polyaniline.

observed with redox polymers. In bilayer electrodes, two polymers arrange themselves on an electrode surface as two distinct layers consisting of an inner and an outer film. Electron transfer from the electrode surface to the outer film, and bulk, is thus via the inner film [1,27]. This kind of set up results into a rectifying property at the interface of the two polymers and may be useful in electronic devices such as zener diodes.

The essential criterion for the successful operation of such a bilayer modified electrode are [9]:-

a) the inner layer should insulate the outer layer from the electrode at all electrode potentials except those where the redox reactions of the inner layer occurs, which are placed so as to mediate electron transfer between the electrode and the outer layer,

b) the outer layer should be permeable to counter ions flow demanded by the redox reactions of the inner layer,

c) there should be minimal overlap of energy distributions of redox levels of inner and outer films,

d) the release of trapped outer states should be feasible e.g. by the exposure of the electrode to a solution containing the monomer in order for repetitive rectification to be observed.

Murray and co-workers [9] were able to achieve charge rectification from a bilayer formed using electrochemically polymerized vinylpyridine and vinylbipyridine complexes of ruthenium and iron on platinum electrodes. This property though was not sustainable.

The area of formation of composites and bilayers, involving conducting polymers, is of great interest to researchers in that it will lead to an improvement in the properties of conducting polymers, hence expanding their applications domain.

(iii) Uses of conductive polymer modified electrodes.

Conducting polymers are currently being used in rechargeable batteries and as electrochromic display devices. These batteries are characterized by low weight as compared to ordinary batteries and are potentially environmental friendly.

In principle, there are three different types of batteries. These are; active polymer being the cathode and the anode or as both the cathode and the anode [27]. However, as most polymers are only oxidizable, recent research has concentrated on developing cells with a polymer cathode and a metal anode. Such a cell is shown in Fig. 1.2.4. A polypyrrole versus Li/Li^+ cell for example has an open circuit voltage near 3.5 V and has an excellent rechargibility [27]. The charging of the polymer electrode has been shown to be accompanied by the migration of ions from the electrolyte solution into the electrode (doping) while during the discharging process, the ions move out of the electrode into the electrolyte solution leaving the electrode neutral - the insulating state [8].

The use of conductive films as electrochromic displays has its basis on the fact that conducting polymers change their visual displays on change of the redox state. These displays are also easy to prepare, have a uniform surface and an unlimited visual angle [27]. Polyaniline appears to be the most promising in that its colour

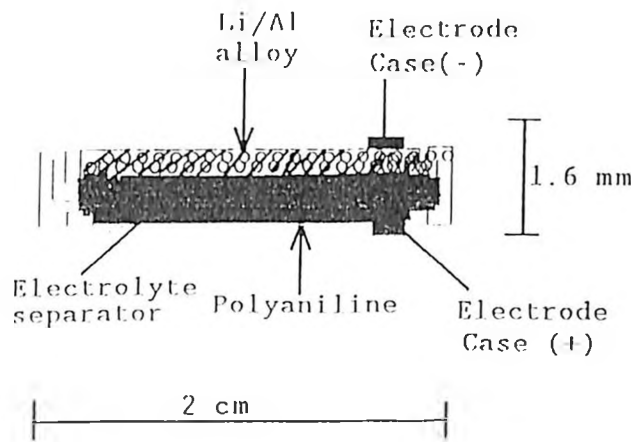


Fig 1.2.4.: Conducting polymer rechargeable battery (Button cell, Bridgestone design)

changes during oxidation to cover the whole spectrum i.e., yellow, green, violet and brown in that order. The response time for its transition from one state to the other lies below 100 mSec. This is acceptable for most practical purposes such as in "smart windows".

The fact that polymer films on the electrode exhibit ion exchange abilities qualifies them for use in place of ion exchangers only with loss of efficiency. For example, an oxidized polyaniline film has been shown to incorporate more anions than cations [8,30]. This is due to the repulsive forces between the positive charge on the polymer and that on the ion.

As already noted, redox polymer modified electrodes have been extensively used in electrocatalysis. The prospect of combining redox polymers and conducting polymers however, is expected to improve the electrocatalytic activity of such electrodes. This is due to the fact that conducting polymers are not only electron carriers but also act as electron reservoirs. For example, it has been shown that the reduction of solvated dioxygen in both protic and aprotic media is electrocatalyzed by an anthraquinone electrodeposited on a polypyrrole modified electrode [55].

Hans and coworkers have successfully devised ways of producing electrically conductive fabrics and textiles by impregnating these two with polypyrrole and polyaniline. These textiles have the same strength and tactility as their commercial counterparts. The fabrics may then be incorporated into the plastic of air frames for the purpose of charge dissipation during lightning strikes, thus, preventing damage to aircraft.

This list is by no means complete and it's growing all the time. However, it's the high time that basic research in this field moves beyond the stage of trial and error. We now need to develop concepts to enable us obtain quantitative information about molecular structures and properties, on the one hand, and the resultant material properties on the other hand.

CHAPTER TWO

2.0 PROPOSED RESEARCH.

The electrochemical investigations will be carried out using cyclic voltammetric technique. Elemental analysis on the montmorillonite and amberlite (cation exchanger) will be studied using X-ray fluorescence spectroscopy.

The investigations will include the following:

- 1) Investigation of electrochemical response of amberlite (a commercial cation exchanger) and bentonite (montmorillonite from Athi river) modified carbon graphite electrodes in various electrolyte solutions.
- 2) A study of the electrochemical response of various metal cations such as lead, copper and tin on these modified electrodes and compared it to that of the unmodified electrode.
- 3) Incorporation of redox species in bentonite and amberlite by means of applying voltage on modified electrodes dipped in a solution containing cations of interest (simultaneous exchange) and soaking these exchangers in a solution containing cations of interest before modification (pre-treated), in order to make them redox active.
- 4) Electrodeposition of polyaniline (a conducting polymer) on each of the above electrodes and comparing its behaviour for the different cations and for the same cation incorporated by the use of the two different methods.

- 5) Determination of the redox activity of soaked ion exchangers by comparing the surface coverage as obtained electrochemically with X-ray fluorescent data.
- 6) Determination of the effect of the nature and number of redox sites in the redox modified electrode on the electrochemistry of polyaniline.

EXPERIMENTAL SECTION

2.1 METHODS OF ANALYSIS

In our experiments, two methods of analysis namely, cyclic voltammetry (for electrochemical analysis) and X-ray fluorescence (for elemental composition) were used.

The electrochemical apparatus comprised of a PAR model 173 Potentiostat/Galvanostat used in conjunction with a model 175 Universal programmer. The output signal was fed into a PAR RE-0089 X-Y recorder. The X-RF apparatus on the other hand comprised of an IBM PC fitted with an AXIL programme for spectrum analysis and a QAES (75) programme for quantitative analysis.

2.1.1. AN OVERVIEW OF THE ELECTROCHEMICAL TECHNIQUE.

Electrochemical methods have now come to be accepted as very important techniques in the chemical characterization process. Many researchers in the fields of organic and inorganic chemistry rank them with IR, NMR spectroscopy, UV-visible and ESR spectroscopy in this respect [72]. Some of the questions that they have been used to address include:-

- a) the standard potentials of a compound's redox process,
- b) electron stoichiometry of a compound's redox process,
- c) evaluation of heterogeneous electron transfer kinetics and mechanism of a compound's reaction,
- d) effect of solvent and electrode material on a compound's electron transfer kinetics,
- e) half lives of unstable intermediates,
- f) determination of the formulas and stability constants of metal complexes and
- g) effect of supporting electrolyte and solution pH on the redox process of a compound [8,72,77,7,66].

Due to this broad applications domain, various electrochemical methods have been developed. These include polarography, linear sweep voltammetry, cyclic voltammetry and rotating disk voltammetry. These methods fall into two broad categories, namely, chronoamperometry and chronopotentiometry.

Chronoamperometric methods involve the controlled variation of voltage while the changing current is monitored. This is achieved by use of a potentiostat. Chronopotentiometric methods on the other hand involve the use of a galvanostat, so as to vary the current in a controlled manner while changes of voltage are monitored.

Cyclic voltammetry is a chronoamperometric technique and it basically involves the use of a stationary electrode, surface area $< 1 \text{ cm}^2$ immersed in an unstirred solution containing a suitable solvent and supporting electrolyte. Voltage is scanned

linearly from a particular potential to a set switching potential (final potential), and back to the initial potential [72,74]. During this process, the current originating from the electrochemical cell is monitored and recorded. A plot of voltage (or time) versus current obtained this way is called a cyclic voltammogram and has the general shape shown in Fig. 2.1. Consider a case where a stationary electrode is dipped into a solution containing the oxidized species, O only. If the scan is began at a potential well positive than the reduction potential $E^{\circ'}$, then, only non-Faradic currents flow for a while (portion AB in Fig. 2.1).

When the electrode potential reaches the vicinity of $E^{\circ'}$, reduction begins and a current starts to flow. As the potential continues to grow more negative, the surface concentration of O drops; hence the flux to the surface (and the current) increases (portion BC). As the potential moves past $E^{\circ'}$, the surface concentration drops to near zero, mass transfer to the electrode reaches a maximum and then declines as depletion effects sets in (portion CD). The voltammogram is as such peaked at C.

When the sweep or scan direction is suddenly reversed, at a time when there is a large concentration of oxidizable species at the electrode surface, a similar peak at E will be observed essentially due to the same behaviour.

The parameters of interest in a cyclic voltammogram include i_{pa} , i_{pc} , E_{pa} , E_{pc} , and the general shape of the peaks.

The chemical nature of the reactants, intermediates, products and the electrode surface determines the kind of interactions between all these four materials [74]. When these forces are weak for example, chemisorption, the reactants, intermediates and/or

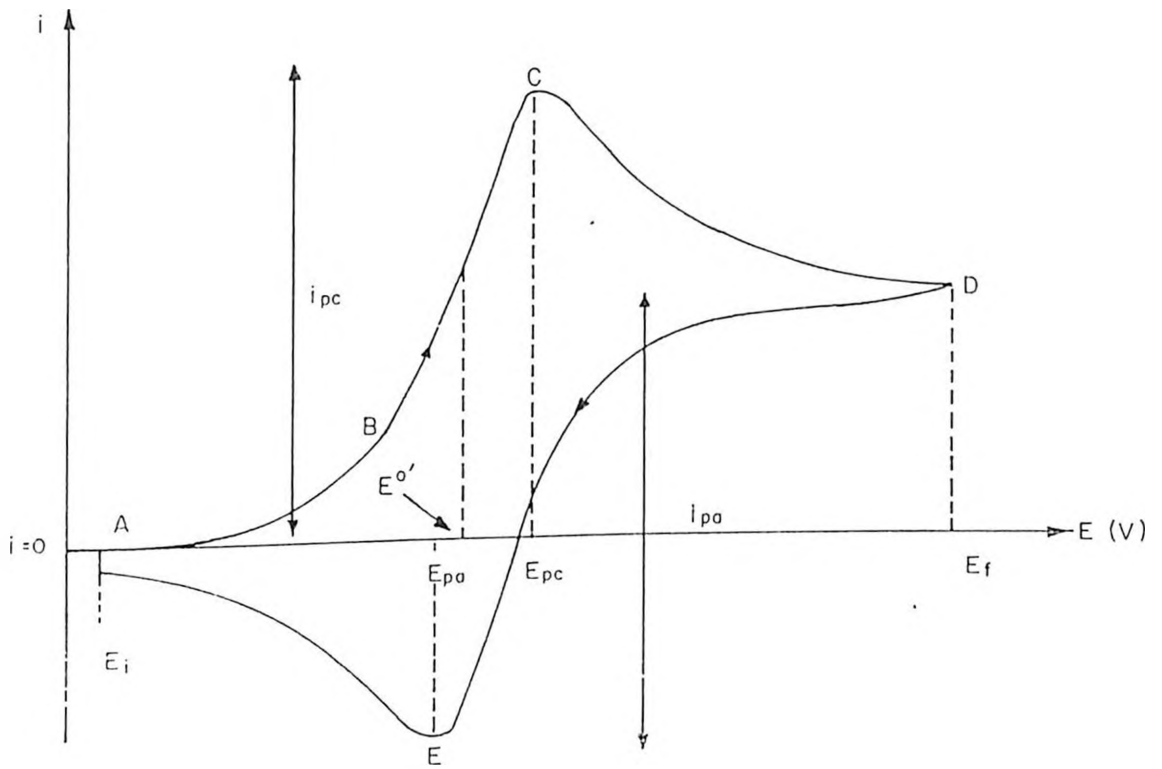


Figure 2.1: The general shape of a cyclic voltammogram E_i and E_f are the initial and final potentials i_{pa} and i_{pc} are the anodic and cathodic peak current E_{pa} and E_{pc} are the anodic and cathodic peak potentials respectively and $E^{o'}$ is the reduction potential

the products diffuse freely to and from the electrode surface. This behaviour yields a nernstian (reversible) voltammogram. When the interactions are strong, the species concerned get adsorbed or bonded to the electrode surface. This kind of behaviour leads to quasi-reversible or totally irreversible systems.

For a reversible redox process at 25°C,

$$i_p = 2.67 \times 10^{-5} AC\sqrt{DVn^3} \dots \dots \dots \text{Equ. 2.1}$$

While the peak separation

$$\Delta E = E_{pa} - E_{pc} = \frac{59}{n} mV$$

and

$$\frac{i_{pa}}{i_{pc}} = 1$$

regardless of the scan rate [72,74].

Where i_p is the peak current (A)

n is the number of electrons involved in the redox process

A is surface area of the electrode (cm²)

D is the diffusion coefficient (cm²/sec)

C is concentration of electroactive species (mol/cm³)

V is scan rate (V/sec).

In this case, ΔE is scan rate independent and only varies slightly with E_r . When either the oxidized or reduced species get adsorbed on the electrode surface, the peak current is now given by

$$i_p = n^2 F^2 x \frac{AFV}{4RT} \dots \dots \text{Equ. 2. 2}$$

while the peak potential is

$$E_p = E^\circ - \frac{RT}{nF} \ln \frac{b_o}{b_R}$$

where

$$b = \alpha n_a \frac{FV}{RT}$$

where α is the transfer coefficient.

Comparing equations 2.1 and 2.2, we note that for diffusion controlled processes, i_p is proportional to $v^{1/2}$ while for cases where either the reactant or products are adsorbed on the electrode surface, i_p is proportional to v . This latter case is similar to what is observed for a purely capacitive current and the area under the peak, corrected for residual current, represents the charge associated with the reduction/oxidation of the adsorbed layer i.e., $nFA\Gamma$ [74] (where Γ is the surface coverage mol/cm²).

The peak currents and peak separations may be used for quantitative and qualitative analysis, determination of the reversibility of a redox process and the diffusion coefficient of an electroactive species.

Cyclic voltammetry also provides information concerning any side processes, such as pre- and post-chemical reactions, which lead to formation of side products or reaction intermediates. It is as such a very important tool to an electrochemist interested with the mechanism of an electrochemical reaction. The high scan rates associated with cyclic voltammetry may also be used to determine the lifetimes of unstable intermediates [72].

For the measurement of kinetic parameters, Nicholson et. al. [73] have developed a number of equation which include

$$\Psi = \gamma^\alpha \frac{K_s}{\sqrt{\pi a D_{ox}}}$$

(for reversible reactions)

Where Ψ is a kinetic parameter for electrochemical processes that are limited by finite rates of electron transfer.

$$\gamma = \frac{D_{ox}}{D_{red}}$$

α is the transfer coefficient

K_s is the heterogenous electrochemical rate constant at E'

and

$$a = \frac{nFV}{RT}$$

a) MODE OF OPERATION OF A POTENTIOSTAT.

A potentiostat is an instrument that controls the voltage across the working and counter electrode pair, and adjusts it in order to maintain the voltage between the working electrode and the reference electrode according to the program supplied by a function generator [74]. It enforces the adjustment by supplying whatever current is required through the counter electrode. It's this current that is actually experimentally recorded.

A potentiostat utilizes operational amplifiers usually of the differential type, where a differential amplifier is represented by a triangle with two input and one output terminals. The potentials of these terminals are usually referred to ground. A positive input applied to the non-inverting (positive) terminal gives a positive output while a positive input applied to the inverting terminal (negative) gives a negative output [72].

The fundamental property of an amplifier is that the output, e_o is the inverted amplified voltage difference e_s , where e_s is the voltage of the inverting input with respect to the non-inverting input (see Fig. 2.2).

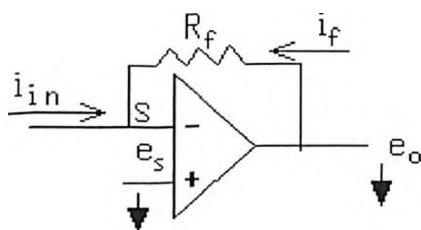


Fig. 2.2: Block diagram of a differential amplifier (current follower) [3]

The amplification factor or the open loop gain A , is thus defined as;

$$A = -\frac{e_o}{e_i}$$

An ideal operational amplifier is characterized by:-

- a) an infinite open loop gain, so that the slightest input voltage e_i , drives the output voltage to the limit of a desirable power supply (usually ± 13 V),
- b) the input terminals must be at the same voltage,
- c) an infinite input impedance, so as to draw negligible current from the voltage source and a zero output impedance so as to be in a position to supply any amount of current demanded by the load and
- d) an infinite bandwidth so as to promptly respond to a signal of any given frequency.

Operational amplifiers have been observed to suffer from a drift of several mV/day, resulting to errors in its operations. This is overcome by the application of an external feedback loop, such that, part of its output is fed back to the inverting input. In Fig. 2.3, the resistor R_f is the feedback element through which a feedback current i_f passes. This then ensures that the current at the summing point, S is zero, making this point a virtual ground.

It then follows that,

$$i_{in} = -i_f$$

and from Ohm's law,

$$i_f = \frac{e_o - e_s}{R_f} = \frac{e_o}{R_f}$$

since $e_s = 0$. Thus,

$$e_o = -i_{in} R_f$$

or, the output voltage of the amplifier is directly proportional to the input current. This amplifier is thus called a current follower [74].

Unlike in the foregoing type of amplifier where part of the output current is fed to the inverting input, there are cases where all the output voltage is fed back to the inverting input terminal through the external feedback loop. Such kind of an amplifier is shown in Fig. 2.3.

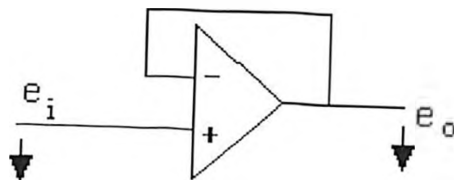


Fig. 2.3: Block diagram of a voltage follower

In this case, $e_o = e_i$ as the two terminals are at the same potential. Such an amplifier is called a voltage follower.

A third type of an operational amplifier is the so called control amplifier, shown in Fig. 2.4. A control amplifier is fed with an input voltage e_i , at the inverting

terminal while the non-inverting input terminal is maintained at ground potential. The potential at point B, e_B , must also then be e_i .

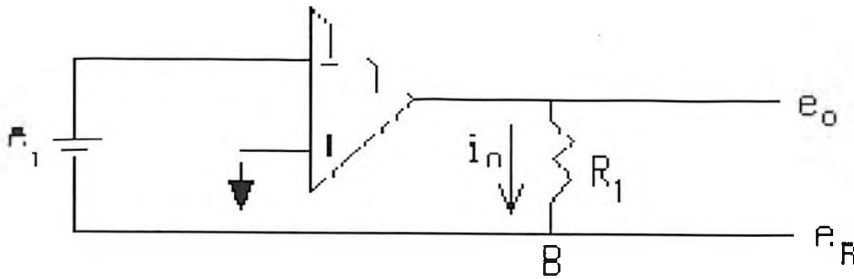


Fig. 2.4: Block diagram of a control amplifier.

To ensure that this condition is maintained, the amplifier is forced to adjust its output, by means of passing the necessary current through the resistors. This type of amplifiers thus offers a means of controlling the voltage at a fixed point in a network of resistors even though these resistances fluctuate during an experiment [74].

For a potentiostat to operate successfully, it must

a) possess a circuit that provides accurate potential control with no iR drops through the signal generator or current measuring resistors. This reduces the potential - control error,

b) Utilize stabilized (single ended) amplifiers in order to have lower potential drifts and

c) allow the signal generator and the current measuring device to be grounded.

This is due to the convenience experienced when all signal inputs and outputs are referred to a common ground.

For a potentiostat to possess all the factors stated above, it's necessary that it incorporates all the three types of amplifiers discussed above (see Fig. 2.5).

The working electrode is maintained at virtual ground by amplifier 4. The output voltage of amplifier 4 is on the other hand given by equation 2.3.

$$E_o = -iR_c \dots \dots \dots \text{Equ. 2. 3}$$

So that E_o is proportional to the current flowing through the working electrode. Amplifier 4 as such acts as a current follower and it's output may be fed into a recorder in order to monitor the current changes in the cell.

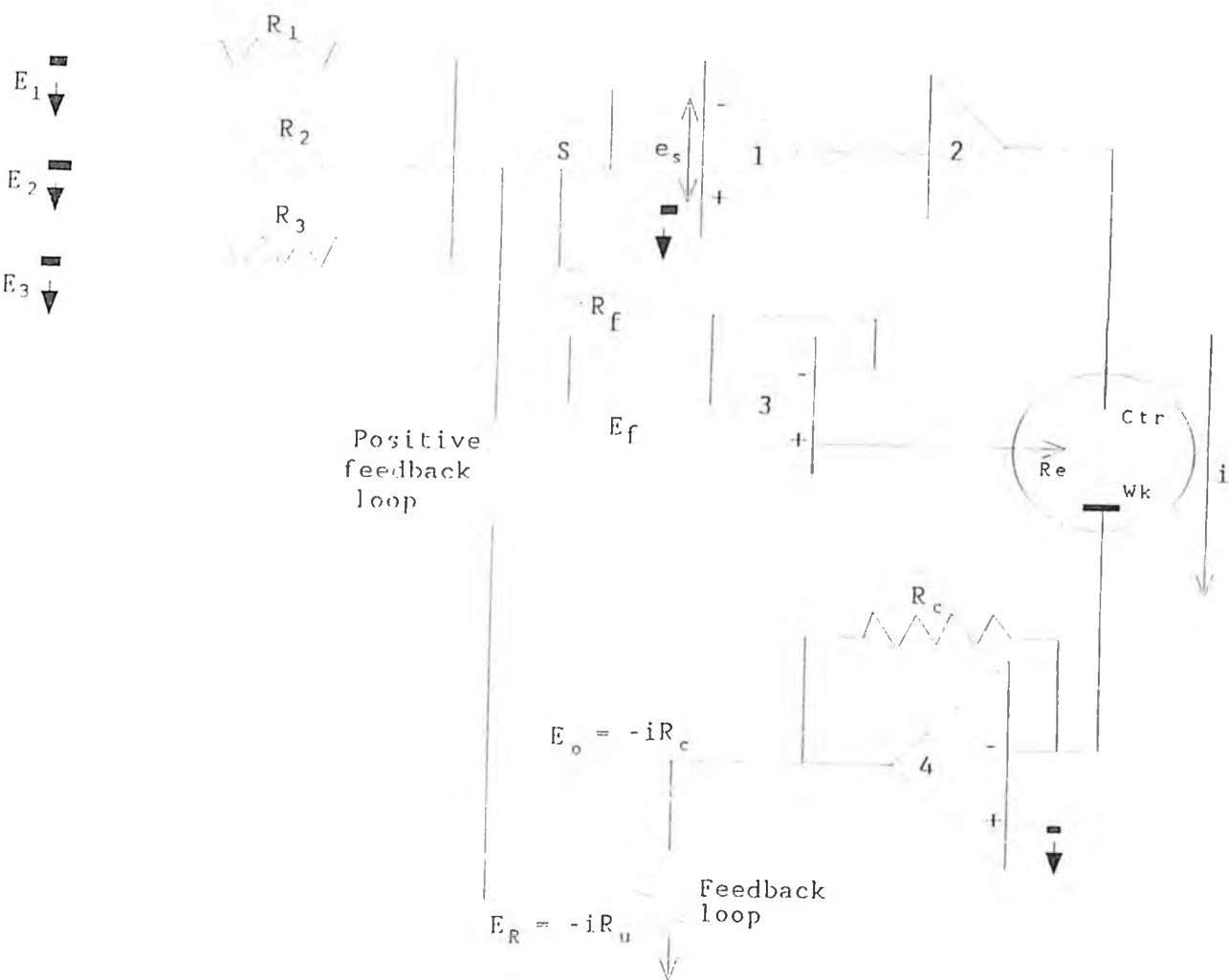
$$E_f = e_f = -E_{cell} = -(E_{wk} - E_{re}) \dots \dots \dots \text{Equ. 2. 4}$$

Amplifier 3, the voltage follower, has an output voltage E_f which is equal to the input voltage e_f . The potential e_f is the potential of the reference electrode measured with respect to the working electrode as shown in equation 2.4.

Equation 2.4 is varied for as long as there is no iR drop from the electrode and the electrolyte solution, the so called uncompensated resistance, R_u . When this resistance is put into consideration, it transforms into Equation 2.5.

$$E_f = -E_{cell} + iR_u \dots \dots \dots \text{Equ. 2. 5}$$

where i is the current passing through the cell (cathodic current taken as positive current while anodic current is taken as negative current).



g. 2.5: An adder potentiostat with a positive feedback compensation [3].
 Amplifier 1 - Control amplifier Amplifier 2 - Booster amplifier
 Amplifier 3 - voltage follower Amplifier 4 - Current follower
 Ctr, Re and Wk are the control, reference and working electrodes respectively.

The control inputs E_1 , E_2 , E_3 and the voltage follower output E_f are added and summed through separate input resistors connected to the summing point S, of amplifier 1, the control amplifier. This amplifier maintains its summing point at virtual ground ($e_s = 0$) by use of a feedback loop consisting of a booster amplifier, counter electrode, reference electrode and the voltage follower. At point S then,

$$\frac{E_1}{R_1} + \frac{E_2}{R_2} + \frac{E_3}{R_3} = 0$$

If

$$R_1 = R_2 = R_3 = R_f$$

then,

$$-E_f = E_1 + E_2 + E_3 \dots \dots \text{Equ. 2. 6}$$

and from equations 2.4 and 2.6, we get

$$E_{cell} = E_1 + E_2 + E_3 \dots \dots \text{Equ. 2. 7}$$

Simply stated then, the control amplifier forces current to flow through the counter and the working electrode to maintain the condition given in equation 2.7. To enable it perform this function, it's usually necessary to complement it with a booster amplifier, amplifier 2, especially for cases where a high current is demanded by the cell [74].

Whenever current is passed through a cell, potential control errors arise due to the uncompensated resistance. Uncompensated resistance originates from capacitance in the double layer, leads of the electrodes and from the solution. For example, when a cathodic current is flowing, the true working electrode potential, E_{true} , will be less negative, as shown in equation 2.5, by an amount iR_u . Even though R_u values are typically low, serious potential control errors arise especially when substantial currents are flowing.

This discrepancy is overcome by the use of a positive feedback compensation scheme. The current follower is in this case connected to the control amplifier through a potentiometer. The potentiometer selects a fraction of the current follower's output in such a way that the feedback voltage E_R is given by equation 2.8.

$$E_R = -iR_u \dots \dots \dots Equ. 2. 8$$

$$E_{true} = E_1 + E_2 + E_3 + -iR_u + iR_u \dots \dots \dots Equ. 2. 10$$

As such, the true working electrode potential versus the reference electrode, E_{true} is given by equation 2.10.

or,

$$E_{true} = E_1 + E_2 + E_3 \dots \dots \dots Equ. 2. 11$$

This circuit is versatile and permits as many control inputs as desired to be connected to the input terminal of the control amplifier, each through its own resistor.

For example, a voltage ramp generator connected to the input provides a linearly varying voltage. The potential at which the voltage scans starts can be varied by applying to a second input a variable voltage source to provide initial potential control. This is the basic configuration used in DC polarography and linear sweep voltammetry. A triangular waveform applied at the inputs enables one to undertake cyclic voltammetry [72].

2.1.2 X-RAY FLUORESCENCE ANALYSIS (X-RF)

In X-RF, quantitative analysis depend upon the correlation of elemental composition with the observed X-ray fluorescence intensities. This correlation is worked through using basic equations derived using fundamental parameters. The equations are general and represent a basis for all different methods of quantitative analysis. Fundamental parameter technique (FPT) is very popular mainly because it is simple, rapid and does not require the use of standards.

In the derivation of these equations, FPT assumes that,

- a) a monochromatic radiation from the primary source is used to excite the characteristic x-rays from the sample,
- b) the sample is homogenous i.e., the density is well defined and constant throughout the sample volume and
- c) a fixed geometry of sample, source and detector is maintained.

The geometry shown in Fig. 2.6 is the one used to calculate intensity, I_i of fluorescent radiation from element i , within the sample and excited by a primary radiation of energy E .

The probability of exciting and detecting the $K\alpha$ x-rays of energy E_i from element i , in the layer of thickness dx at a distance x , in the sample is represented as a product of three probabilities as follows [78],

$$P_1 = I_0 \Omega_1 \exp -\mu(E) \rho x \csc \Phi_1 \dots \dots \dots Equ. 2. 12$$

Which is the probability that primary radiation will reach a depth x

$$P_2 = \sigma(E) \rho_i dx \csc \Phi_1 B \Phi \omega f^i \dots \dots \dots Equ. 2. 13$$

being the probability that element i will absorb the primary radiation in the layer of thickness dx and emit k x-rays of energy E_i and

$$P_3 = \Omega_2 \exp -[\mu(E) \rho x \csc \Phi_2] \epsilon(E_i) \dots \dots \dots Equ. 2. 14$$

which is in turn the probability that k x-rays of energy E_i emitted by element i in the sample will penetrate out of the sample and be detected.

The fluorescent intensity dI_i , being a contribution from the atoms of element i , at depth x , can be written as

$$dI_i = I_0 \Omega_1 \Omega_2 \csc \Phi_1 \rho_i \sigma(E) \cdot B \cdot \omega f^i \epsilon(E_i) \exp -(a \rho x) dx \dots \dots \dots Equ. 2. 15$$

where

$$a = \mu(E) [csc \Phi_1 + csc \Phi_2]$$

On integration to obtain the total contribution of element i , to the detected fluorescence throughout the sample thickness, one gets

$$I_i = I_o \Omega_1 \Omega_2 csc \Phi_1 \sigma(E) B \omega^i f^i \epsilon(E_i) (\rho_i d) \frac{1 - e^{-a \rho d}}{a \rho d} \dots \text{Equ. 2. 16}$$

which may be broken down to

$$I_i = G_o K_i (\rho_i d) \frac{1 - e^{-a \rho d}}{a \rho d} \dots \dots \dots \text{Equ. 2. 17}$$

where

$$G_o = I_o \Omega_1 \Omega_2 csc \Phi_1$$

i.e., the geometric constant (count/sec)

$$K_i = \sigma(E) f^i \omega^i B \epsilon(E_i)$$

i.e., the relative detection efficiency (cm²/g).

and a is the combined absorption coefficient for primary and fluorescent x-rays in the sample.

A summary of the definitions of the terms in the above equations is as follows,

I_i fluorescent intensity (counts/sec)

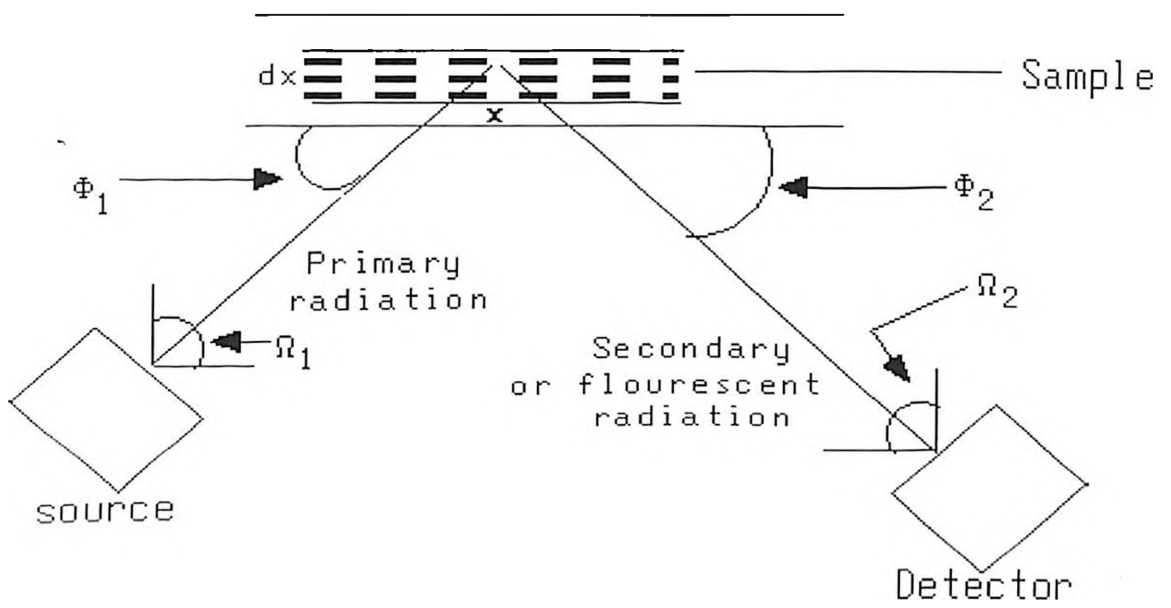


Fig. 2.6: A Schematic representation of X-RF geometry [82]

Ω_1 and Ω_2 are the solid angles formed by directions of the primary and fluorescent (characteristic) radiations with the sample surface,

ρ_1 and ρ_2 are the density of the sample and partial density of element i, within the sample respectively,

$\sigma(E)$ is the photoelectric cross section of element i for primary radiation (cm^2/g),

$\mu(E)$ is the total mass absorption co-efficient of the sample for the characteristic (cm^2/g)

$B = 1 - 1/J_k$ and is the relative probability (fraction) for the photoelectric process to occur in the K-shell of element i

K is the absorption jump

J_k the ratio between the value of maximum and minimum photoelectric cross section at the K absorption edge of element i

ω^i the fluorescent yield of k x-rays of element i

$$f^i = \frac{P(K_\alpha)}{P(K_\alpha) + P(K_\beta)}$$

the relative transition probability for K_α x-rays of element i where P's are the transition probabilities

$\epsilon(E_i)$ is the relative efficiency for the detection of x-rays of energy E_i .

The values of μ , $\sigma(E)$, J_k , ω^i and f^i may be obtained from tables in references 10 and 11, while the values of $\epsilon(E_i)$ must be evaluated for the particular detector used.

The measured intensity of the fluorescent x-rays I_i , would be directly proportional to the concentration of the relevant element in the sample, $\rho_i d$ according to equation 2.17 if it were not for the absorption correction factor

$$\frac{1 - e^{-a \rho d}}{a \rho d}$$

This factor is a function of the combined absorption coefficient a , in the sample, which is implicitly dependent on the concentration of all elements comprising the sample. It strongly depends on the product $a \rho d$. For cases where $a \rho d \ll 1$, implying a thin sample, then, equation 2.17 transforms into

$$I_i = G_o K_i (\rho_i d) \dots \dots \dots Equ. 2. 18$$

while for thick samples, i.e., $a \rho d \gg 1$,

$$I_i = G_o K_i \alpha_i \frac{1}{a}$$

and for $0.1 < a \rho d < 2$ i.e., a transparent sample,

$$I_i = G_o K_i \alpha_i \frac{1 - e^{-a \rho d}}{a} \dots \dots \dots Equ. 2. 20$$

To eliminate the absorption correction factor in quantitative analysis using FPT, a thin sample should be used.

Another matrix that has also to be corrected for is the inter-elemental effects. These arise in the form of enhancement effects [81], which occur in cases where

fluorescence radiation of element i , is excited not only by the primary radiation but also by the fluorescence radiation of other elements in the sample. This is usually observed in both thick and transparent samples.

a) X-RF INSTRUMENTATION

A X-RF unit consists of a X-ray excitation source and a x-ray spectrometer. The spectrometer consists of a solid state detector Si(Li) or HPGE, a pre-amplifier, an amplifier and a multichannel analyzer (MCA) to which a microcomputer with the relevant interface may be incorporated (see Fig. 2.7).

The detector is a crystal of germanium or silicon that is processed to form a diode. When operated in the reverse bias, electron-hole pairs produced by the interaction with x-rays, are swept out of the crystal by the applied electric field. To minimize other sources of charge carriers, the impurities in silicon are compensated with lithium in a process called lithium drifting. The lithium drifted crystals, as well as high purity germanium crystals (HPGE), crystals are operated at liquid nitrogen temperature to reduce thermal noise [81].

Lithium drifted silicon or germanium detectors must be maintained at this temperature at all times for lithium to remain in place. HPGE may however be left at room temperature when not in use as it does not require lithium drifting.

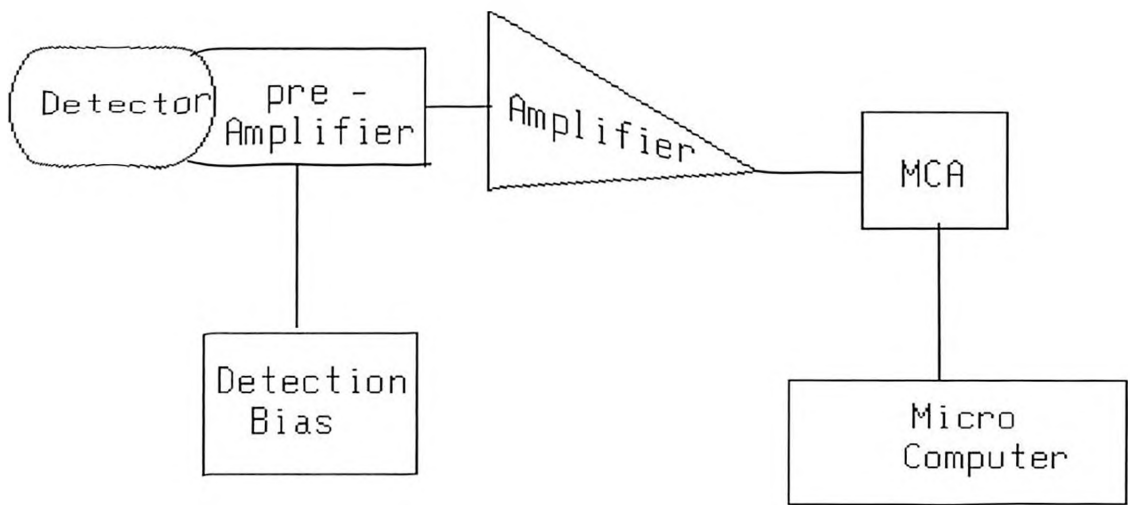


Fig.2.7: Block diagram of the electronic set-up of a X-RF unit.

The pre-amplifier converts the burst of electrons, resulting from the absorption of x-rays, into a voltage signal which may be conveniently transmitted to the measurement system. The pre-amplifier also minimizes any noise which may degrade the resolution of the spectrum. This is achieved by using a field effect transistor (FET) input charge sensitive pre-amplifier.

The pre-amplifier is then followed by a shaping amplifier which acts as a shaper of the pulse as well as to amplify it and make the pulse suitable for precise pulseheight analysis by the MCA. It gives a near Gaussian shape with a time constant of 6-10 μ Sec. The MCA on the other hand sorts out the pulses according to their heights and accumulates the respective pulse height distribution in its memory (channels).

The radiation excitation source used in our analysis was ^{109}Cd , a radioisotope with a half-life of 453 days which decays by electron capture. This source is very useful for analysis of the elements Ca to Mo by K x-rays and W to U by L x-rays [81].

b) SAMPLE PREPARATION

This method may be used to analyze both liquid and solid samples and has found a lot of application in the elemental determination in samples of biological, geological and industrial origins.

The sample preparation techniques are adopted to ensure that the samples are homogenous and transparent or thin. This is in a bid to utilize equations 2.18 and 2.20 for quantitative analysis.

The bulk solid samples are initially crushed to small pieces and then pulverized. Further manual pulverization of the sample in an agate mortar is done so as to reduce the particle size to less than 50 microns. Two types of samples are usually made, namely,

a) Scotch tapes- in this case, the sample is spread out on a scotch tape approximately $1\text{mg}/\text{cm}^2$, and

b) thin pellets diluted with pure starch or cellulose powder. The starch helps in binding the sample material into a stable pellet. This was the technique used in our X-RF analysis. The pellet weights were in the range 0.1-0.2 g and had a surface area of 4.91 cm^2 .

This method has been shown to detect elements with a concentration as low as 10^{-8} g/g of sample [81] with statistical errors of measurement being less than 1 %.

In liquid samples, it's necessary that the elements be pre-concentrated as these solutions are usually very dilute. The pre-concentration procedures usually used include evaporation, complexing and precipitation. Precipitation of dissolved elements with organic precipitating reagents e.g., ammonium-1-pyrrolidine dithiocarbamate (APDC), is most popular. The digestion of solid samples followed by selective precipitation has been observed to provide a higher sensitivity than is obtained with

pellets [81]. It's however necessary that the pH of the solution be selected carefully to enable maximum precipitation of the elements.

2.2 CHEMICAL REAGENTS

The chemicals used, copper sulphate, sulphuric acid, hydrochloric acid, lead (II) sulphate, potassium nitrate and maize starch, were of ANALAR grade and were used as received without further purification. Aniline (BDH) was triply distilled to a colourless liquid prior to use.

The amberlite CG50 (BDH) and Athi river bentonite, the materials used for electrode modification, were also used as received. Amberlite CG50 is a commercial cation exchange which consists of weakly acidic active groups, $-\text{COO}^-$. It has a mesh size of 200 (US.S.S); wet density of about 0.7 g/ml on rehydration; exchange capacity of 5.3 meq/ml (wet) and 10 meq/ml (dry) and is most suited for use in the pH range 5-14.

Athi river bentonite is a montmorillonite and it's composition as determined by x-ray fluorescence is shown in Table 2.1

2.3 ELECTRODES

A three electrode assembly in an undivided cell was used throughout our experiments. These consisted of a bare or modified carbon graphite electrode as the working electrode, saturated calomel electrode as the reference electrode and a platinum wire as the auxiliary electrode.

Table 2.1: Elemental composition of bentonite as determined by x-ray fluorescence

Element	Conc. g/g of bentonite x 10 ²
K	1.08
Ca	2.58
Ti	0.506
Cr	0.0031
Mn	0.0292
Fe	4.98
Cu	0.00525
Zn	0.00882
Ga	0.00197
Pb	0.00193
Rb	0.00707
Sr	0.028
Y	0.00289
Zr	0.0144
Nb	0.0017

The residual matrix was composed of a mixture of aluminosilicates and oxides of not measured light elements (Atomic number less than 19).

2.3.1 MODIFICATION OF THE WORKING ELECTRODE.

The modification of the working electrode was done by mixing about 40 mg of the modification material with about 0.04 ml of a non-electroactive binder (Henkel (K) Ltd). The paste so obtained was then thinned onto the electrode surface after the electrode, surface area 0.38 cm², had been polished on a felt cloth using alumina. The thickness of the electrode modification material after drying of the binder for 24 hours at room temperature was about 0.16 mm. The electrode surface area after

modification was found to be 0.64 cm^2 , representing an 80 % increase compared to the bare electrode.

The materials used for the purpose of modification were as follows:-

a) Amberlite soaked in a solution containing 0.01 M CuSO_4 for 24 hours (5 g amberlite in 100 ml of solution)

(A-NAC).

b) Amberlite soaked in a solution containing 0.01 M CuSO_4 and $0.1 \text{ M H}_2\text{SO}_4$ for 24 hours (5 g of amberlite in 100 ml of solution)**(A-WAC).**

c) Amberlite soaked in a solution containing 0.01 M lead (II) nitrate for 24 hours (5 g of amberlite in 100 ml of solution)**(A-NPN).**

d) Amberlite soaked in a solution containing 0.01 M lead (II) nitrate and 0.1 M KNO_3 for 24 hours(5 g of amberlite in 100 ml of solution)**(A-WPN).**

e) **Bare amberlite**

Similar material were made for bentonite and were designated **B-NAC**, **B-WAC**, **B-NPN**, **B-WPN** and **Bare bentonite**.

The soaking process was carried out under continuous stirring to ensure homogenous exchange of the cations in the exchangers.

2.3.2 REFERENCE ELECTRODES

The fact that the potential of a working electrode or a half cell is not absolute makes the use of reference electrodes inevitable. Conventionally, the standard

hydrogen electrode (SHE) has been arbitrarily assigned zero potential and all other half cell potentials are referred to it. It consists of

Pt^(s)/ H⁺_(aq) (a=1)/ H_{2(g)}(1 atm.) half cell and a cell reaction



Although this electrode is very reproducible, it's hardly used in electrochemical analysis mainly due to its cost of maintenance (lasting 7-20 days) and its inconvenient set-up.

Other half cells, which meet the following conditions, have as such been developed and utilized as reference electrodes,

a) are reversible and obey Nernst's equation (Equation 2.21).

$$E = E^{\circ} - \frac{RT}{nF} \ln \frac{a_{red}}{a_{ox}} \dots \text{Equ. 2. 21}$$

b) have stable potentials over long periods of time and

c) exhibit no hysteresis on passage of small currents or with temperature cycling.

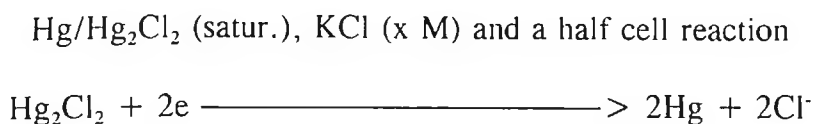
This include calomel electrodes, silver/silver chloride electrode e.t.c. These are then grouped into three classes, namely;

a) reference electrodes of the first kind- half cell involving a metallic or soluble phase in equilibrium with its ion e.g, H⁺/H₂, Ag⁺/Ag

b) reference electrode of the second kind- involving a metallic phase in equilibrium with its sparingly soluble salt e.g., Ag/AgCl, Hg₂Cl₂/Hg, HgSO₄/Hg and

c) reference electrode of the third kind which include all miscellaneous electrodes e.g., glass electrode, ion-specific electrodes e.t.c.

The most commonly used of these electrodes in electrochemical analysis is the calomel electrodes, whose half cell may be represented by



where x represents the molar concentration of KCl in the solution. This in turn determines the electrode potential as it controls the Cl⁻ ion activity. The half cell potentials of the various calomel electrodes used versus SHE, are shown in Table 2.2

Table 2.2: Standard potentials for the various types of calomel electrodes in the form (Pt)/H_{2(g)}/H⁺ (a=1); KCl/Hg₂Cl₂ (satur.)/Hg [72].

Name	KCl conc. (x M)	E° vs SHE at 25°C
Decimolar	0.1	0.336
molar	1.0	0.283
SCE	4.2 (saturated)	0.245

The decimolar and molar electrodes are preferred for very accurate work as they reach their equilibrium potentials more quickly as compared to the SCE. They also show very little hysteresis on temperature cycling. The SCE is however the most widely used reference electrode due to its easy preparation and maintenance. This is in disregard to its more pronounced hysteresis on temperature cycling [76].

A commercial calomel electrode consists of a tube 5-15 cm in length and 0.5 - 1.0 cm in diameter. The mercury, mercury (II) chloride (calomel) and potassium chloride paste is contained in the inner tube (see Fig. 2.8) which is connected to the

potassium chloride solution in the outer tube by means of glass wool plugged in the end of the inner tube. The whole electrode then interacts with the analyte present in the cell via the asbestos fibre at the end of the outer tube. Such an electrode has a resistance of about 200-300 Ω and has a very limited current carrying capacity before exhibition of severe polarization [76]. It however makes it difficult for ions to move in or out of the reference electrode. This helps prevent contamination.

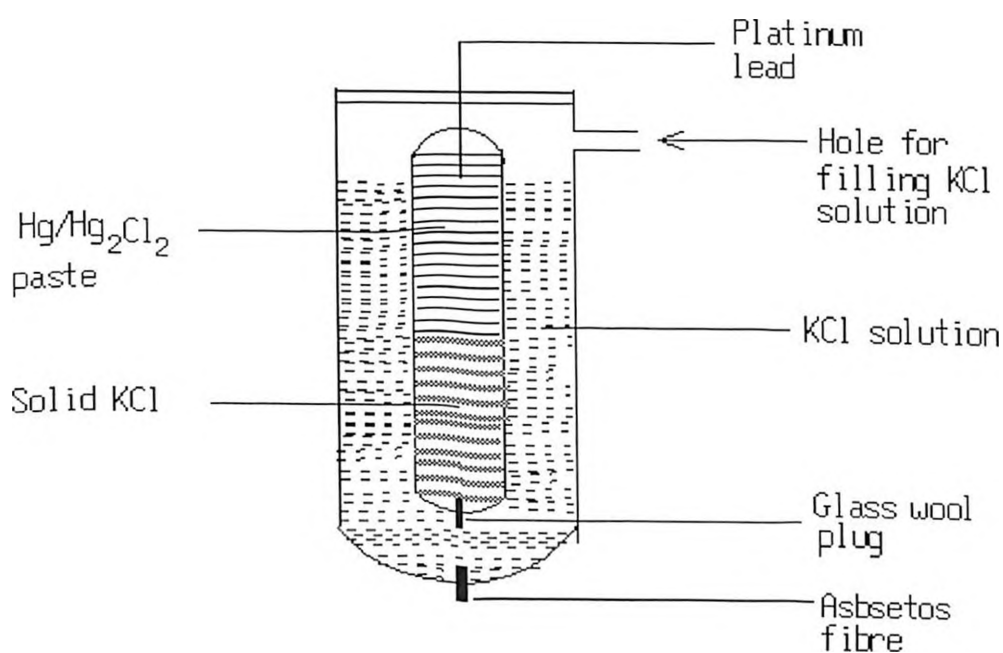


Fig. 2.8: A commercial calomel electrode [4].

CHAPTER THREE

RESULTS AND DISCUSSION

3.1) ENHANCEMENT OF LEAD REDOX CHARACTERISTICS AND DETECTION BY CLAY MODIFICATION OF THE WORKING ELECTRODE.

3.1.1 ELECTROCHEMISTRY OF LEAD ON A CARBON GRAPHITE ELECTRODE.

Lead electrochemical behaviour was initially studied on a bare carbon graphite electrode. This was done by dipping the electrode into a solution containing 1×10^{-3} M lead (II) nitrate and 0.1 M potassium nitrate and cycling the potential in the range -0.8 V to 0.4 V at a scan rate of 20 mV/sec. The cyclic voltammetric response (see Fig. 3.1.1) is characterized by a highly symmetrical and sharp oxidation peak at -0.39 V and a relatively broader reduction peak at -0.66 V.

The difference between the charges under the peaks is approximately 20 % of the total charge for both peaks. This value has been computed using the area under the voltammogram.

It was further observed that a nucleation loop was forming on reversal of the current direction, crossing at approximately -0.51 V and -0.56 V, and this may be attributed to the deposition of lead. On continued cycling, the voltammogram remained invariant suggesting a non-changing electrode surface [85]. It is also worth mentioning that hydrogen evolution was not observed within the potential range used in this analysis.

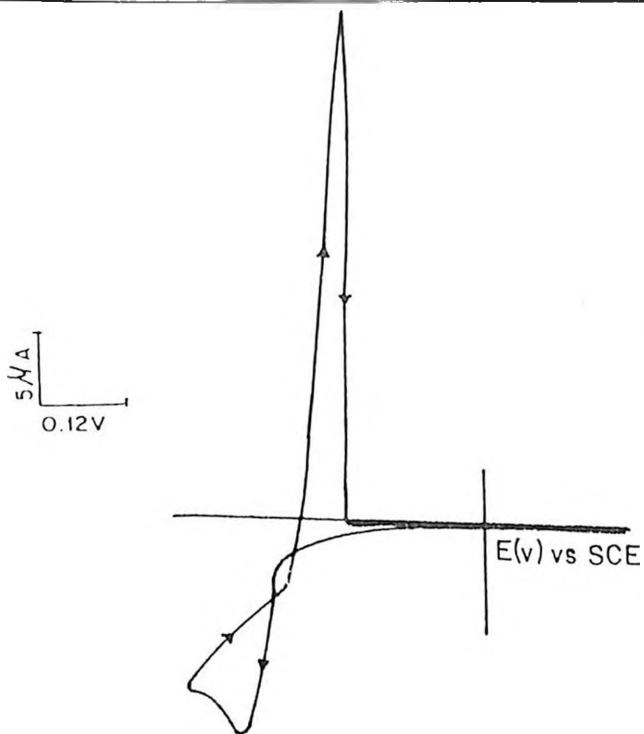


Fig. 3.1.1: Cyclic voltammetric response for bare carbon graphite electrode in a solution containing 0.001 M $\text{Pb}(\text{NO}_3)_2$ and 0.1M KNO_3 Potential range -0.8V to 0.4V scan rate 20 mV/sec.

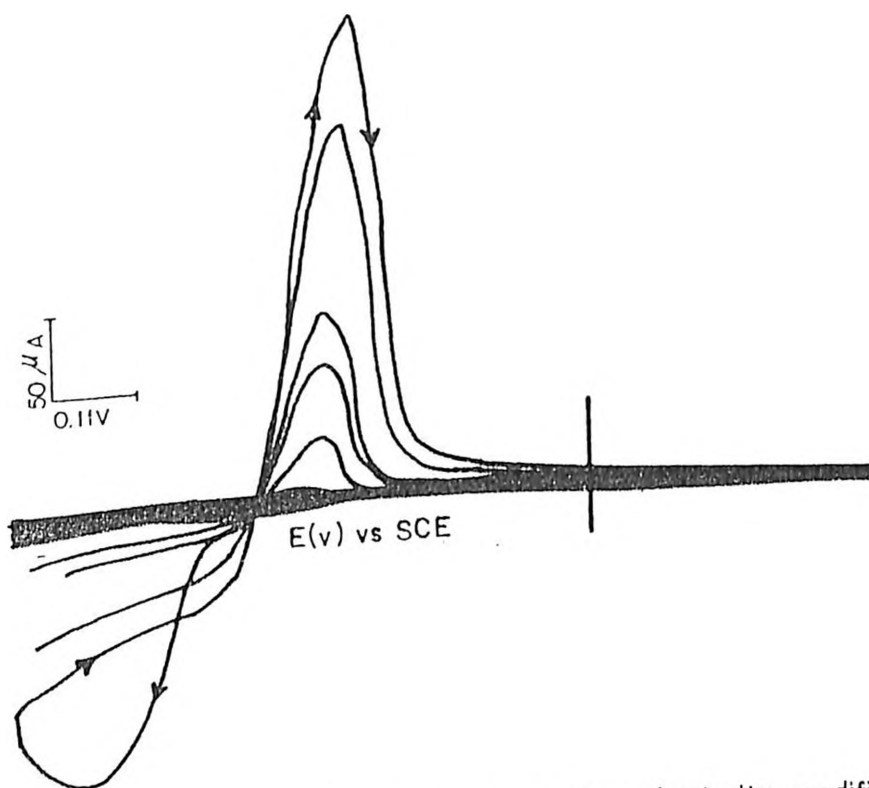


Fig. 3.1.3: Cyclic voltammetric response for a bentonite modified electrode in a solution containing 0.1M $\text{Pb}(\text{NO}_3)_2$ and 0.1M KNO_3 potential range -0.8V to 0.4V scan rate 50mV/sec.

Scan rate studies gave linear plots for anodic peak current versus square root of scan rate (see Fig. 3.1.2). This suggests that the process is diffusion limited, a fact enhanced by the peak tailing characterising the voltammogram. From the gradient of this plot, the diffusion coefficient was calculated to be 1.21×10^{-6} cm²/sec.

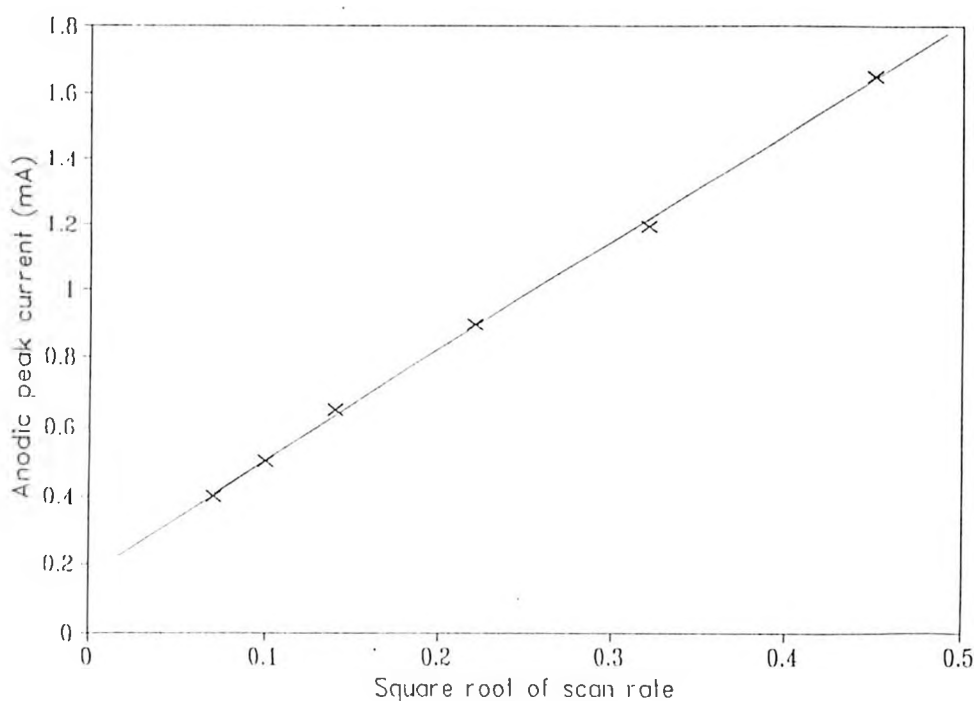


Fig. 3.1.2: A plot of anodic peak current versus square root of scan rate for a bare carbon electrode in a solution containing 0.001 M $\text{Pb}(\text{NO}_3)_2$ and 0.1 M KNO_3 . Potential range -0.8 V to 0.4 V.

3.1.2. REDOX CHEMISTRY OF LEAD ON A BENTONITE MODIFIED ELECTRODE.

The working electrode was then modified with bentonite (clay mineral) and dipped into a solution containing 0.1 M lead(II) nitrate and 0.1 M potassium nitrate, and the potential scanned from -0.8 V to 0.4 V at a scan rate of 50 mV/sec. The

resulting cyclic voltammetric response is shown in Fig. 3.1.3. The oxidative peak potential is now observed to have shifted by approximately 24 mV towards positive potentials as compared to the bare carbon electrode case. The reduction peak potential remains invariant i.e., -0.66 V. It is interesting to note that, the oxidative peaks are now much broader as compared to the bare electrode case. This is probably an indication of slow electron transfer in bentonite modified electrodes.

This observation is supported by the fact that during the first scan in the bare carbon electrode case, the total anodic charge was 6.37×10^{-3} coulombs while in the case of the bentonite modified electrode, the anodic charge was 1.25×10^{-3} coulombs on the eighteenth scan i.e., approximately 19 % of the bare electrode anodic charge.

Unlike in the case of the bare carbon electrode where the anodic and cathodic peak currents remained relatively constant on continued potential cycling (a fact which was attributed to a non-changing electrode surface), the anodic peak current for lead increased at the rate of 1.08×10^{-2} mA/min on the bentonite modified electrode.

A fresh bentonite electrode was next dipped into a solution containing 0.1 M $\text{Pb}(\text{NO}_3)_2$ and 0.1 M KNO_3 and potential scanned in the same range and at the same scan rate until the anodic charge was 7.89×10^{-4} coulombs. It was then transferred into a solution containing 0.1 M potassium nitrate only (no lead), and the potential cycled from -0.8 V to 0.4 V at a scan rate of 50 mV/sec. The cathodic and anodic peak currents were observed to decrease on continued potential cycling. The anodic peak current dropped at a rate of 1.06×10^{-2} mA/min.

This value is almost equal to that recorded for the rate of increase of anodic peak current and based on this observation, it can be inferred that leaching of the lead ions incorporated in the bentonite matrix is significant. This is probably due to the fact

that, the concentration of the electrolyte solution is high, hence solutions ion-exchange with the lead cations in the bentonite matrix is substantially high. The diffusion of lead cations from the bentonite matrix into the solution could also be playing a major role.

The next set of experiments involved studies on the effect of varying the concentration of the lead (II) nitrate, while maintaining that of potassium nitrate constant, at 0.1 M. When the concentration of lead nitrate was varied from 1.0 mM to 10 mM lead electrochemistry was not observed in the various samples, when the potential was scanned from -0.8 V to 0.4 V at a scan rate of 20 mV/sec.

When the bentonite electrodes used in the foregoing analysis were transferred separately into a solution containing 1.0 M hydrochloric acid, lead electrochemistry was registered in the form of current spikes at -0.50 V (see Fig. 3.1.4). The intensity of the spikes increase with the concentration of the lead (II) nitrate. It is apparent that despite the 150 mV shift towards negative potentials as compared to experiments conducted in 0.1 M KNO_3 , the current spikes/peaks represent the lead redox process. The shift in the potential probably has no electrochemical significance and could probably be related to proton activity within the interlamellar region [83]. This observation is very important and might prove useful in lead detection studies, more so now that lead is a major pollutant.

3.1.3 ELECTRODE MODIFICATION WITH PRE-TREATED BENTONITE

When a B-NPN modified electrode was dipped into a solution containing 0.1 M potassium nitrate, and the potential cycled from -0.8 V to 0.8 V at a scan rate of 20 mV/sec, the resultant cyclic voltammetric response (see Fig. 3.1.5) showed no evidence of lead electrochemical activity. A freshly prepared B-NPN modified

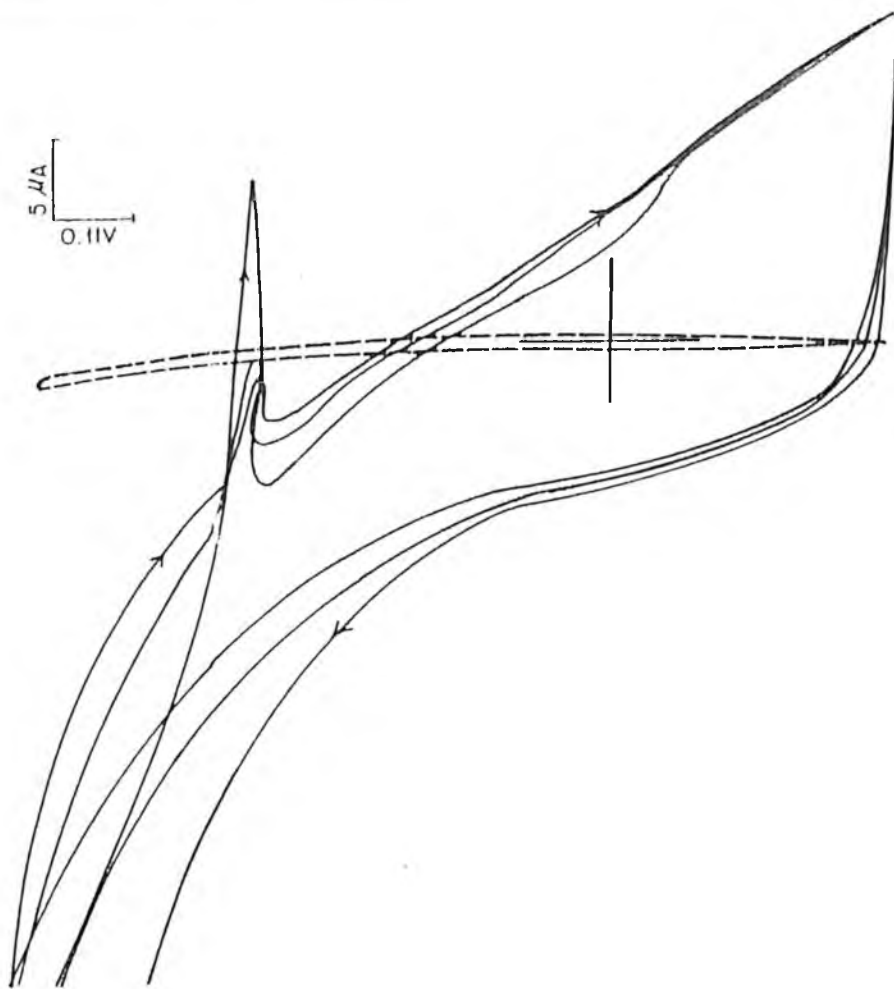


Fig. 3.1.4: Cyclic voltammetric response for a bentonite modified electrode in a solution containing 1M HCl (full lines) after transfer from a solution containing 1mM $\text{Pb}(\text{NO}_3)_2$ and 0.1M KNO_3 (dashed line). Potential range -0.8V to 0.4V . Scan rate $20\text{mV}/\text{sec}$.

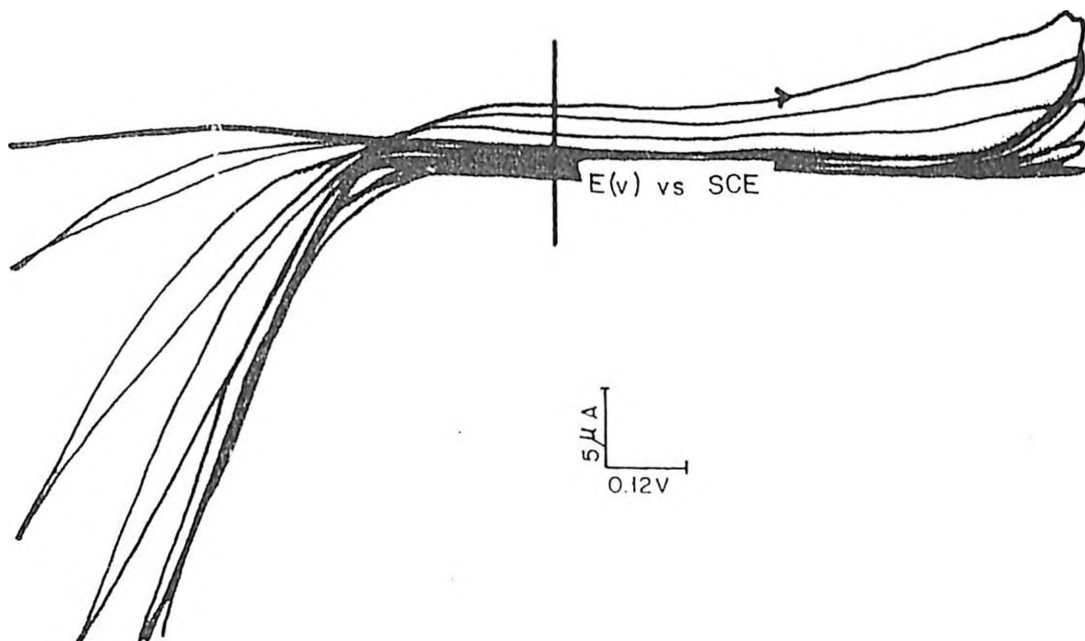


Fig. 3.1.5: Cyclic voltammetric response for a B-NPN modified electrode in a solution containing 0.1M KNO₃ potential range -0.8V to 0.8V. scan rate 20mV/sec.

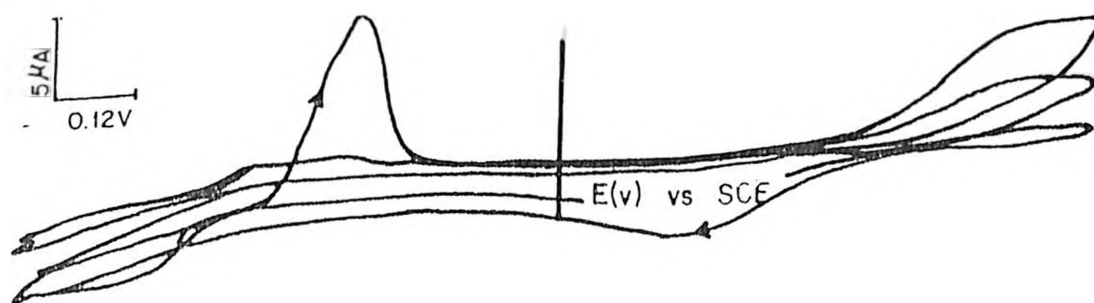


Fig. 3.1.6: Cyclic voltammetric response for a B-NPN modified electrode in a solution containing 1.0M H₂SO₄ potential range -0.8V to 0.8V Scan rate 20mV/sec.

electrode subjected to the same potential range and scan rate as for the foregoing case but now in a solution containing 1.0 M sulphuric acid, showed lead oxidation and reduction peaks at approximately -0.28 V and -0.57 V (see Fig. 3.1.6). This represents a shift of about 110 mV and 80 mV towards positive potentials for the oxidation and reduction peaks respectively compared to that of bare and bentonite modified electrodes in 0.1 M KNO_3 . On the second scan after the appearance of the lead oxidation peak however, its oxidation peak current dropped almost to zero.

It is important to mention that conventionally, lead electrochemistry in sulphuric acid has always been complicated by precipitation of lead sulphate. Hence, the fact that it was possible to observe, at least momentarily, lead redox characteristics in sulphuric acid when it is adsorbed on a clay mineral stresses the significance of electrode modification. The robust lead electrochemical activity during the first scan in sulphuric acid may be attributed to the high proton activity in the interlamellar region before the *ion pairing effect* of the SO_4^{2-} sets in leading to the precipitation of lead sulphate and complete reduction in electrochemical activity [83].

B-WPN modified electrodes were subjected to similar electrochemical investigations i.e., the electrode dipped in a solution containing 0.1 M potassium nitrate and 1.0 M sulphuric acid and potential cycled from -0.8 V to 0.8 V at a scan rate of 20 mV/sec. The cyclic voltammetric responses were very different compared to that of B-NPN in 0.1 M KNO_3 (see Fig. 3.1.7). An even more well defined electrochemical response was recorded in a solution containing 1.0 M sulphuric acid (see Fig. 3.1.8) on cycling the potential within the same range and at the same scan rate. The anodic and cathodic peaks in 0.1 M KNO_3 and 1.0 M H_2SO_4 media occurred

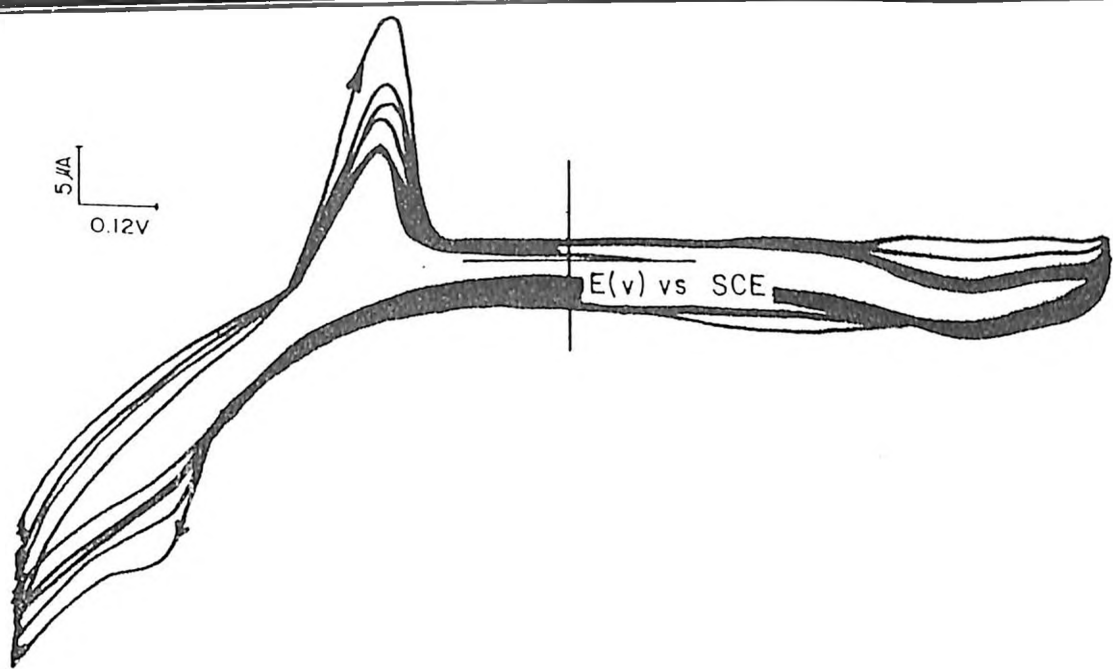


Fig. 3.1.7: Cyclic voltammetric response for a B-WPN modified electrode in a solution containing 0.1M KNO_3 . Potential range -0.8V to 0.8V . Scan rate $20\text{mV}/\text{sec}$.

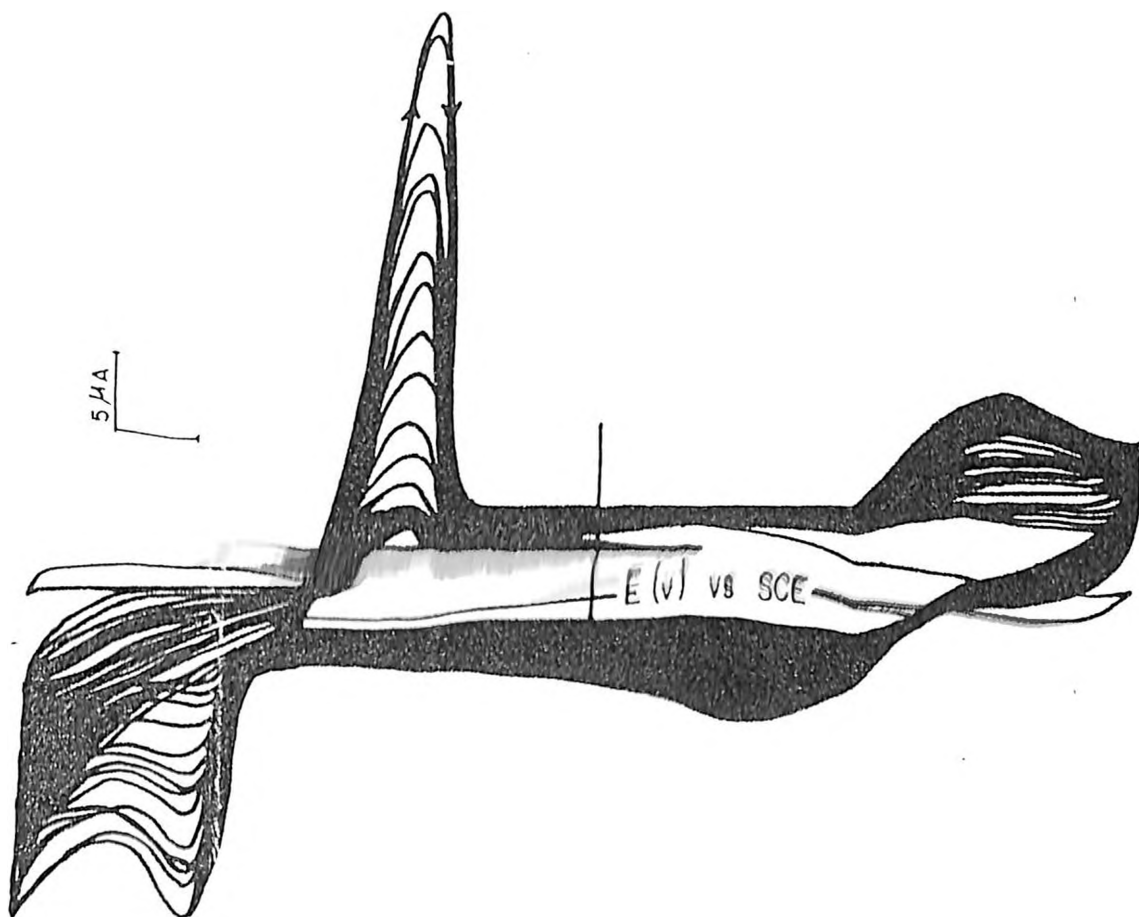


Fig. 3.1.8: Cyclic voltammetric response for a B-WPN modified electrode in a solution containing 1.0M H_2SO_4 . Potential range -0.8V to 0.8V . Scan rate $20\text{mV}/\text{sec}$.

at -0.26 V/-0.54 V and -0.29 V/-0.56 V respectively with a redox efficiency of about 58 % in 1 M H₂SO₄.

The difference in lead electrochemical activity in B-WPN and B-NPN electrodes was attributed to the increased level of potassium ion (K⁺) concentration in the bentonite (B-WPN) matrix through isomorphous substitution of exchangeable cations in the bentonite and/or adsorption on the surface of the clay mineral. The K⁺ probably facilitates charge transport, leading to the enhancement of the observed peak currents.

3.1.4 ELECTROCHEMICAL ANALYSIS OF POLYANILINE REDOX PROPERTIES ON PRE-TREATED BENTONITE HOST-MATRIX

In the next set of experiments, the B-NPN and B-WPN modified electrodes were used as host matrices for the electrodeposition of a polyaniline - a conducting polymer.

Freshly prepared B-NPN and B-WPN electrodes were dipped into a solution containing 1.0 M sulphuric acid and 0.1 M aniline. The potential was then cycled from -0.8 V to 0.80 V at a scan rate of 20 mV/sec. The B-NPN electrode yielded the cyclic voltammogram shown in Fig. 3.1.9. While the voltammograms yielded by B-WPN are shown in Fig. 3.1.10. Polyaniline oxidation and reduction peaks were observed at 0.17 V and 0.036 V for B-NPN modified electrode. The lead redox activity diminishes as already mentioned earlier. The polyaniline redox chemistry on a B-WPN electrode was relatively similar to that on a B-NPN electrode i.e., the oxidation and reduction peaks occurred at approximately 0.18 V and 0.036 V respectively while lead oxidative peak occurred at -0.29 V.

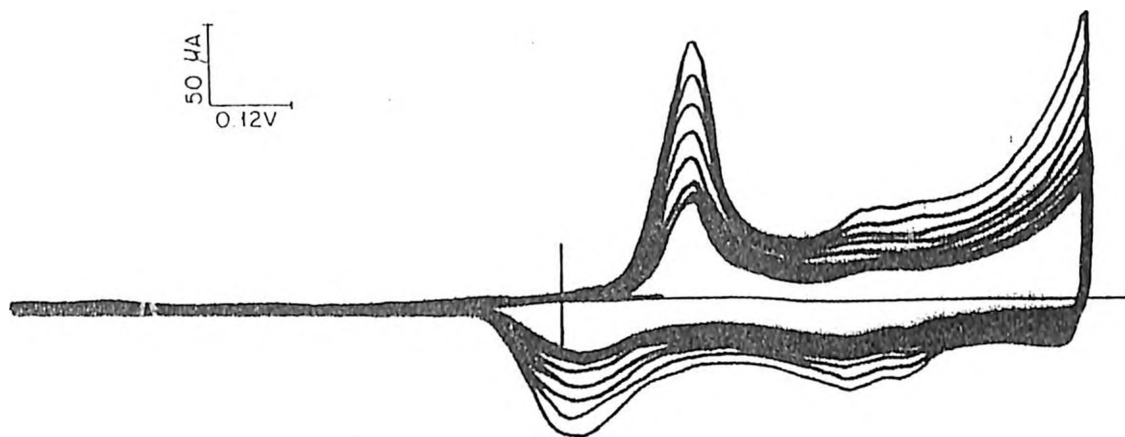


Fig. 3.1.9 Cyclic voltammetric response for a B-NPN modified electrode in a solution containing 1.0M H_2SO_4 and 0.1M aniline. Potential range -0.8V to 0.8V. Scan rate 20mV/sec.

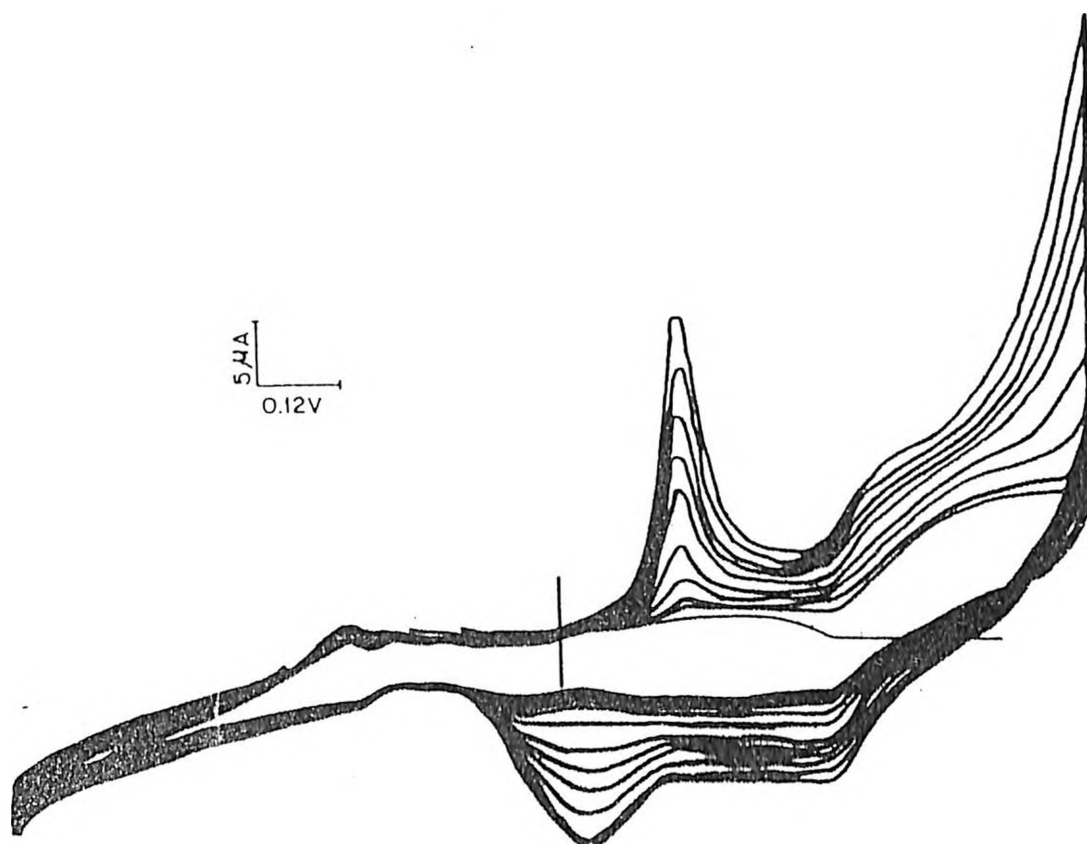


Fig. 3.1.10 Cyclic voltammetric response for a B-WPN modified electrode in a solution containing 1M H_2SO_4 and 0.1M aniline. Potential range -0.8V to 0.8V. Scan rate 20 mV/sec.

The modification of the electrode with B-NPN or B-WPN does not appear to alter significantly the electrochemistry of polyaniline vis-a-vis that obtained on unmodified (bare) carbon and bentonite modified electrodes where the oxidation/reduction peaks appear at around 0.2 V/0.04 V respectively [8].

The rates of change of anodic peak current for polyaniline on a bare bentonite, B-NPN and B-WPN modified electrodes and the polyaniline redox efficiency on each of these electrodes are shown in Table 3.1.

Table 3.1: Rate of change of i_{pa} and redox efficiency of polyaniline on various types of bentonite modified electrodes.

Electrode Material	Rate of Change of i_{pa} (mA/min)	Polyaniline Redox Efficiency (%)
Bare bentonite	1.20×10^{-3}	50
B-NPN	1.70×10^{-3}	50
B-WPN	4.25×10^{-3}	63

The results show clearly that the presence of lead in the host matrix affects the electrodeposition of polyaniline. This could probably be by electron transfer mediation. This occurs despite the fact that the two redox centres are about 500 mV apart. These values are however not significantly different, suggesting that ion exchange kinetics for the anilinium radical cation (which is the precursor to polyaniline) is not strongly affected by the presence of lead (II) cations. The anilinium cation radicals can migrate into the clay mineral matrix as the basal spacing is not fixed. In the case of pillared bentonite, the anilinium radical cation would probably have been excluded due to its size [84].

It is also difficult to speculate on the formation of a bilayer between the B-NPN/B-WPN and polyaniline interface, as no electrochemical features such as charge rectification, which are characteristic of bilayer electrode were observed.

3.2 LEAD (II) AND POLYANILINE ELECTROCHEMISTRY ON AN ION-EXCHANGE RESIN MODIFIED ELECTRODE.

3.2.1 ELECTROCHEMISTRY OF LEAD ON AN AMBERLITE MODIFIED ELECTRODE

A bare amberlite modified electrode was dipped into a solution containing 0.1 M potassium nitrate and potential cycled from -0.8 V to 0.8 V at 20 mV/sec so as to test its stability in this electrolytic media. It was found that these electrodes could stay for up to 6 hours in the solution without developing any major/or visible cracks. This period was even much longer for those cases where the modification material had previously been soaked in the target metal cation solution i.e., A-WPN and A-NPN.

Cycling potential from -0.8 V to 0.4 V at a scan rate of 20 mV/sec in a solution containing 0.1 M lead (II) nitrate and 0.1 M potassium nitrate, gave the cyclic voltammetric response shown in Fig. 3.2.1. It can be observed that broad but well defined oxidation and reduction peaks appear, at approximately -0.29 V and -0.70 V respectively. This represents a shift of 100 mV towards positive potential for the oxidation peak and 40 mV towards the negative potentials for the reduction peak. The nucleation loops crosses at -0.44 V and -0.62 V in this case as compared to -0.51 V and -0.56 V for the bare electrode.

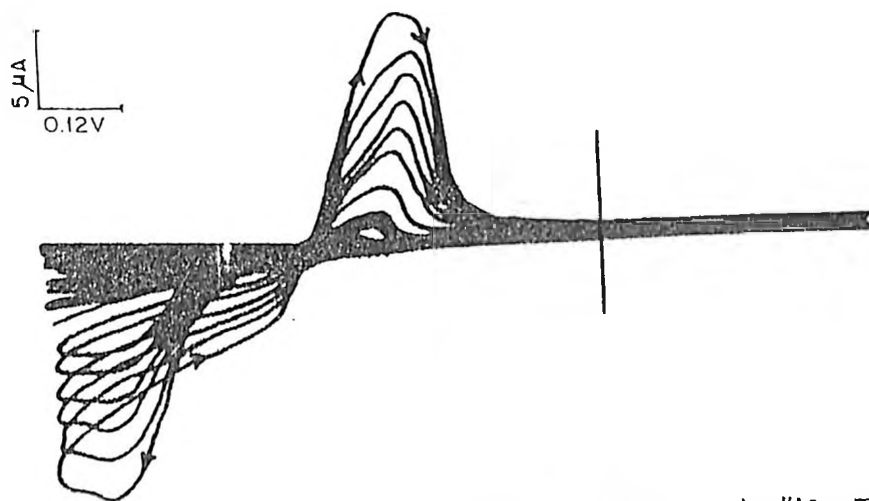


Fig. 3.2.1 Cyclic voltammetric response for an amberlite modified electrode in a solution containing 0.1M $\text{Pb}(\text{NO}_3)_2$ and 0.1M KNO_3 . Potential range -0.8V to 0.4V . Scan rate $20\text{mV}/\text{sec}$.

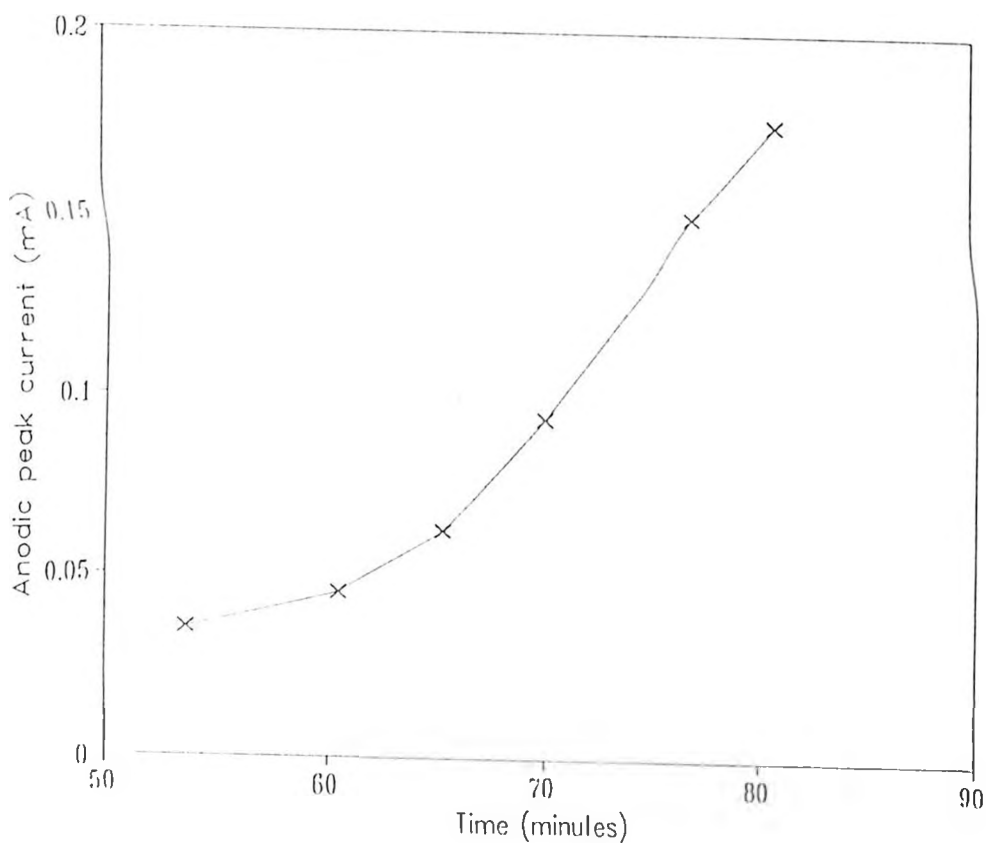


Fig. 3.2.2: A plot of anodic peak current versus time for an amberlite modified electrode in a solution containing 0.1 M $\text{Pb}(\text{NO}_3)_2$ and 0.1 M KNO_3 . Potential range -0.8 V to 0.4 V. Scan rate 20 mV/sec.

It was also observed that the oxidation peak current increased on continued cycling of the potential. The rate of change of the anodic peak current as given by the slope of the plot of anodic peak current versus time (see Fig. 3.2.2) is 7.5×10^{-3} mA/min.

It is important to mention that the average time taken, for the first lead redox peaks to appear varied largely for different electrodes. These differences, ranging from 20 to 70 minutes can be attributed to non-reproducibility of the surface

morphology. The importance of surface morphology on electrochemical response has also been observed with clay minerals [52].

The electrodes used in the foregoing analysis were then transferred to solutions containing only 1.0 M sulphuric acid. The general electrochemical pattern observed was that on cycling the potential from -0.8 V to 0.4 V, there was an increase in both the anodic and cathodic peak currents for the first two minutes followed by a reduction (see Fig. 3.2.3). This increase, may as the case of bentonite, be attributed to the presence of protons within the matrix. This enhances the conductivity of lead.

The ratio of anodic to cathodic peak currents i_{pa}/i_{pc} during the increase was greater than unity i.e., approximately 2.0. The measurements were made from the zero current baseline. This can be attributed to the fact that electron transfer was from the Pb(II) trapped in the amberlite matrix [52]. The ratio i_{pa}/i_{pc} was still greater than unity in the decreasing peak current case too.

The mean stripping rate obtained for different samples on calculating the slope of the plot of anodic peak current versus time (see Fig. 3.2.4) was found to be 8.75×10^{-2} mA/min. It is important to mention that during both current phases characterized by an increase in the peak current followed by a decrease, the peak potentials shifted towards negative potentials for both the anodic and cathodic peaks by about 135 mV and 30 mV respectively. This as already mentioned was due to the changing electrode surface.

When similar experiments were repeated but now in an electrolytic media containing only 0.1 M potassium nitrate, large decrease in anodic peak currents were observed i.e., from 240 μ A to 150 μ A during the first scan and from 150 μ A to 90 μ A during the second scan. There were equally large shifts in anodic peak potentials

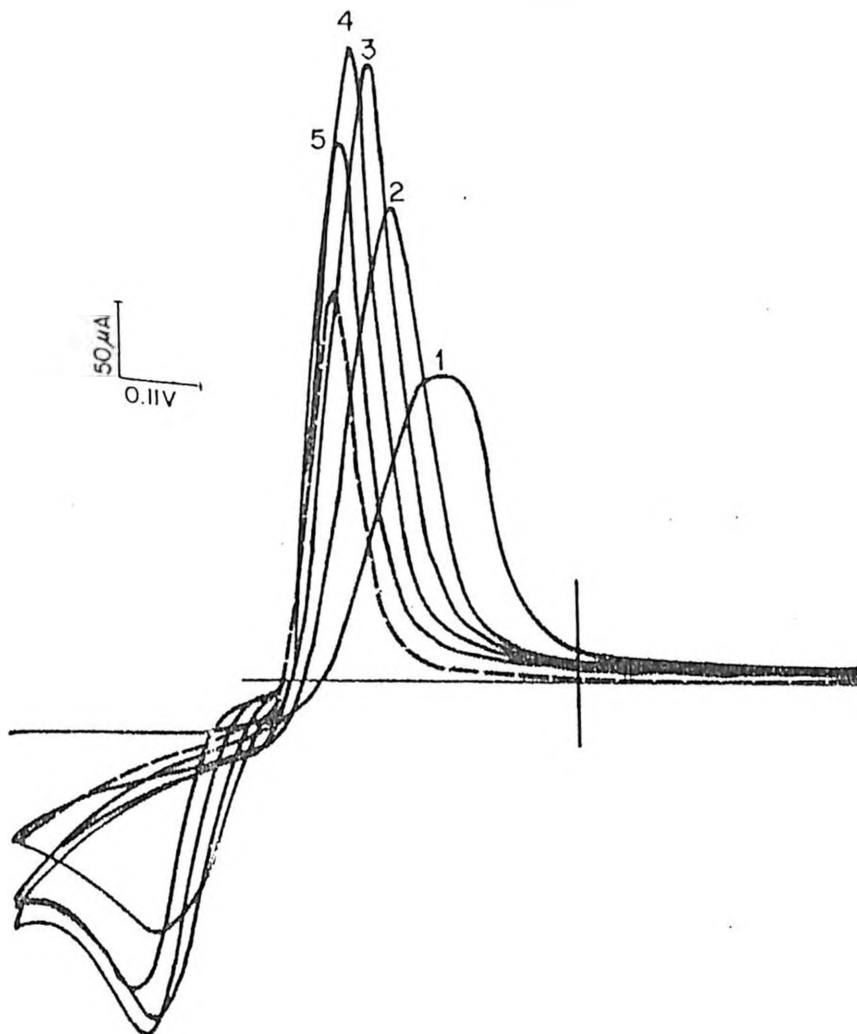


Fig. 3.2.3: Cyclic voltammogram response for an amberlite modified electrode on transfer into a solution containin 1.0M H_2SO_4 (full lines) from a solution containing 0.1M $Pb(NO_3)_2$ and 0.1M KNO_3 (dashed line). Potential range $-0.8V$ to $0.4V$. Scan rate $20mV/sec$.

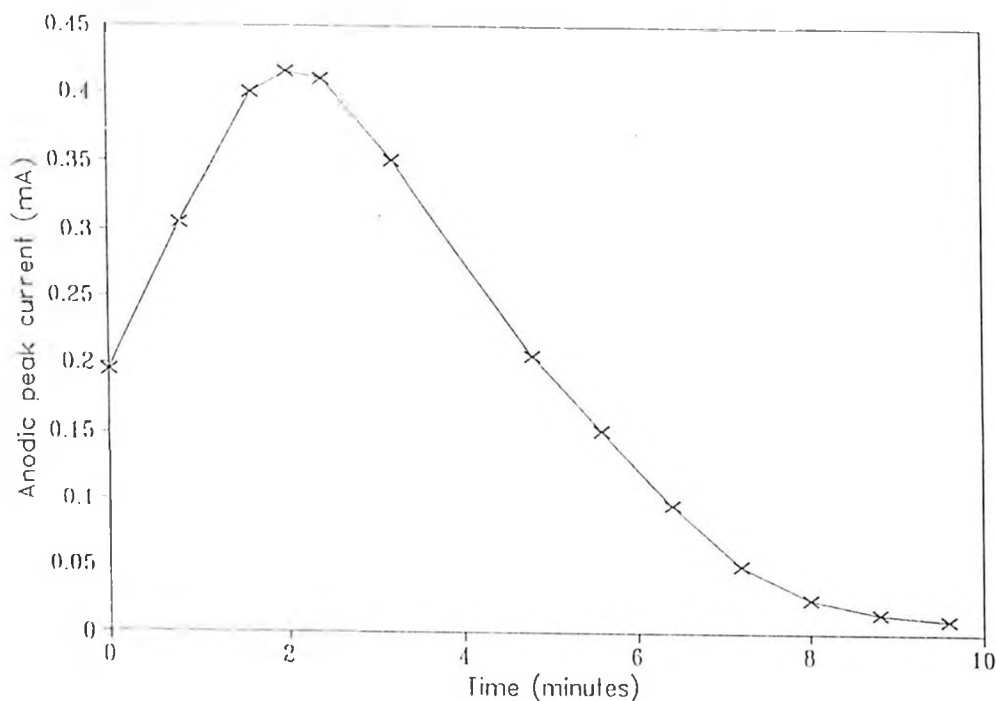


Fig. 3.2.4: A plot of anodic peak current versus time for an amberlite modified electrode (after incorporation of lead (II) from solution) after being transferred in a solution containing 1.0 M H_2SO_4 .

towards negative potentials i.e., 106 mV and 71 mV during the first and second scan respectively (see Fig. 3.2.5). The average rate of decrease of anodic peak current for these electrodes was determined to be about 1.2×10^{-2} mA/min. The significant changes during the leaching of Pb(II) were attributed to changes in the electrode surface, and solutions ion-exchange with ions in the resin matrix. The latter will be dependent on the nature/type of the cation and concentration of the supporting electrolyte [52,53,84].

Fresh amberlite electrodes were dipped into a solutions containing 0.1 M potassium nitrate and varying concentrations of lead i.e., 10^{-5} , 10^{-4} , 10^{-3} , 10^{-2} and 10^{-1}

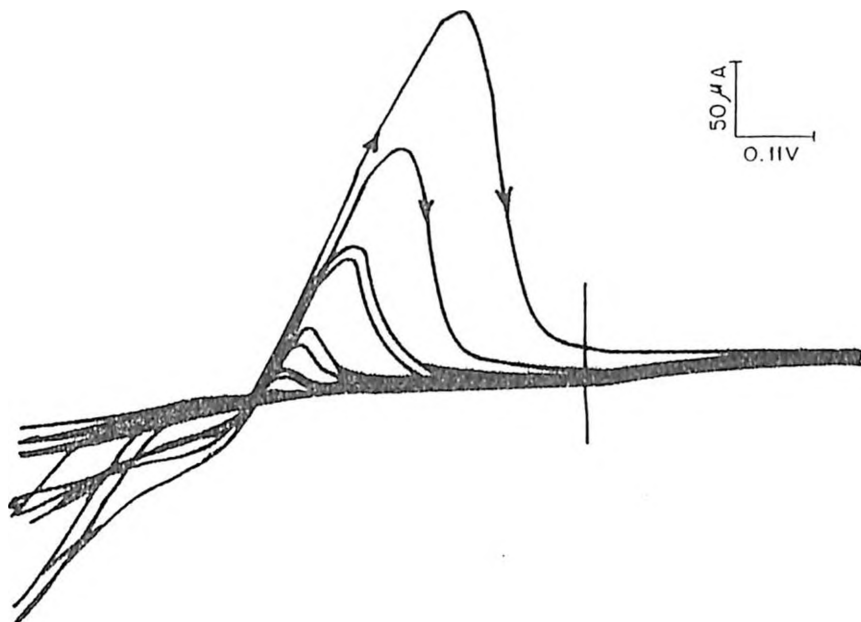


Fig 3.2.5: Cyclic voltammetric response on transfer of an amberlite modified electrode (after incorporation of lead (II) from solution) into a solution containing 0.1M KNO_3 . Potential range -0.8V to 0.4V. Scan rate 20mV/sec.

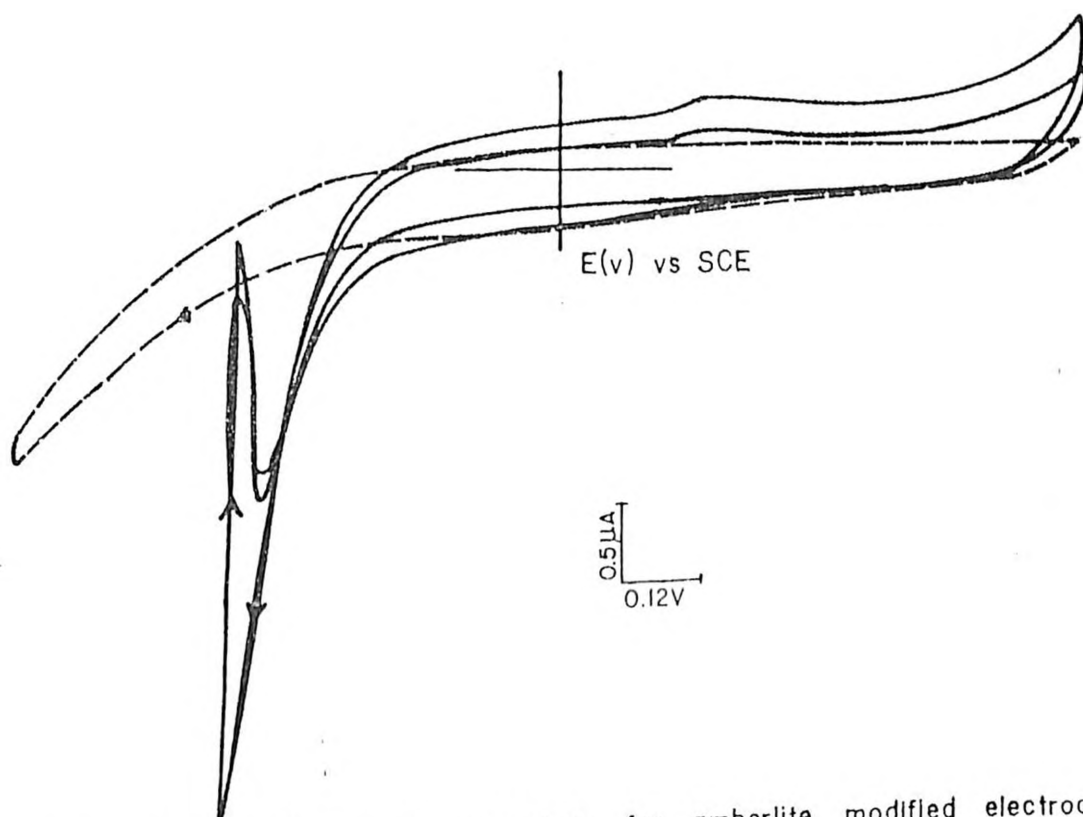


Fig. 3.2.6: Cyclic voltammetric response for amberlite modified electrode on transfer into a solution containing 1.0M HCl (full lines) from a solution containing 10^{-5} $\text{Pb}(\text{NO}_3)_2$ and 0.1M KNO_3 (dashed line). Potential range -0.8V to 0.4V. Scan rate 20mV/sec.

M and potential cycled from -0.8 V to 0.4 V at 20 mV/sec. It was observed that lead (II) electrochemical activity was only observable in solutions of concentrations greater than 10^{-3} M. This was also applicable to the bare carbon electrode.

However, on cycling the potential of an amberlite modified electrode for about one hour in solutions containing lead (II) nitrate concentrations of even up to 10^{-6} M and 0.1 M potassium nitrate (constant), from -0.8 V to 0.4 V at 20 mV/sec, and then transfer the electrode into a solution containing 1.0 M hydrochloric acid, it was observed that lead (II) oxidation peaks appeared at -0.45 V. This represents a shift of 160 mV towards negative potentials (see Fig. 3.2.6). The important electrochemical feature to note is that the size of the current spikes were observed to decrease with the concentration of lead (II) nitrate. This shows that an amberlite modified electrode is even more sensitive than the bentonite modified electrode. This property seems inherent of ion exchangers due to their ability to pre-concentrate lead ions from the dilute solutions. It is thus important that ion exchangers with a high preference for lead be investigated and this procedure be improved as a method of quantitative and qualitative analysis of lead.

3.2.2 ELECTRODE MODIFICATION WITH PRE-TREATED AMBERLITE

In this set of experiments, the electrode was modified with amberlite prepared in the manner described in section 2.3.1.

A A-WPN modified electrode was dipped into a solution containing 1.0 M sulphuric acid and the potential cycled from -0.8 V to 0.8 V at a scan rate of 20 mV/sec. There was no evidence of Pb(II) electrochemical activity (see Fig. 3.2.7). On

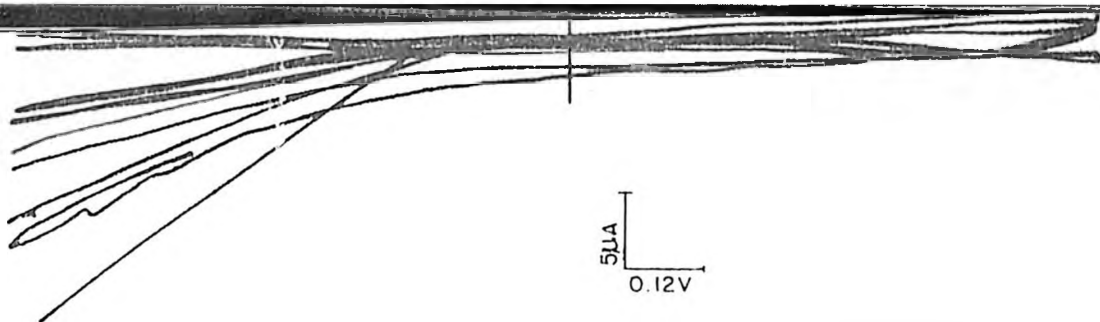


Fig. 3.2.7: Cyclic voltammetric response for a A-WPN modified electrode in a solution containing 1.0M H_2SO_4 . Potential range $-0.8V$ to $0.8V$. Scan rate $20mV/sec$.

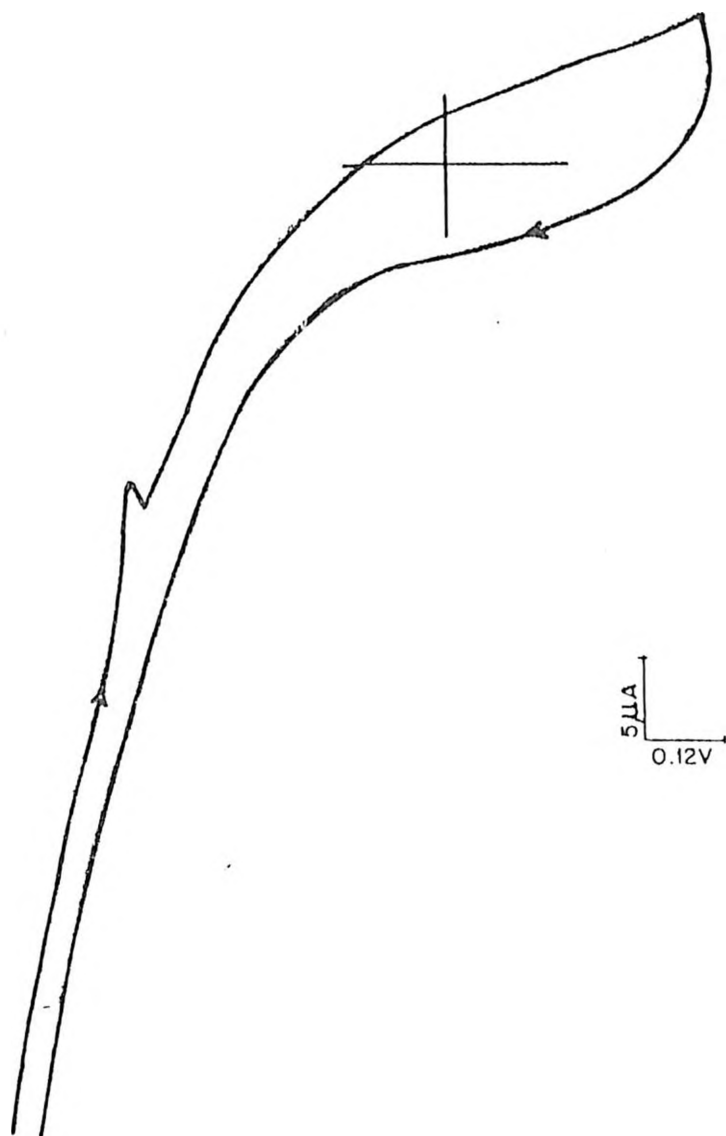


Fig. 3.2.8: Cyclic voltammetric response for a A-WPN modified electrode in a solution containing 1.0M H_2SO_4 . Potential range $-0.8V$ to $0.8V$. Scan rate $20mV/sec$.

the contrary, the A-NPN modified electrode under the same electrochemical environment yielded cyclic voltammograms characterized by a lead oxidation peak at -0.46 V. These peaks were in form of spikes (see Fig. 3.2.8). A plot of i_{pa} versus square root of scan rate yielded a linear plot as shown in Fig. 3.2.9. From the slope of this plot, we obtained the apparent diffusion coefficient for Pb(II) to be 8.32×10^{-5} cm²/sec.

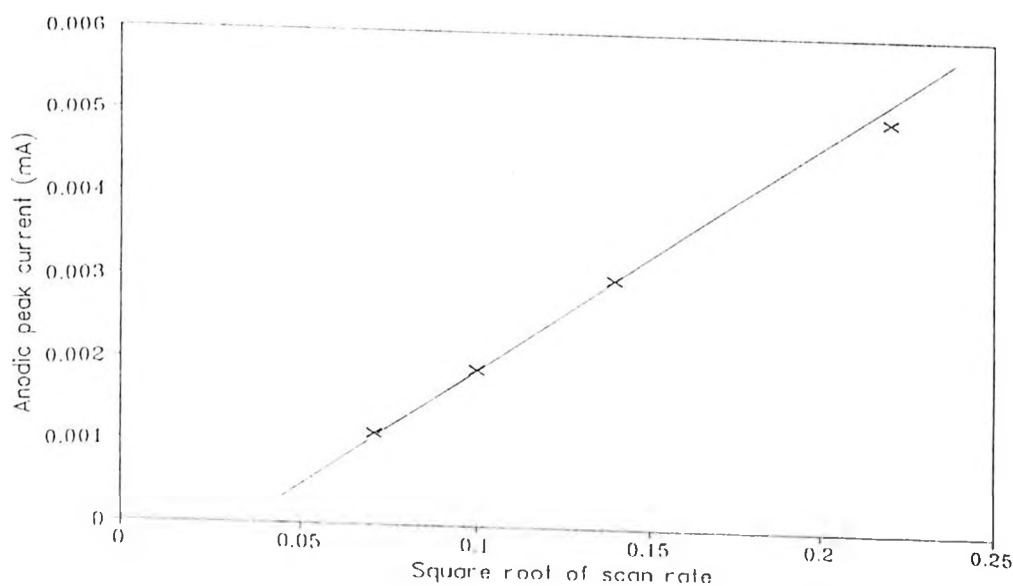


Fig. 3.2.9: A plot of anodic peak current versus square root of scan rate for a A-NPN modified electrode in a solution containing 1.0 M H₂SO₄. Potential range -0.8 V to 0.8 V.

This is quite high as compared to that of cations in clay minerals [84]. This difference can be attributed to the fact that we are dealing with a cation exchanger with anionic sites favouring cation incorporation. Even though we do have oxyanions requiring charge compensation by cations in montmorillonites such as 2:1 phyllosilicates [52,84], the kinetics of cation transport in clays is probably much slower than in the case of an exchange resin.

3.2.3 POLYANILINE REDOX FEATURES ON A PRE-TREATED AMBERLITE MODIFIED ELECTRODE

In this experiments polyaniline was electrodeposited on an A-NPN modified electrode, by cycling the potential from -0.8 V to 0.8 V in a solution containing 1.0 M sulphuric acid and 0.1 M aniline at 20 mV/sec. The resultant cyclic voltammetric response is shown in Fig. 3.2.10. It may be observed that polyaniline oxidation and reduction peaks appeared at 0.20 V and 0.036 V respectively. No lead redox peaks were observed even after 213 minutes. Similar experiment were repeated using A-WPN modified electrode. The overall electrochemical features of the cyclic voltammograms were the same, except that the rate of change of peak current was lower than in the case of A-NPN i.e., 8.5×10^{-5} mA/min for A-WPN and 1×10^{-4} mA/min for A-NPN. When the slopes of plots for cathodic versus anodic peak currents were computed to obtain the redox efficiency of the process, it was found that the redox efficiency was about the same in both cases i.e., 65 % for A-WPN and 67 % A-NPN.

The low rate of electrodeposition of polyaniline in the presence of K^+ ions (for A-WPN modified electrode) can be attributed to the competition between the anilinium radical cation (or aniline monomer) and K^+ to exchange into the resin matrix. The favoured process is probably exchange of K^+ due to its small size.

Plots of anodic peak currents versus scan rate, for polyaniline were linear. This suggest that polyaniline is a surface attached [8].

In our next experiment, an amberlite modified electrode was dipped into a solution containing 0.1 M lead nitrate and 0.1 M potassium nitrate and the potential cycled from -0.8 V to 0.8 V at 20 mV/sec. The electrode was then transferred into

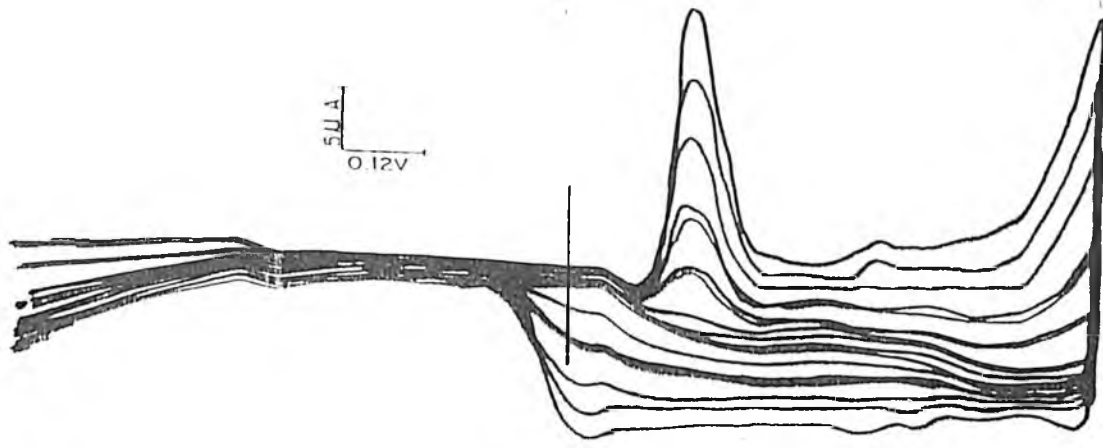


Fig 3.2.10 Cyclic voltammetric response for a λ -WfN modified electrode in a solution containing 1.0M H_2SO_4 and 0.1M aniline. Potential range -0.8V to 0.8V. Scan rate 20 mV/sec.

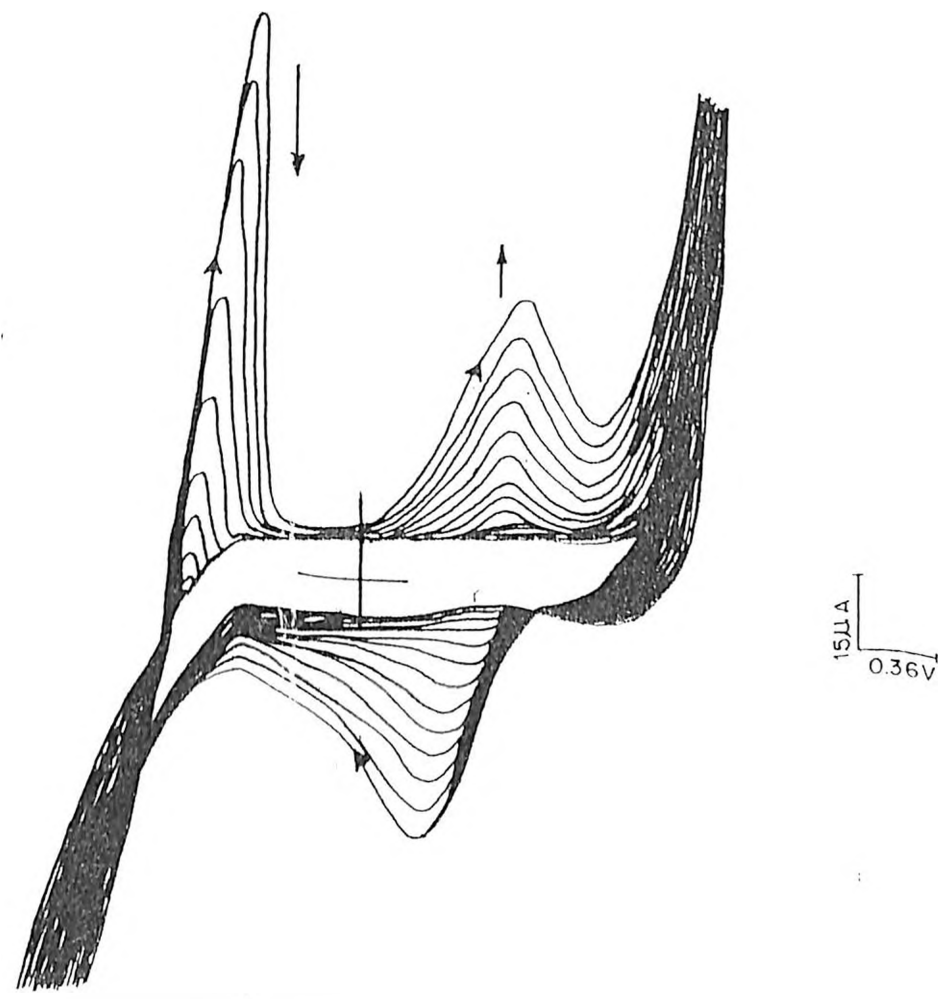


Fig. 3.2.11 Cyclic voltammetric response for an amberlite modified electrode (after incorporation of lead (II) from solution) in a solution containing 1.0M H_2SO_4 and 0.1M aniline. Potential range -0.8V to 0.8V. Scan rate 20mV/sec

a solution containing 1 M sulphuric acid and 0.1 M aniline for the purpose of electrodepositing polyaniline on it. The lead oxidation peak appearing at -0.37 V was found to be diminishing. An anodic and a cathodic peak were observed to be growing at 0.34 V and 0.2 V respectively (see Fig. 3.2.11). This was attributed to the shifting of the polyaniline redox peaks towards positive potentials due to the high internal pH of the amberlite host matrix. This behaviour is typical of polyaniline and has been observed by other researchers [8].

3.3 POLYANILINE-COPPER REDOX CHEMISTRY ON CLAY MINERAL(BENTONITE) HOST MATRIX.

3.3.1 ELECTROCHEMISTRY OF COPPER ON A BARE CARBON GRAPHITE ELECTRODE

In the set of experiments to be discussed, the key objective was to study the electrochemical interaction between two redox centres whose formal potentials are close. In our case, the redox centres were those of copper and polyaniline.

The copper redox centre was to be attached to a host matrix with cationic exchange properties and polyaniline electrodeposited on the matrix thereafter. The formation of a bilayer was anticipated more so because of the closeness of the oxidation peaks displayed by these two centres. Electrochemical analysis were started by studying the copper redox process on a bare carbon electrode.

The carbon graphite working electrode was dipped into a solution containing 0.01 M copper sulphate and 0.1 M sulphuric acid and the potential cycled from -0.3 V to 0.6 V, at a scan rate of 20 mV/sec. The cyclic voltammogram obtained (see Fig. 3.3.1), is characterized by an oxidation peak at 0.12 V and a reduction peak at -0.19 V. On continued cycling, both the oxidative and reductive peak currents remain relatively constant. From the cyclic voltammogram it was observed that the difference between anodic and cathodic charge is approximately 17 %. This is based on the difference between the areas under the peaks compared to the total area. A bentonite modified electrode dipped into a solution containing 0.1 M sulphuric acid and 0.01 M copper sulphate and potential cycled from -0.3 V to 0.6 V at a scan rate of 20 mV/sec gave the cyclic voltammetric response is shown in Fig. 3.3.2. It can be

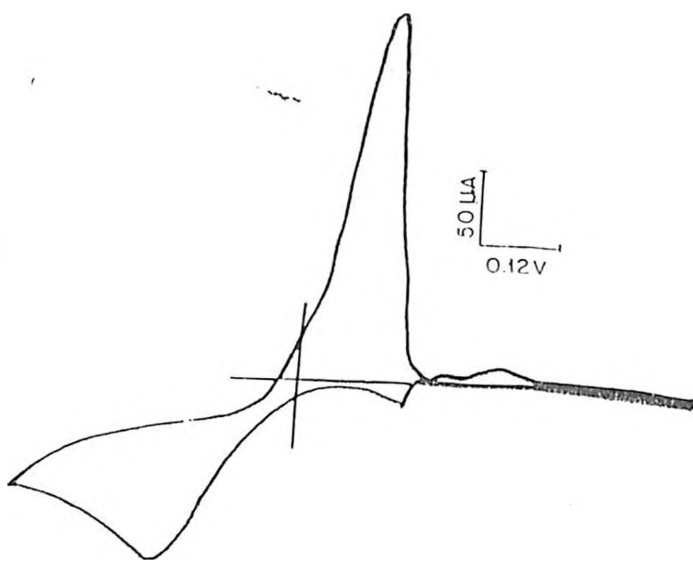


Fig 3.3 1: Cyclic voltammetric response on a bare carbon electrode in a solution containing 0.1M H_2SO_4 and 0.01M $CuSO_4$. Potential range $-0.3V$ to $0.6V$. Scan rate of $20mV/sec$.

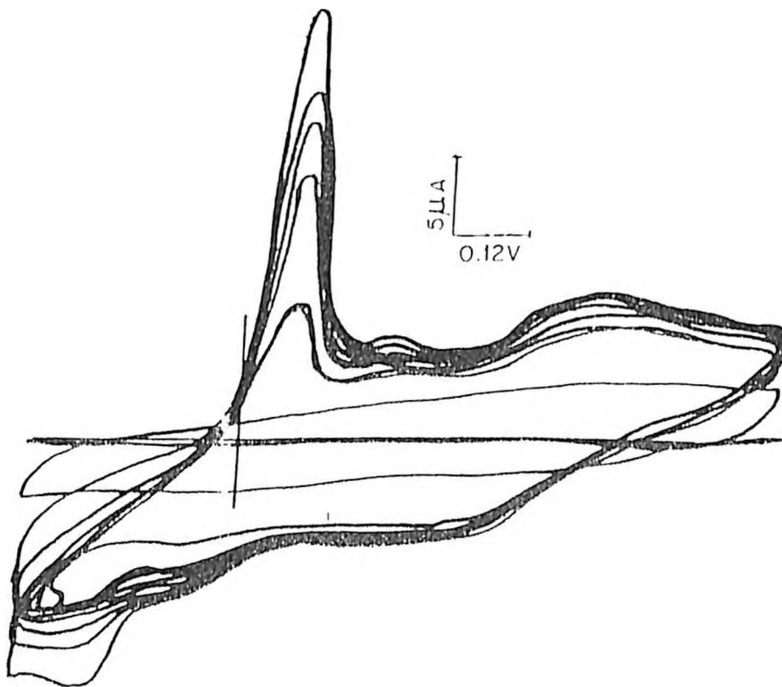


Fig 3.3 2: The cyclic voltammetric response for a bentonite modified electrode in a solution containing 0.1M H_2SO_4 and 0.01M $CuSO_4$. Potential range $-0.3V$ to $0.6V$. Scan rate $20mV/sec$.

3.3.2 ELECTROCHEMISTRY OF COPPER ON A BENTONITE MODIFIED ELECTRODE.

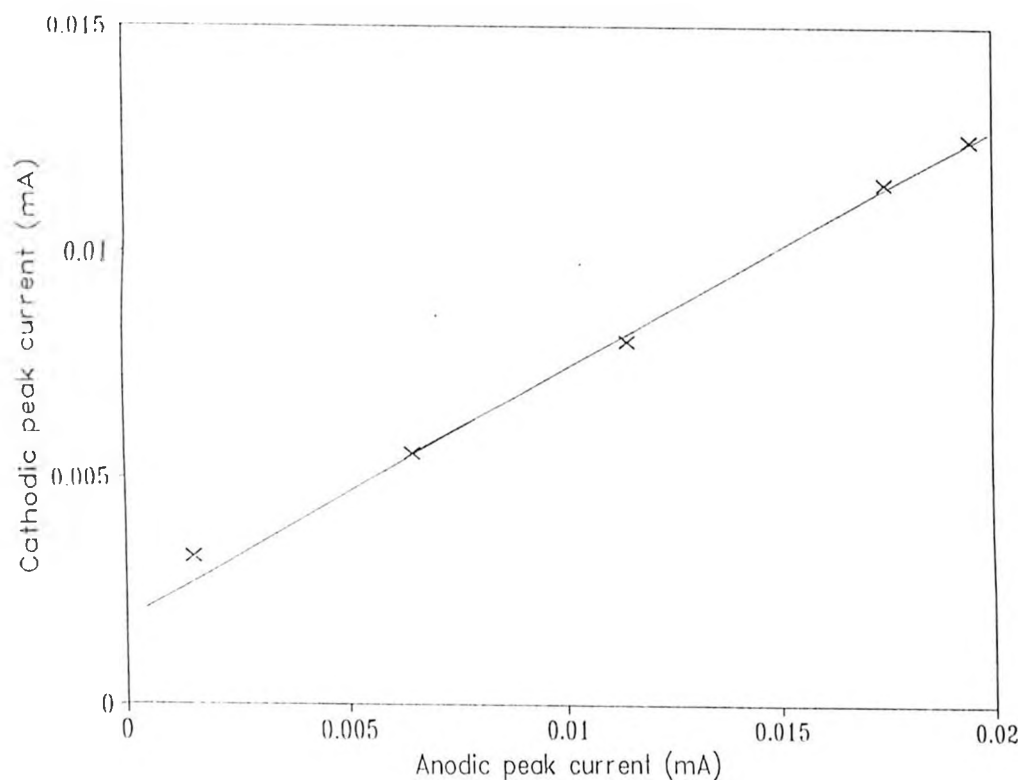


Fig. 3.3.3: A plot of the cathodic versus anodic peak current used in calculating the redox efficiency for copper redox process on a bentonite modified electrode.

observed that a well defined anodic peak, with a peak potential of approximately 0.1 V, and a cathodic peak at -0.21 V were formed. These peaks are attributed to the oxidation of copper [3]. The redox efficiency of this process as obtained from plot of cathodic versus anodic peak currents (see Fig. 3.3.3) was 45 %, while the rate of change of the anodic peak current was found to be 3.57×10^{-4} mA/min. This shows that the rate of dissolution of copper is much higher in the case of a bentonite

modified electrode than on a bare carbon electrode, where the anodic peak current had been observed to remain relatively unchanged.

Plots of the variation of the anodic peak current with the square root of scan rate i.e., i_p vs $v^{1/2}$ yielded plots with linear dynamic range confined to values below 80 mV/sec (see Fig. 3.3.4). The curvature in the i_p vs $v^{1/2}$ plot at high scan rate values can probably be attributed to the fact that, the concentration of the electroactive species (adsorbed) decreases during the recording of the voltammograms at different scan rates as a result of leaching [84].

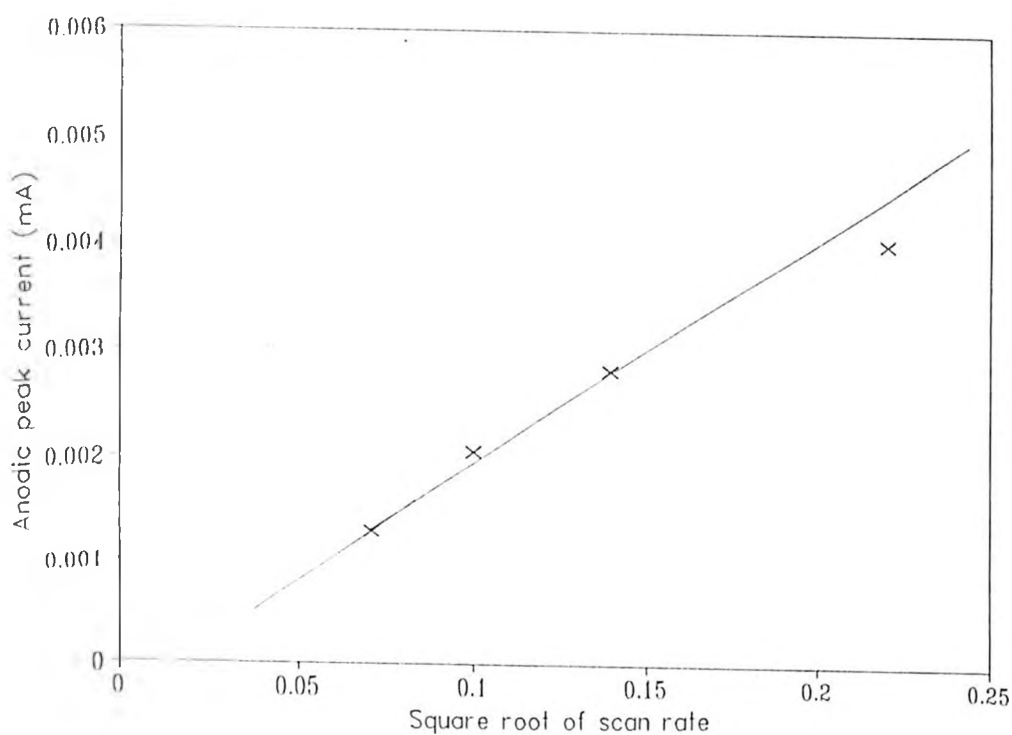


Fig. 3.3.4: A plot of anodic peak current versus square root of scan rate for a bentonite modified electrode in a solution containing 0.1 M H_2SO_4 and 0.01 M $CuSO_4$. Potential range -0.3 V to 0.6 V.

Thus the values of the apparent diffusion coefficient (D_{app}) obtained from the slopes of the plot is just an estimate of its accurate value. Despite all this, the value of D_{app} obtained i.e., 3.6×10^{-11} cm/sec is in good agreement with those published for cations in clay modified electrodes [67,83].

Table 3.2: Peak current ratios at different scan rates for a bentonite modified electrode.

Scan rate MV/sec	$i_{pa} \times 10^3$ mA	$i_{pc} \times 10^3$ mA	i_{pa}/i_{pc}
5	1.30	7.50	0.17
10	2.05	10.00	0.21
20	2.80	13.50	0.22
50	4.05	20.00	0.20
100	4.35	28.50	0.15

The peak current ratio (i_{pa}/i_{pc}) at different scan rates (see Table 3.2) was found to be less than unity i.e., (approximately 0.20) and the differences could be attributed to error during evaluation of the values.

The fact that the cathodic peak current is increasing with scan rate rules out significant leaching. Similarly the increase in anodic peak current with scan rate suggests insignificant contribution to electron transfer by atoms in the bentonite lattice [67,84,86].

The electrode used in the foregoing analysis was then transferred to a solution containing 0.1 M sulphuric acid and the potential scanned from -0.3 V to 0.6 V. The anodic peak current dropped from 43 μ A on the first scan to 23 μ A within 105 seconds. This drop in the peak current continued but at a much reduced pace up to 17

μA on the sixth scan. This was attributed to leaching [84]. This data is particularly important in that the ratio of the peak current can be used as a factor in the correction for leaching effect during computation for the total amount of copper adsorbed by the clay mineral.

Another strong support for the leaching concept is the fact that, the redox peaks were not regenerated after the electrode had been left standing for 24 hours. This would have been the case if the drop in the peak currents were due only to reduction of the adsorbed copper.

3.3.3 ELECTRODE MODIFICATION WITH PRE-TREATED BENTONITE

An electrode modified with B-WAC was transferred into a solution containing 1.0 M sulphuric acid and the potential cycled from -0.3 V to 0.6 V at a scan rate of 20 mV/sec. The resultant cyclic voltammetric response is shown in Fig. 3.3.5. The copper oxidation peak is sharp, well defined and occurs at 0.11 V while the reduction peak appears at -0.2 V.

The same electrochemical procedure was repeated but this time with an electrode modified with B-NAC. The rate of change of the anodic peak current for the B-NAC modified electrode was found to be almost twice that of electrode modified using B-WAC i.e., 6.5×10^{-3} mA/min.

It is worth noting that during the first fourteen scans for a B-NAC modified electrode, the anodic peak for copper occurred at approximately 0.36 V while the

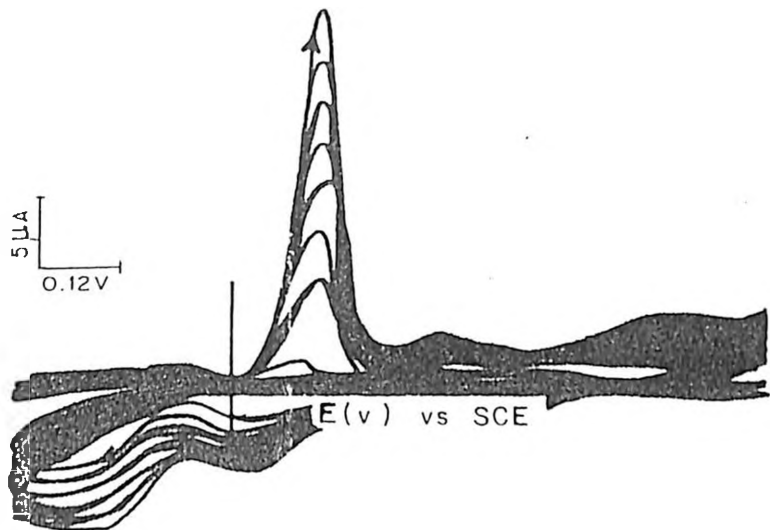


Fig. 3.3.5 Cyclic voltammetric response for a B-WAC modified electrode in a solution containing 1.0M H_2SO_4 . Potential range -0.3V to 0.8V. Scan rate: 20mV/sec.

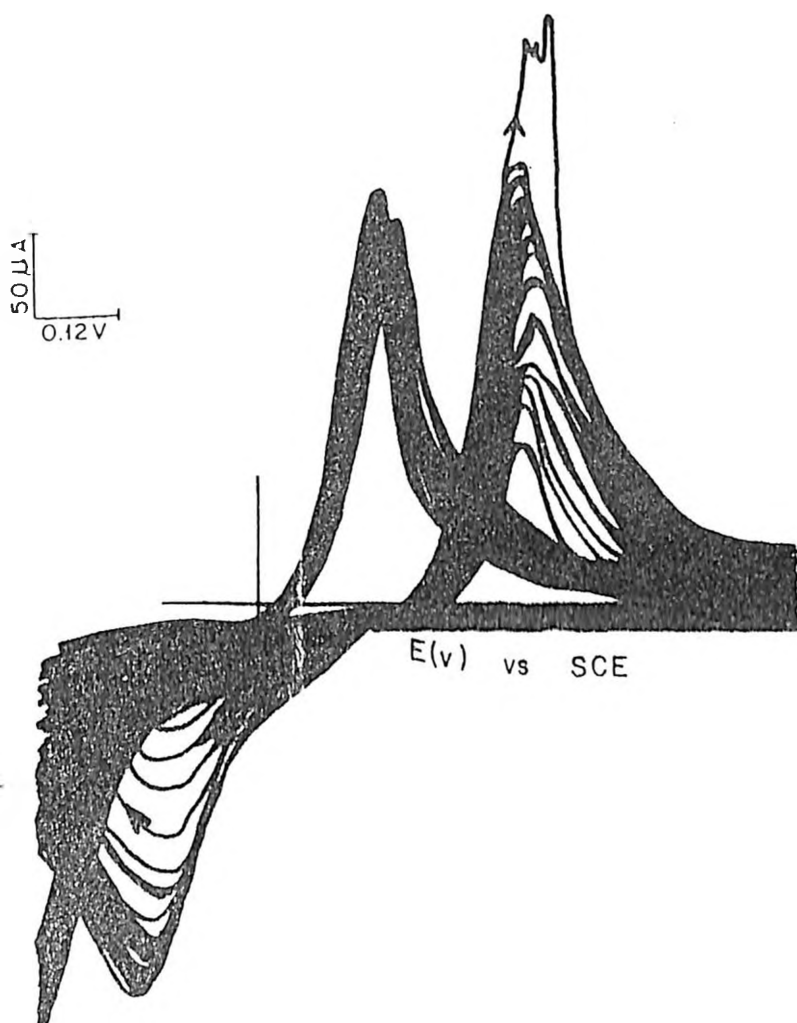


Fig 3.3.6: Cyclic voltammetric response for a B-NAC modified electrode in a solution containing 1M H_2SO_4 . Potential range -0.3 to 0.8V. Scan rate 20mV/sec

reduction peak appeared at -0.14 V. There was then a slight but sudden increase in the anodic peak current followed by a big shift in the anodic peak towards negative potentials to 0.143 V. After this 217 mV shift in the anodic peak potential, the rate of change of the anodic peak current was now substantially reduced (see Fig. 3.3.6) and the cathodic peak disappeared. It was proposed that this shift was probably related to the location of the electroactive copper in the bentonite matrix i.e., whether adsorbed on the surface or trapped in the vacant octahedral sites in the bentonite lattice.

The redox efficiency of the copper redox processes in B-WAC modified electrode is found to be approximately half that of copper in B-NAC modified electrode i.e., 27 % and 50 % respectively.

Attempts to correlate the maximum anodic peak current obtainable for various amounts of B-WAC and B-NAC used in the electrode modification yielded the results tabulated in Tables 3.3 and 3.4.

Table 3.3: Maximum anodic peak current versus mass of B-NAC used in electrode modification.

Mass of B-NAC (g)	Max i_{pa} (mA)
0.040	0.13
0.041	0.22
0.046	0.18
0.048	0.17
0.050	0.2

Table 3.4: Maximum anodic peak current versus mass of B-WAC used in electrode modification.

Mass of B-WAC (g)	Max i_{pa} (mA)
0.040	0.02
0.041	0.03
0.043	0.04
0.047	0.01
0.048	0.04
0.051	0.09

Due to the haphazard nature of this data, too much emphasis cannot be placed on it. This was probably due to the fact that it is not possible to produce electrodes with the same surface morphology. These points could therefore not be used to make plots of anodic peak current (maximum) versus mass of the electrode modification material (for both B-WAC and B-NAC) to be used as a calibration curve.

It is however worth noting that the maximum anodic peak currents for B-NAC electrodes are generally about four times higher than those obtained for the B-WAC electrodes. This shows, as would be expected, that there is more exchanged copper in absence on protons.

XRF measurements were then conducted to determine the concentration of copper in bentonite, B-WAC and B-NAC and the results obtained are shown in Table 3.5.

Table 3.5: X - ray fluorescence measurements on various samples of bentonite.

Sample	Conc. x 10 ³ g/g
Bentonite	0.05
B-WAC	7.10
B-NAC	24.90

Calculations from cyclic voltammograms obtained for B-WAC and B-NAC modified electrodes yielded a surface coverage for electroactive copper as being approximately 4.5×10^{-10} mol/cm². This corresponds to 1.07×10^{-6} grams of copper/gram of electrode modification material. Thus electroactive copper constitutes 0.015 % and 0.004 % of the copper present in B-WAC and B-NAC respectively. The fact that the amount of electroactive copper is much higher in B-WAC is not surprising, because there is a large proton population in it. As such, isomorphous substitution of exchangeable cations from bentonite lattice by the protons will take place.

This denies copper cations (adsorbed) the opportunity to occupy these sites, which would have put them in remote locations not favouring electron transport. This would have cut down the population of electroactive copper.

3.3.4 ELECTRODEPOSITION OF POLYANILINE ON A COPPER LOADED BENTONITE MODIFIED ELECTRODE.

The B-WAC and B-NAC modified electrode were next used as host matrices for the electrodeposition of polyaniline.

The cyclic voltammetric response obtained with the B-WAC and B-NAC modified electrodes when their potential was cycled in a solution containing 0.1 M

aniline and 1.0 M sulphuric acid in the range -0.8 V to 0.8 V at 20 mV/sec are shown in Figs. 3.3.7 and 3.3.8. The polyaniline oxidation peak occurs at approximately 0.18 V in both cases. An initial increase in the copper redox peaks followed by a decrease as polyaniline is electrodeposited were observed. The two redox centres are distinct from each other as can be seen in the voltammograms. It can also be observed that, in the case of B-NAC modified electrode there was formation of a distinct nuclear loop upon reversal of current direction. Such nucleation have been observed by other researchers during copper deposition [3]. This process is probably related to the internal pH of the bentonite matrix, as a similar phenomena is not observed with B-WAC electrodes.

On continued cycling, the polyaniline redox peaks dominate the electrochemical scene for both B-WAC and B-NAC cases as shown in Fig. 3.3.9. In this case also there was no evidence of formation of bilayer electrodes such as charge rectification. The decrease in the copper redox peaks on continued electrodeposition of polyaniline is probably due to combination of leaching and outright displacement by the polyaniline polymer.

The rate of change of anodic peak for polyaniline was 4.82×10^{-4} mA/min for B-WAC and 6.7×10^{-3} mA/min for B-NAC with a redox efficiency of 52 % and 60 % respectively. This shows catalytic effect of a redox centre in the matrix. This, as already noted, is achieved through electron transfer mediation by the redox centre between the electrode surface and the aniline monomers.

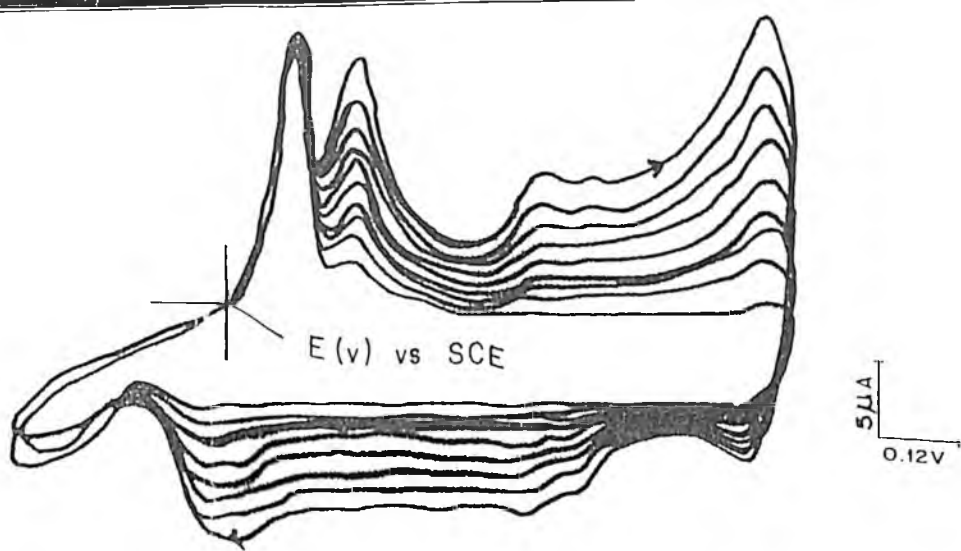


Fig. 3.3.7: Cyclic voltammetric response for a B-WAC modified electrode in a solution containing 0.1M aniline and 1.0M H_2SO_4 . Potential range -0.3V to 0.85V . Scan rate $20\text{mV}/\text{sec}$.

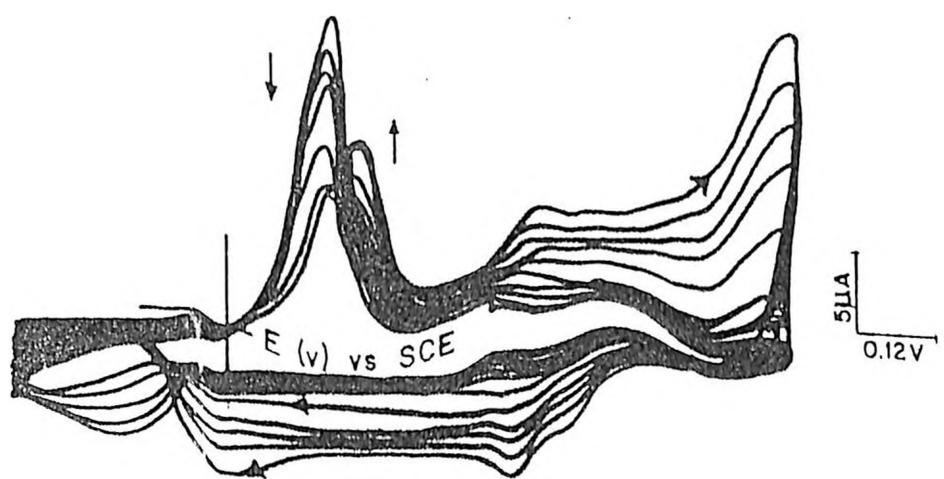


Fig. 3.3.8: Cyclic voltammetric response for a B-WAC modified electrode in a solution containing 0.1M aniline and 1.0M H_2SO_4 . Potential range -0.3V to 0.85V . Scan rate $20\text{mV}/\text{sec}$.

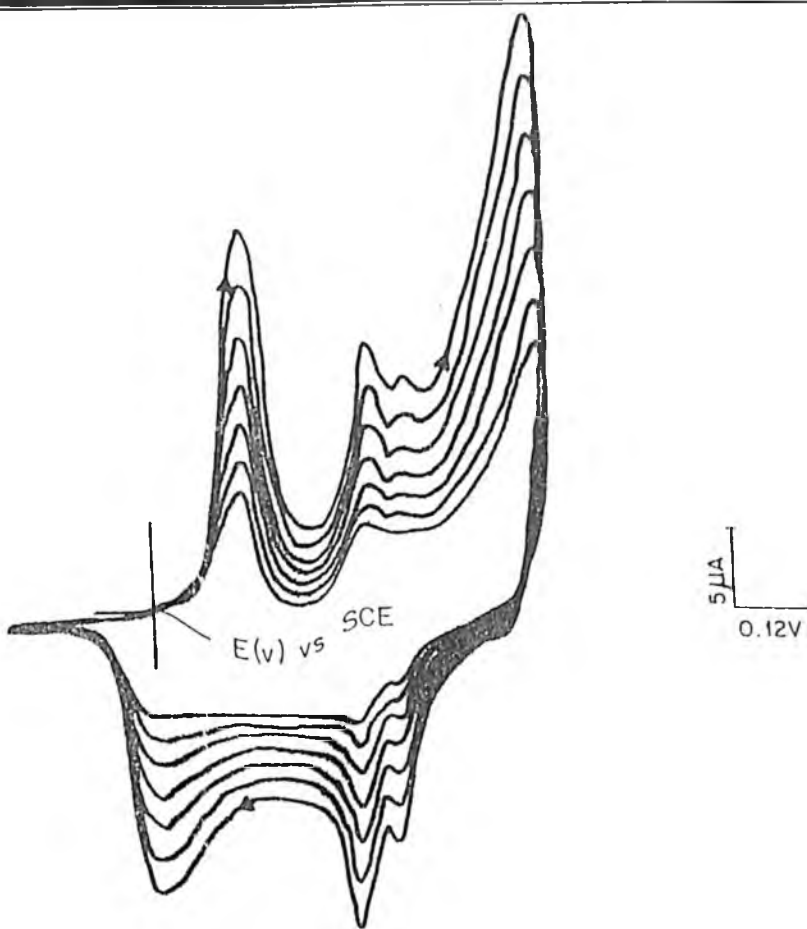


Fig. 3.3.9: Cyclic voltammogram depicting only the polyaniline redox peak. The solution contains 0.1M aniline and 1.0M H₂SO₄. Potential range -0.3V to 0.85V. Scan rate 20mV/sec.

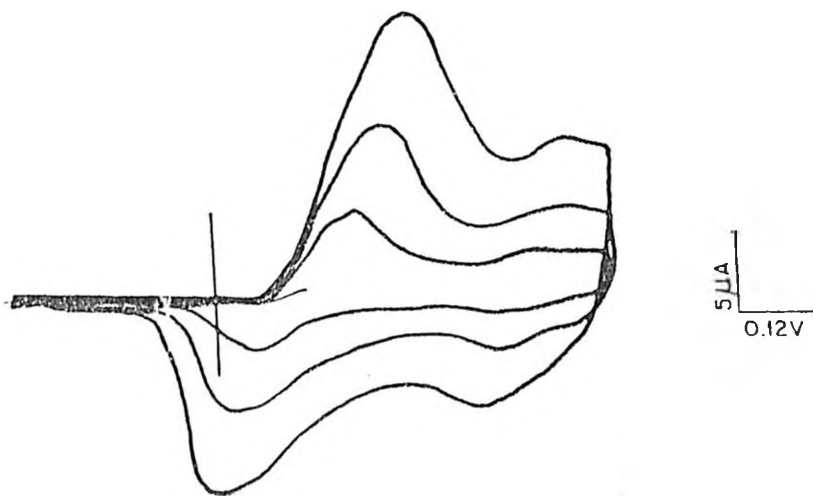


Fig. 3.3.10 Scan rate studies on B-WAC modified electrode after the merging of copper and polyaniline oxidation peaks in a solution containing 1M H₂SO₄. Potential range -0.3V to 0.6V.

Scan rate studies conducted after the merging of the two oxidation peaks (see Fig. 3.3.10) show a peak whose peak potential varies linearly with $v^{1/2}$. This is typical of quasi reversible systems [74]. A plot of i_{pa} versus v was linear showing that the species were surface attached.

3.4 CHARGE STATE TRAPPING AT A CONDUCTING POLYMER-REDOX ION EXCHANGER INTERFACE - A BILAYER ELECTRODE.

3.4.1 ELECTROCHEMICAL BEHAVIOUR OF COPPER ON AN AMBERLITE MODIFIED ELECTRODE

The cyclic voltammetric response obtained from the amberlite modified electrode during the cycling of potential in the range -0.3 V to 0.6 V in a solution of 0.1 M sulphuric acid and 0.01 M copper sulphate displayed the same electrochemical features as those exhibited in the bare carbon case, the only difference being that the oxidation peak potential now occurred at 0.1 V. This represents a shift of approximately 20 mV towards negative potentials. The shift probably has no electrochemical significance other than, being due to iR drop in the electrode (see Fig. 3.4.1).

A plot of the oxidative peak current versus time (see Fig. 3.4.2) yielded linear plots for different electrode samples under the same experimental conditions. The slopes had a value of approximately 3.4×10^{-3} mA/min with a redox efficiency of 80 %.

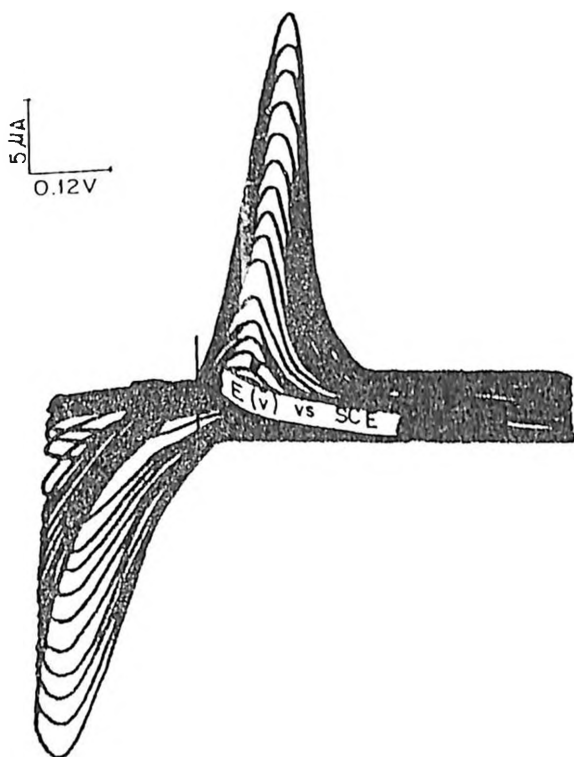


Fig. 3.4.1: Cyclic voltammetric response for an amberlite modified electrode in a solution containing 0.1M H_2SO_4 and 0.01M $CuSO_4$. Potential range $-0.3V$ to $0.6V$. Scan rate $20mV/sec$.

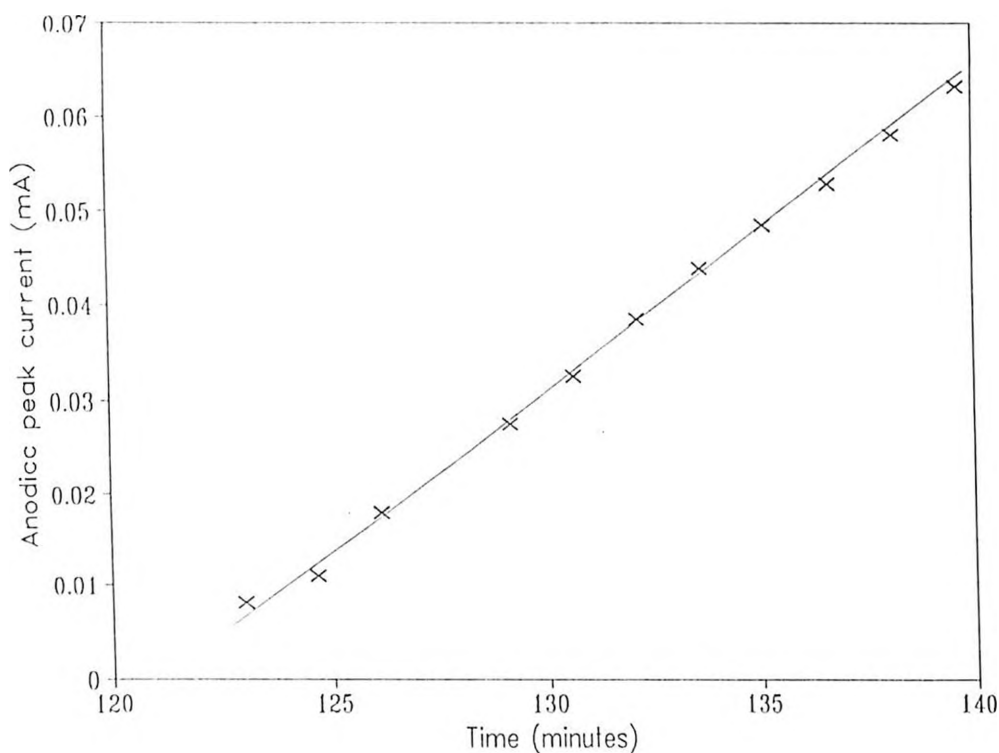


Fig. 3.4.2: A plot of anodic peak current versus time for an amberlite modified electrode in a solution containing 0.1 M H_2SO_4 and 0.01 M CuSO_4 . Potential range -0.3 V to 0.6 V. Scan rate 20 mV/sec.

On transfer of the electrode into a solution containing 0.1 M sulphuric acid, a shift of about 20 mV was observed. The copper oxidation and reduction peaks were stable and lasted for over 50 minutes. Electrodes made this way were latter used for the purpose of electrodeposition of polyaniline (section 3.4.3).

3.4.2 ELECTRODE MODIFICATION USING PRE-TREATED AMBERLITE

The next set of experiments involved electrodes modified with copper loaded amberlite. These electrodes were dipped into a solution containing 1 M sulphuric acid

(no copper sulphate) and the potential cycled from -0.3 V to 0.8 V at a scan rate of 20 mV/sec. An oxidation peak at 0.16 V for Λ -NAC and 0.06 V for Λ -WAC were observed. The reductive peak occurred at -0.2 V for Λ -NAC and was **indistiguishable** for the Λ -WAC case.

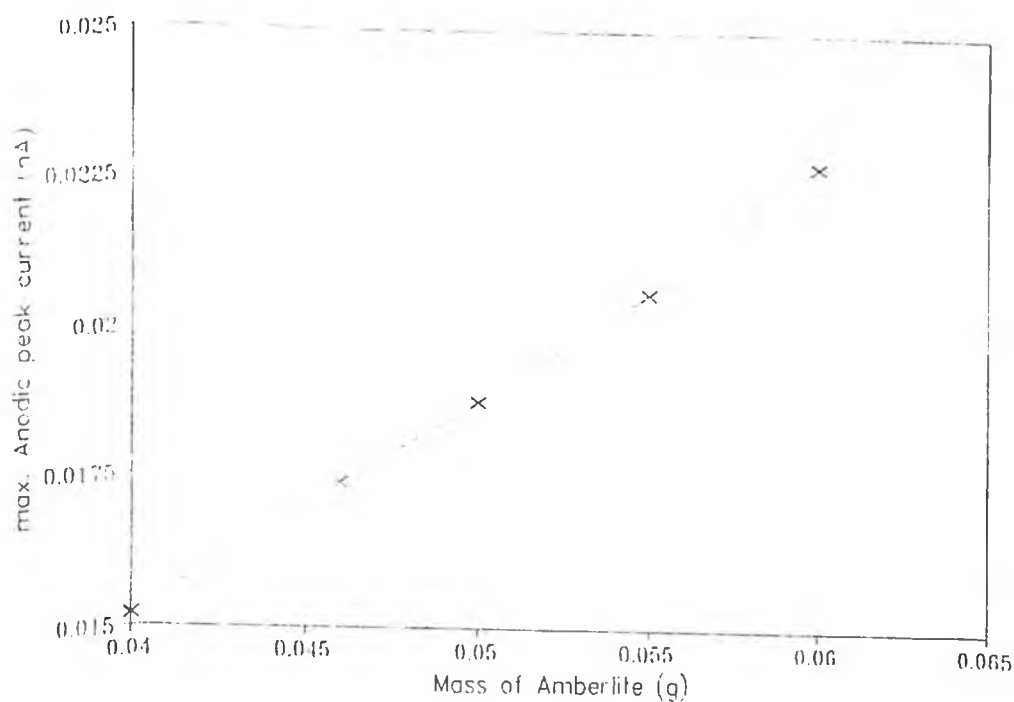


Fig. 3.4.3: A plot of maximum anodic peak current versus amount of Λ -WAC used in the electrode modification on dipping the electrode in 1 M H_2SO_4 . Potential range -0.3 V to 0.8 V. Scan rate 20 mV/sec.

The 80 mV shift towards the positive potentials of the copper oxidation peak, for Λ -NAC modified electrode as compared to that of bare carbon, was attributed to the fact that exchanged copper is a little more difficult to oxidize than copper ions in solution.

Plots for anodic versus cathodic peak current were linear, giving a redox efficiency as high as 87%.

In the next set of experiments an attempt to relate the maximum anodic peak current obtainable to the amount of material used in the electrode modification was made. This was done by dipping a copper loaded amberlite modified electrode in 1.0 M sulphuric acid and cycling the potential in the range -0.3 V to 0.8 V. Several of such experiments were conducted, but only representative results have been shown in Fig. 3.4.3 for A-WAC. When these were used as calibration curves to establish the expected surface coverage for a given mass of amberlite used in electrode preparation, an error of 10 % for A-NAC and 5 % for A-WAC was realised. This was attributed to non-reproducibility of the surface morphology. The slope of these plots were found to be 1.5×10^{-8} mol/cm² per gram of A-WAC and 37.8×10^{-8} mol/cm² per gram of A-NAC. This corresponds to a value of 2.4×10^{-6} grams of copper per gram of A-WAC and 6.02×10^{-5} grams of copper per gram of A-NAC based on the equation;

$$\Gamma_{\text{copper}} \times \text{Mol. weight of CuSO}_4 \times \text{Electrode area}$$

X-ray fluorescence (XRF) analysis done to determine the amount of copper in A-NAC and A-WAC gave the results shown in Table 3.6. Electroactive copper, therefore constitutes approximately 0.16 % of the copper contained in the A-WAC and 0.38 % of copper contained in A-NAC. This suggests that most of the copper in the amberlite is not electroactive. This low value of Γ_{Cu} (electroactive) can be attributed

to the fact that the electroactive copper is that adsorbed onto the surfaces of the cation exchanger or on sites resulting from defects i.e., holes.

Table 3.6: Copper concentration in A-WAC and A-NAC as determined by XRF analysis.

Sample	Copper conc. x 10 ³ (g/g)
A-WAC	1.49
A-NAC	16.0

3.4.3 ELECTROCHEMICAL BEHAVIOUR OF POLYANILINE ON A PRETREATED AMBERLITE MODIFIED ELECTRODE.

In the next set of experiments a conducting polymer - polyaniline was electrodeposited on pre-treated amberlite modified electrode. The experiments were started by cycling the potential of an amberlite (no copper) modified electrode from -0.3 V to 0.8 V at a scan rate of 20 mV/sec, in a solution containing 1.0 M sulphuric acid and 0.1 M aniline. The polyaniline oxidation peak occurred at 0.19 V. It is surprising that there was no significant difference in the oxidation potentials of polyaniline electrodeposited on an amberlite electrode as compared to that electrodeposited on a bare carbon electrode. This had been expected due to electrostatic interaction between cationic sites generated on oxidation of polyaniline (see scheme VI) and those of the anionic sites (weakly acidic group such as -COO⁻), found in the cation exchange resin to affect the redox potentials. The absence of electrostatic interference between polyaniline and the cation exchange resin is probably a veiled pointer to the two units being distinctly separate i.e., bilayer arrangement.

When a similar experiment was repeated but this time using a copper loaded amberlite (in a solution containing 1 M sulphuric acid and 0.1 M aniline) as the electrode modification material, different results were obtained. The results obtained also depended very strongly on the mode of attachment of the copper redox centre on the amberlite i.e., simultaneous exchange (SE) or physical adsorption (PA) e.g. A-WAC. Experiments conducted on the SE-amberlite electrode revealed copper oxidation/reduction peaks which were decreasing while three other oxidation peaks were building up at 0.19 V, 0.36 V and 0.71 V (see Fig. 3.4.4).

The oxidation peak at 0.19 V results from the polyaniline oxidation process, while those at 0.36 V and 0.71 V are attributed to quinone - quinone imine derivatives, characteristic of polyaniline at very positive potentials [8].

When similar experiments were conducted on the A-WAC electrode, the polyaniline redox peaks were observed to start as a shoulder off the copper oxidation peak, gradually developing into a well defined peak (see Fig. 3.4.5). The double humped copper-polyaniline peak finally merges into one distinct peak where the peak potential of this new peak corresponds to that characteristic of polyaniline (see Fig. 3.4.6).

The interesting thing is that at some stage during the electrochemical process, the copper redox state appear "trapped" i.e., invariant as the polyaniline redox peaks develops. This status is maintained throughout until when the polyaniline peak becomes dominant. This charge trapping is a further pointer to bilayer formation [86].

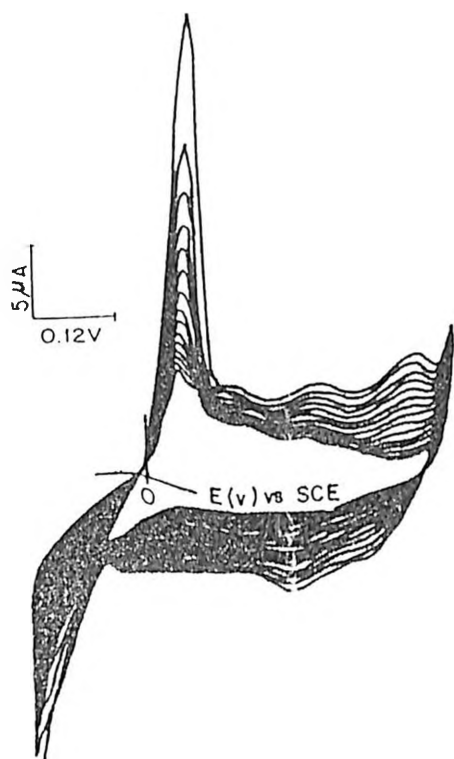


Fig. 3.4.4: Cyclic voltammetric response on transferring a copper loaded amberlite (by simultaneous exchange) into a solution containing 1M H_2SO_4 and 0.1M aniline. Potential range $-0.3V$ to $0.8V$. Scan rate $20mM/sec$.

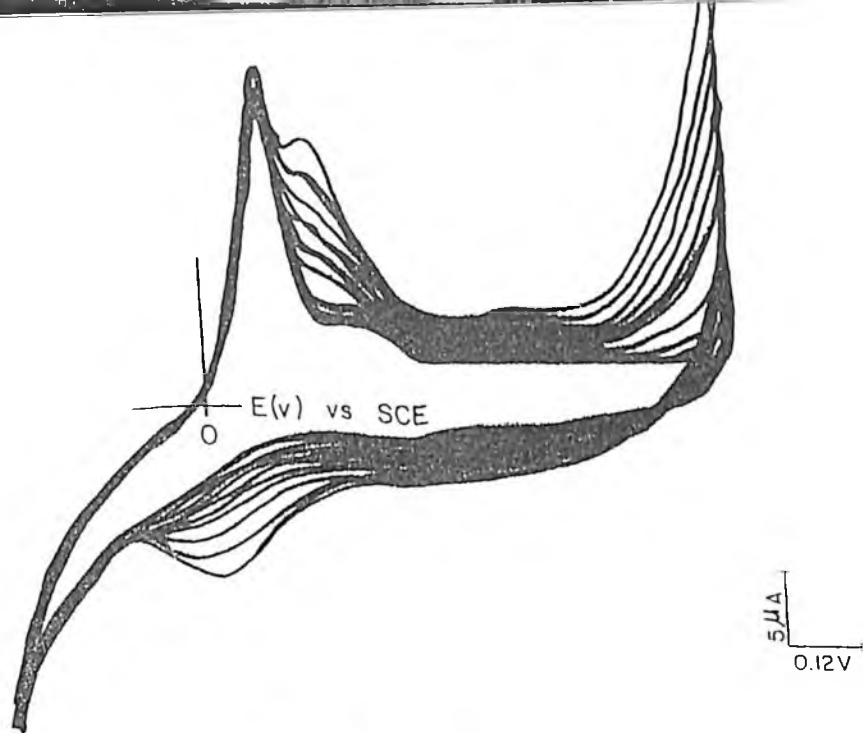


Fig. 3.4.5: Cyclic voltammetric response for A-WAC modified electrode in a solution containing 1M H_2SO_4 and 0.1M aniline. Potential range $-0.3V$ to $0.8V$. Scan rate $20mV/sec$.

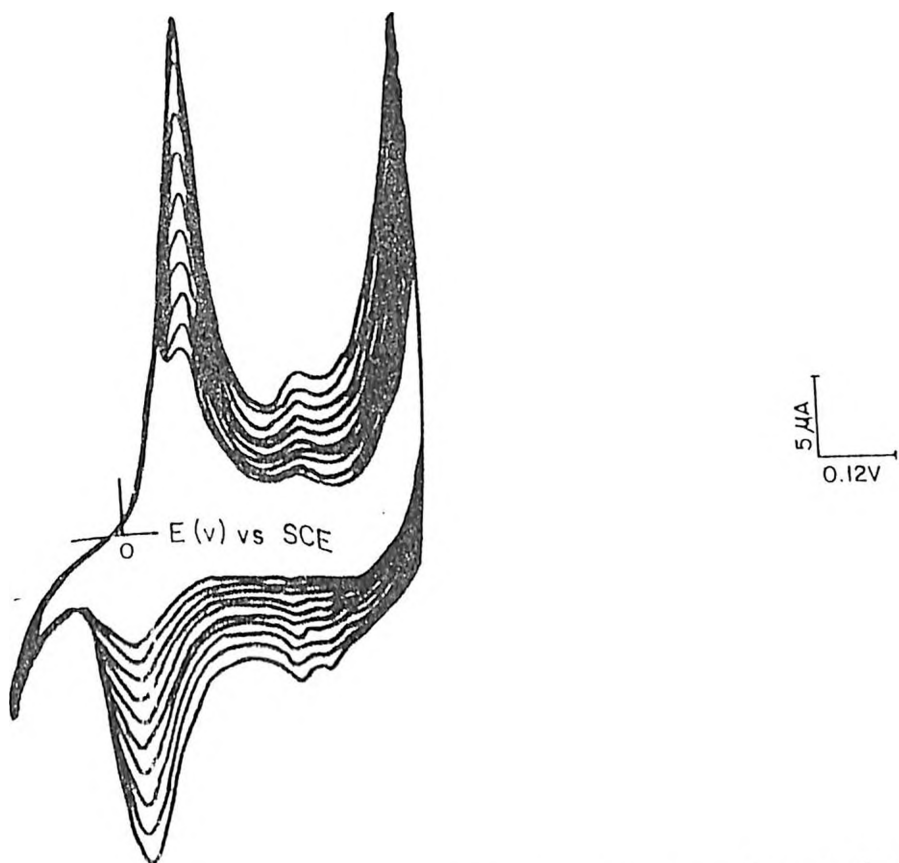
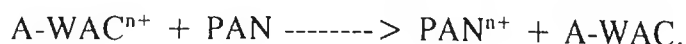


Fig. 3.4.6: Cyclic voltammograms obtained after the merging of the copper and polyaniline oxidation peaks for A-WAC modified electrode.

If A-WAC is treated as the inner film and polyaniline as the outer film, then the current controlling steps will include oxidation of copper redox sites, electrochemical charge transfer through the A-WAC and polyaniline film, and finally *electron* transfer between the redox centres i.e., copper in A-WAC and polyaniline. The rate determining step will be electron transfer between the PA-amberlite and polyaniline redox centres, as the other processes are relatively fast i.e., the peak currents are proportional to scan rate implying that charge transport is fairly rapid.

The electron transfer at the PA-amberlite and polyaniline (PAN) interface may then be expressed by the following equation;



The K_{eq} for the above reaction, calculated from the equation;

$$\frac{RT}{nF} \ln K_{eq} = (E_{in} - E_{out})$$

where n - is the number of electrons involved in the reaction, E_{in} and E_{out} represent the formal potential of the inner and outer layer respectively, is 1×10^2 (for $n = 2$).

This value is twice that obtained for the poly-Ru(VB)₃/poly-VDQ⁺ (vinyl diquat) bilayer electrode [86].

Using the equation;

$$E_p = E_{1n} - \frac{RT \ln M}{nF}$$

where

$$M = \frac{RT}{nFV} K^{interf} X \frac{\Gamma_{1n}^{interf} \Gamma_{out}^{interf}}{\Gamma_{out}}$$

one obtains a value of $M = 100$. Where Γ_{in}^{interf} gives the amount in mol/cm² of the inner and while Γ_{out}^{interf} gives the amount in mol/cm² of the outer film redox sites in contact at the interface between the two layers and v is the scan rate in volts/sec and E_p is the peak potential in volts. (For further discussion of the equations, see reference [86]).

Using the value of $M = 100$, the product

$k^{interf} X \Gamma_{in}^{interf} X \Gamma_{out}^{interf}$ approximately equals 68 for n is two and v equals 20×10^{-3} v/sec.

and using the equation;

$$i_{pa} = \frac{nAFV^2}{eRT} \Gamma_{out}$$

we obtain $\Gamma_{out} \approx 6.03 \times 10^{-10}$ mol/cm², taking an $i_{p,a}$ value of $20 \mu A$ obtained from the cyclic voltammogram. It is important to mention that the A-WAC was treated as the inner layer, even though on peeling off the electrode one can clearly see polyaniline film next to the working electrode.

On comparing this value to that of electroactive copper contained in 40 mg of A-WAC used in the electrode modification (i.e., 6×10^{-10} mol/cm² of copper) It is observed that the ratio of the copper to polyaniline redox centres is approximately 1 : 1. The fact that we have equal amounts of copper and polyaniline redox centres yet the latter is dominant is a veiled pointer to the fact that the copper redox state is "trapped". A situation classically associated with bilayer electrodes.

CONCLUSION

Electrode modification with ion exchangers has been shown to bring out salient electrochemical features which cannot be observed on a bare electrode. It is thus important that other cationic exchange materials be investigated for the same ability. Investigations on the overall electrochemical effect on the redox properties of various cations on an electrode modified with pillared bentonite may be interesting. Such an electrode may also be used as a host matrix for polyaniline.

The use of ion exchangers especially amberlite and the cheaper bentonite as traps of lead from waste products may offer a solution to environmental lead pollution. The study of the enhancement of the redox properties of lead, when adsorbed on an exchanger may further be refined as a technique for quantitative and qualitative analysis of lead.

The fact that the redox ion exchange material may be peeled off the electrode surface after the electrodeposition of polyaniline is of significance in that it may be subjected to further analysis. Also, now that we have successfully formed a bilayer on such an electrode, it is worthwhile that other cations in conjunction with other conducting polymers be investigated. This could be a major breakthrough in the world of electronics especially in the field of diodes.

REFERENCES

1. Murray, R.W.; (1984) Chemically modified electrodes (ed by Bard A.J.) in *Electroanal. Chemistry* 13, Marcel Dekker Inc. NY 191.
2. Murray, R.W. and Moses, P.R.; (1976) Chemically modified electrodes 3. SnO₂ and TiO₂ electrodes bearing an electroactive reagent, *J. Am. Chem. Soc.*, **98**, 7435.
3. Lane, R.F. and Hubbard, A.T.; (1973) Electrochemistry of chemisorbed molecules I. Reactions connected to electrodes through olefinic substituents, *J. Phys. Chem.*, **77**, 1401.
4. Lane, R.F. and Hubbard, A.T.; (1973) Electrochemistry of chemisorbed molecules II. The influence of charged chemisorbed molecules on the electrode reactions of platinum complexes, *J. Phys. Chem.*, **77**, 1411.
5. Watkins, B.F., Behling, J.R. and Kariv, E.; (1975) Chiral electrodes, *J. Am. Chem. Soc.*, **97**, 3549.
6. O'Grady, W., Iwakura, C., Huang, J. and Yeager, E.; (1974) Electrocatalysis (ed by Breiter, M.W.), *Electroc. Soc. Symposium Series*, Princeton NY, 286.
7. Miller, L.L. and Van De Mark, M.R.; (1978) Electrode surface modification via polymer adsorption, *J. Am. Chem. Soc.*, **100**, 639.
8. Orata, D.O. and Buttry, D.A.; (1987) Determination of ion population and solvent content as functions of redox state and pH in polyaniline, *J. Am. Chem. Soc.*, **109**, 3574.

9. Abruna, H.D., Denisevich, P., Umana, M., Meyer, T.J. and Murray, R.W.; (1981) Rectifying interfaces using two-layer films of electrochemically polymerized vinylpyridine and vinylbipyridine complexes of Ruthenium and Iron on electrodes, *J. Am. Chem. Soc.*, **103**, 1.
10. Orata, D.O. and Osoro, F.K.; (1993) Electrochemical degradation of a metallated polyaniline, *Reactive polymers*, **20**, 81.
11. Wrington, M.S., Palazzatto, M.C., Bocarsly, A.B., Bolts, J.M., Fischer, A.B. and Nadjo, L.; (1978) Preparation of chemically derivatized platinum and gold electrode surfaces, *J. Am. Chem. Soc.*, **100**, 7264.
12. Merz, A. and Bard, A.J.; (1978) A stable surface modified platinum electrode prepared by coating with electroactive polymer, *J. Am. Chem. Soc.* **100**, 3222.
13. Arnold, B.B. and Murphy, G.W.; (1961) Studies on the electrochemistry of carbon and chemically modified carbon surfaces, *J. Phys. Chem.*, **65**, 135.
14. Firth, B.E., Miller, L.L., Mitani, M., Rogers, T., Lennox, J. and Murray, R.W.; (1976) Anodic and cathodic reactions on a chemically modified edge surface of graphite, *J. Am. Chem. Soc.*, **98**, 8271.
15. Koval, C.A. and Anson, F.C.; (1978) Electrochemistry of the ruthenium (3+/2+) couple attached to graphite electrodes, *Anal. Chem.*, **50**, 223.
16. Fox, M.A., Nabs, F.J. and Voynick, T.A.; (1980) Covalent attachment of arenes to SnO₂ - semiconductor electrodes, *J. Am. Chem. Soc.*, **102**, 4029.

17. Thornton, E.W. and Harrison, P.G.; (1975) Part I - Surface hydroxyl groups and the chemisorption of carbon dioxide and carbon monoxide on tin (IV) oxide, *J. Chem. Soc. Faraday Trans. 1*, **71**, 461.
18. Aderson, S., Constable, E.C., Dare-Edwards, M.P., Goodenough, J.B., Hamnett, A., Seddon, K.R. and Wright, R.D.; (1970) Chemical modification of a titanium (IV) oxide electrode to give stable dye sensitisation without a supersensitizer, *Nature*, **280**, 571.
19. Bolts, J.M. and Wrington, M.S.; (1978) Chemically derivatized n-type semiconducting germanium photoelectrodes. Persistent attachment and photochemical activity of ferrocene derivatives, *J. Am. Chem. Soc.*, **100**, 5257.
20. Wrington, M.S., Austin, R.G., Borcarsly, A.S., Bolts, J.M., Haas, D., Legg, K.D., Nadjjo, L. and Palazzatto, M.C.; (1978) Design and study of a photosensitive interface: A derivatized n-type silicon photoelectrode, *J. Am. Chem. Soc.*, **100**, 1602.
21. Murray, R.W.; (1980) *Silylated surfaces* (eds Leyden, D.E. and Collins, W.) Gordon and Breach NY.
22. Brown, A.P., Koval, C. and Anson, F.C.; (1976) Illustrative electrochemical behaviour of reactants irreversibly adsorbed on graphite electrode surfaces, *J. Electro. Chem.*, **72**, 379.
23. Mattson, J.S. and Mark, H.B.; (1971) *Activated carbon: surface chemistry and adsorption from solution*, Marcel Dekker, NY.
24. Elliot, C.M. and Murray, R.W.; (1976) Chemically modified carbon electrodes, *Anal. Chem.*, **48**, 1247.

25. Lennox, J.C. and Murray, R.W.; (1978) Chemically modified electrodes 10. Electron spectroscopy for chemical analysis and alternating current voltammetry of glassy carbon bound tetra(aminophenyl)porphyrins, *J. Am. Chem. Soc.*, **100**, 3710.
26. Dautartas, M.F., Evans, J.F. and Kuwana, T.; (1978) Studies of O-tolidine attachment to pyrolytic graphite electrodes via cyanuric chloride, *Anal. Chem.*, **50**, 104.
27. Heinze, J. and Merz, A.; (1990) *Topics in current chemistry*, Springer Verlag Berlin.
28. Murray, R.W., Wier, L. and Moses, P.R.; (1975) Chemically modified tin oxide electrode, *Anal. Chem.*, **47**, 1882.
29. Orata, D.O. and Osoro, F.K.; (1993) Stabilization of polyaniline films in the presence of P-aminophenol, *Bull. Chem. Soc. Ethiop.*, **6(1)**, 27.
30. Paul, E.W., Ricco, A.J. and Wrington, M.S.; (1985) resistance of polyaniline films as a function of electrochemical potential and the fabrication of polyaniline devices, *J. Phys. Chem.*, **89**, 1441.
31. MacDiarmid, A.G., Chiang, J.C., Halpern, M., Huang, M.S., Mu, S.L., Somesiri, N.D.L., Wu, W. and Yaniger, S.I; (1985) Polyaniline: Interconversion of metallic and insulating forms, *Mol. Crys. Liq. Cryst.*, **121**, 173.
32. Helfferich, F.; (1962) *Ion exchange* McGraw Hill Series in Advance Chemistry.
33. Harm, F. and Rümpler; (1903) 5th Inter. Congr. Pure and Appli. Chem. **59**.

34. Juda, W. and McRae, M.A.; (1950) Coherent ion exchange gels and membranes, *J. Am. Chem. Soc.*, **72**, 1044.
35. Barrer, R.M. and Samma, D.C.; (1975) Exchange equilibrium in crystals of chabazite, *J. Chem. Soc.*, 2838.
36. Forslind, E.; (1953) The Clay-water system II. Water adsorption and cationic exchange in montmorillonites, *Acta. Polytech.*, **115**, CA, **47** 10949.
37. Green-Kelly, R.; (1956) The swelling of orgophilic montmorillonites in liquids, *J. Colloid Sci.*, **11**, 77.
38. Cotton, F.A. and Willinkison, G.; (1972) *Advanced inorganic chemistry*, 3rd ed. Wiley Eastern, New Delhi, India.
39. Jenny, H; (1932) Studies on the mechanism of ionic exchange in colloidal aluminium silicates, *J. Phys. Chem.*, **36**, 2217.
40. Marshel, C.E.; (1949) *The colloid chemistry of the silicate materials*, Academic, Press NY.
41. Van Olphen, H; (1977) *An introduction to clay colloid chemistry*, 2nd ed. Wiley NY.
42. Barrer, R.M.; (1948) Synthesis of a zeolitic mineral with chabazite-like sorptive properties, *J. Chem. Soc.*, 127.
43. Reed, T.B. and Breek, D.W.; (1956) Crystalline zeolites II. Crystal structure of synthetic zeolites type A, *J. Am. Chem. Soc.* **78**, 5972.

44. Pulfrey, W.; Timau and Athi river clays, *Unpublished reports*, Mines and geology Dept., Kenya.
45. Behramann, A.S. and Gustafson, H.; (1938) *Ind. Eng. Chem.*, **30**, 1011.
46. Barrer, R.M.; (1948) Synthesis and reactions of mordenite, *J. Chem. Soc.*, 2158.
47. Norrish, K. and Quirk, J.P.; (1954) Crystalline swelling of montmorillonites, *Nature*, **173**, 255.
48. Gregor, H.P., Dolar, D. and Hoeschele, G.K.; (1955) Polythiolstyrene - a new oxidation/reduction ion exchange resin, *J. Am. Chem. Soc.* **77**, 3675.
49. Howe, P.G. and Kitchener, J.A.; (1955) Fundamental properties of cross-linked poly(methylacrylic acid) ion exchange resins, *J. Chem. Soc.*, 2143.
50. Osborn, G.H.; (1961) *Synthetic ion exchangers*, 2nd ed. Chapman and Hall Ltd. London, 2.
51. Mahlman, H.A., Leddicotte, G.W. and Moora, F.L.; (1954) Separation of cobalt and zinc by liquid-liquid extraction, *Anal. Chem.*, **26**, 1939.
52. Bard, A.J. and Itaya, K.; (1985) Clay modified electrodes 5. Preparation and electrochemical characterization of pillared clay-modified electrodes and membranes, *J. Phys. Chem.*, **89**, 5565.
53. Ege, D., Ghosh, P.K., White, J.R., Egey, J.F. and Bard, A.J.; (1985) *J. Am. Chem. Soc.*, **107**, 5644.

54. Amos, L.J., Duggal, A., Mirsky, E.J., Ragonesi, P., Bocarsly, A.B. and Fitzgerald-Bocarsly, P.A.; (1988) Morphological variation at the $[\text{NiFe}(\text{CN})_6]^{2-/-}$ derivatized nickel electrode, *Anal. Chem.*, **60**, 245. sensitivity for Na and Cs.
55. Auderbert, P., Bedan, G. and Kowski, M.; (1986) Reduction by two successive one electron transfers of anthraquinone units bonded to electrodeposited polypyrrole films, *J. Chem. Soc. Chem. Comm.*, 887.
56. Shigehara, K., Oyama, N. and Anson, F.C.; (1981) Evaluation of rate constants for redox self exchange reactions from electrochemical measurements with rotating disk electrodes coated with polyelectrolytes, *Inorg. Chem.*, **20**, 518.
57. Schnelder, J.R. and Murray, R.W.; (1982) Quantitative aspects of ion exchange partition of redox cations into organosilane - styrenesulfonated copolymer films on electrodes, *Anal. Chem.*, **54**, 1508.
58. Kuwana, T. and Tse, D.C.S.; (1978) Electrocatalysis of dihydronicotinamide adenosine diphosphate with quinones and modified quinones electrodes, *Anal. Chem.*, **50**, 1315.
59. Evans, J.F. Kuwana, T., Henne, M.T. and Royer, J.P.; (1977) Electrocatalysis of solution species using modified electrodes, *J. Electroanal. Chem.*, **80**, 409.
60. Kanatidis, M.G.; (1990) Conductive polymers (*special report*), Dec, 3rd, 36.
61. Goodings, E.P.; (1975) Polymeric conductors and superconductors, *Endeavour*, **34**, 123.

62. Ikehata, S., Kaufer, J., woerner, T., Pron, A., Druy, A.M, Sivak, A., Heeger, A.J. and McDiarmid, A.G.; (1980) Solitons in polyacetylene: Magnetic susceptibility, *Phy. Rev. Lett.*, **45**, 1123.
63. Bredas, J.L., Scotts, J.C., Yakushi, K. and Street, G.B.; (1984) Polarons and bipolarons in polypyrrole, *Phy. Rev. B.*, **30**, 1023.
64. Kaufman, J.H., Caloneri, N., Scott, J.C. and Street, G.B.; (1984) Evaluation of the band stucture and optical spectrum upon doping, *Phy. Rev. Lett.*, **53**, 1005.
65. Green, R.L. and Street, G.B.; (1984) Conducting organic materials, *Science*, **226**, 651.
66. Orata, D.O., and Matheka.. Munge... Ma;(1993) *Macrol. Mol.*, **257**, 71.
67. Ghosh, P.K. and Bard, A.J.; (1985) Clay modified electrodes, *J. Am. Chem. Soc.*, **105**, 5691.
68. Daunert, S., Wallace, S., Florido, A. and Bachas, L.G.; (1991) Anion selective electrodes based on electropolymerized porphrin films, *Anal. Chem.*, **63**, 1676.
69. Gazard, M.; (1986) *Handbook of conducting polymers*, Marcel Dekker NY 673.
70. Labes, M.M., Love, P. and Nicholas, L.F.; (1979) Polysulfurnitride - a metallic superconducting polymer, *Chem. Rev.*, **79**, 1.

71. Chiang, C.K., Druy, M.A., Gau, S.C., Heeger, A.J., Louis, E.J., MacDiarmid, A.G., Park, A.G. and Shirakawa, H; (1977) *Phy. Rev. Lett.*, **39**, 1098, *J. Am. Chem. Soc.*, **100**, 1013.
72. Sawyer, D.T. and Roberts, R.L.; (1974) *Experimental electrochemistry for chemists* Wiley and sons NY.
73. Nicholson, R.S. and Shain, I; Theory of stationary electrodes polarography - single scan and cyclic methods applied to reversible, irreversible and kinetic systems, *Anal. Chem.*, **36**, 706.
74. Bard, A.J. and Faulkner, L.R.; (1980) *Electrochemical methods-Fundamental and applications*, John Wiley NY.
75. Skoog, D.A. and West, D.M.; (1985) *Analytical chemistry*, Holt, Rinehart and Winston, NY, 3rd ed. 355.
76. Skoog, D.A.; *Principals of instrumental analysis*, Saunders, NY 3rd ed. 600.
77. Orata, D.O. and Kamau. S.D.; (1995) Effect of supporting electrolyte and cation population on the redox chemistry of polyaniline electrodeposited on a montmorillonite modified electrode, Submitted to *Macrol. Mol.*
78. Giaouque, R.D., Jakleiric, J.M.; (1971) Rapid quantitative analysis by X-ray spectroscopy in K.J.F. Heinrich et. al. eds., *Advances in X-ray Analysis*, Plenium press **15**, 164.
79. Storm, E. and Isreal, H.I.; (1970) *Nuclear data tables*, **A7**,

80. Bambynet; (1972) X-ray fluorescent yields, Auger, and coaster-kronig, Transition probabilities, *Rev. Mod. Phys.*, **44**, 716.
81. Kinyua, A.N.; (1982) Multielemental analysis of solid and liquid samples by X-ray fluorescence, *MSc. Thesis, University of Nairobi*.
82. Yamagishi, A., and Aramata, I.; (1984) *J. Chem. Soc. Chem. Commun.*, 452.
83. Bard, A.J. and Rudzinski, W.E.; (1990) Clay modified electrodes- Part 6 Aluminium and silicon pillared clay modified electrodes, *J. Electroanal. Chem.*, **199**, 323.
84. Bard, A.J. and Villemure, G.; (1990) Clay modified electrodes- Part 9 electrode studies of the electroactive fraction of adsorbed species in reduced charge and preadsorbed clay films, *J. Electroanal. Chem.*, **282**, 107.
85. Lee, J. and Tan, T.C.; (1990) Cyclic voltammetry of electrodeposition of metal on electrosynthesized polypyrrole film, *J. Electrochem. Soc.*, **137**, 1403.
86. Bard, A.J., Man, A.W.H. and Ghosh, P.C.; (1981) *J. Am. Chem. Soc.*, **103**, 4727, *J. Electroanal. Chem.*, **169**, 315.